

Indoor Localisation
By Using Wireless Sensor Nodes

By

HAKAN KOYUNCU

A Doctoral Thesis

Submitted in Partial fulfilment
of the requirements for the award of

Doctor of Philosophy

of

Loughborough University

December 2014

Copyright 2014 Hakan Koyuncu

ACKNOWLEDGEMENTS

I would like to thank my supervisor Prof Dr Shuang-Hua Yang for his advice and encouragements in the supervision of this study.

He has always assisted in all details throughout the study and he has had a great influence and become my inspiration in my research.

I would also like to thank Dr Eran Edirisinghe for his guidance.

Furthermore I would like to thank Loughborough University for supporting with departmental facilities which helped me accomplish my research work.

I would like to relay my special thanks to my friends Fang Yao and Huanjia Yang who helped me, providing and sharing equipment to use in my research work.

Finally, I would also like to thank to my family who motivated and encouraged me throughout my studies with great patience and moral support.

ABSTRACT

This study is devoted to investigating and developing WSN based localisation approaches with high position accuracies indoors. The study initially summarises the design and implementation of localisation systems and WSN architecture together with the characteristics of LQI and RSSI values.

A fingerprint localisation approach is utilised for indoor positioning applications. A k-nearest neighbourhood algorithm (k-NN) is deployed, using Euclidean distances between the fingerprint database and the object fingerprints, to estimate unknown object positions. Weighted LQI and RSSI values are calculated and the k-NN algorithm with different weights is utilised to improve the position detection accuracy. Different weight functions are investigated with the fingerprint localisation technique. A novel weight function which produced the maximum position accuracy is determined and employed in calculations.

The study covered designing and developing the centroid localisation (CL) and weighted centroid localisation (WCL) approaches by using LQI values. A reference node localisation approach is proposed. A star topology of reference nodes are to be utilized and a 3-NN algorithm is employed to determine the nearest reference nodes to the object location. The closest reference nodes are employed to each nearest reference nodes and the object locations are calculated by using the differences between the closest and nearest reference nodes.

A neighbourhood weighted localisation approach is proposed between the nearest reference nodes in star topology. Weights between nearest reference nodes are calculated by using Euclidean and physical distances. The physical distances between the object and the nearest reference nodes are calculated and the trigonometric techniques are employed to derive the object coordinates.

An environmentally adaptive centroid localisation approach is proposed. Weighted standard deviation (STD) techniques are employed adaptively to estimate the unknown object positions. WSNs with minimum RSSI mean values are considered as reference nodes across

the sensing area. The object localisation is carried out in two phases with respect to these reference nodes. Calculated object coordinates are later translated into the universal coordinate system to determine the actual object coordinates.

Virtual fingerprint localisation technique is introduced to determine the object locations by using virtual fingerprint database. A physical fingerprint database is organised in the form of virtual database by using LQI distribution functions. Virtual database elements are generated among the physical database elements with linear and exponential distribution functions between the fingerprint points. Localisation procedures are repeated with virtual database and localisation accuracies are improved compared to the basic fingerprint approach.

In order to reduce the computation time and effort, segmentation of the sensing area is introduced. Static and dynamic segmentation techniques are deployed. Segments are defined by RSS ranges and the unknown object is localised in one of these segments. Fingerprint techniques are applied only in the relevant segment to find the object location.

Finally, graphical user interfaces (GUI) are utilised with application program interfaces (API), in all calculations to visualise unknown object locations indoors.

Keywords: Wireless Sensor Node (WSN), Fingerprinting, Localisation, Application Program Interface (API), Link Quality indicator (LQI), Received Signal Indicator (RSSI), Centroid Localisation (CL), Weight Centroid Localisation(WCL), Graphical User Interface (GUI)

Hakan Koyuncu, 2014

PUBLICATIONS

Peer reviewed Journal Publications

- 1) **H.Koyuncu and Shuang Hua Yang**, “A survey of Indoor Positioning and object locating systems” ,international Journal of Computer Science and Network Security, Vol. 10, No. 5, May 2010, pp 121-128 ,ISSN 1738-7906
- 2) **H.Koyuncu and Shuang Hua Yang**, “A 2D positioning system using WSNs indoor environment “ International Journal of Electrical & Computer sciences, Vol. 11, No. 03, June 2011, pp 70-77,ISSN 2077-1231
- 3) **H.Koyuncu and Shuang Hua Yang**, “A study of indoor positioning by using trigonometric and weight centroid localisation techniques”, International Journal of computer Engineering Research, Vol. 2(2), Sept 2011, ISSN 2141-6474
- 4) **H.Koyuncu and Shuang Hua Yang**, “Comparisons of Indoor Position Enhancements by Using Mean and Kalman Filtering Techniques”, Journal of computer science and engineering, Vol. 11, issue 2, February 2012. pp 9- 15
- 5) **H.Koyuncu and Shuang Hua Yang**, “Virtual 2D positioning System by using Wireless Sensors in indoor environment”, International Journal of Wireless and mobile networks (IJWMN), Vol. 5,No. 6 ,December 2013, pp 21 -36
- 6) **H.Koyuncu and Shuang Hua Yang**, “An improved adaptive localisation approach for indoor positioning by using environmental thresholds with wireless sensor nodes”, IET Wireless sensor systems. 2014, pp. 1–9, doi: 10.1049/iet-wss.2013.0100

Conference Publications

- 1) **H.Koyuncu and Shuang Hua Yang**, “Determination of 3D indoor object locations by using wireless sensor nodes and RSSI techniques”, Proceedings of 16th international conference on Automation & Computing, University of Birmingham, UK,11 September 2010, pp 37-41, ISBN 978-0-9555293-6-8

- 2) **H.Koyuncu and Shuang Hua Yang**, “Comparisons of Indoor localisation techniques by using reference nodes and weighted k-NN algorithms”, 3rd European conference of computer science. 3 December 2012, pp 46-51, ISBN 978-1-61804-140-1
- 3) **H.Koyuncu and Shuang Hua Yang**, “Indoor Positioning with Virtual Fingerprint mapping by using linear and exponential taper functions”, IEEE International conference on Systems, Man and Cybernetics (CSMC) ,IEEE Proceedings, October 2013, pp. 1052 - 1057, ISSN 978-1-4799-0652-9
- 4) **H.Koyuncu and Shuang Hua Yang**, “Improved Fingerprint localisation by using static and dynamic segmentation” International Conference on Computational Science and Computational Intelligence (CSCI14), IEEE CPS proceedings, March 2014, Las Vegas USA, pp. 149 - 156

ABBREVIATIONS

<i>AP</i>	<i>: Access point</i>
<i>ADC</i>	<i>: Analogue to Digital convertor</i>
<i>APS</i>	<i>: Ad Hoc positioning systems</i>
<i>APIT</i>	<i>: A point of triangulation</i>
<i>AOA</i>	<i>: Angle of arrival</i>
<i>CL</i>	<i>: Centroid Localisation</i>
<i>DB</i>	<i>: Database</i>
<i>EM</i>	<i>: Electro Magnetic</i>
<i>GPS</i>	<i>: Global positioning system</i>
<i>GUI</i>	<i>: Graphical user Interface</i>
<i>IEEE</i>	<i>: Inst. of Electrical and Electronics Engineering</i>
<i>IR</i>	<i>: Infra Red</i>
<i>K-NN</i>	<i>: k – nearest neighbourhood</i>
<i>LAN</i>	<i>: Local Area network</i>
<i>LQI</i>	<i>: Link Quality Indicator</i>
<i>LSE</i>	<i>: Least square estimation</i>
<i>MAC</i>	<i>: Medium Access control</i>
<i>MMSE</i>	<i>: Minimum mean square error</i>
<i>MS</i>	<i>: Mobile systems</i>
<i>PAN</i>	<i>: Personal area network</i>
<i>PDA</i>	<i>: Personal digital assistant</i>

<i>PHY</i>	: <i>Physical layer</i>
<i>PIT</i>	: <i>Point of triangulation</i>
<i>RF</i>	: <i>Radio Frequency</i>
<i>RFID</i>	: <i>Radio Frequency identification devices</i>
<i>RSS</i>	: <i>Received signal strength</i>
<i>RSSI</i>	: <i>Received signal strength Indicator</i>
<i>STD</i>	: <i>Standard deviation</i>
<i>TDOA</i>	: <i>Time difference of arrival</i>
<i>TOA</i>	: <i>Time of arrival</i>
<i>TOF</i>	: <i>Time of Flight</i>
<i>WAN</i>	: <i>Wireless area network</i>
<i>WCL</i>	: <i>Weighted Centroid Localisation</i>
<i>WPAN</i>	: <i>Wide personal area network</i>
<i>WSN</i>	: <i>Wireless sensor node</i>
<i>ZC</i>	: <i>Zigbee coordinator</i>
<i>ZED</i>	: <i>Zigbee end device</i>
<i>ZR</i>	: <i>Zigbee router</i>

LIST OF SYMBOLS

A	:	sub area
b	:	beacon node
cm	:	centimetre
G_t	:	gain transmitter
G_r	:	gain receiver
m	:	meter
P	:	power
T_x	:	transmitter
R_x	:	receiver
v	:	velocity
x	:	x-coordinate
y	:	y- coordinate
t	:	time
dBm	:	decibel meter
D_i	:	i^{th} Euclidean distance
P_{t_x}	:	transmitter power
P_{r_x}	:	received power
Θ	:	angle in radian
α	:	Angle
β	:	environmental factor
e	:	localisation error

TABLE OF CONTENTS

Acknowledgments	II
Abstract	III
Publications	V
Abbreviations	VII
List of symbols	IX
Table of contents	X
Table of figures	XIII
Table of tables	XVII
Chapter 1 introduction	1
1.1 Overview	1
1.2 Wireless sensor Networks	5
1.2.1 Wireless Sensor Network applications.....	7
1.2.2 Wireless sensor node architecture	8
1.2.3 Wireless sensor communication architecture.....	10
1.2.4 Wireless sensor network standards	11
1.2.4.1 IEEE 802.15.4 standards	12
1.2.4.2 ZigBee network standards	12
1.2.5 Localisation applications	13
1.2.5.1 Localisation parameters	15
1.3 Research objectives	16
1.4 Main contributions of the thesis	17
1.5 Thesis layout	20
Chapter 2 Localisation Systems	23
2.1 Background	23
2.2 Localisation Design Considerations	24
2.3 Localisation Techniques	25
2.3.1 Triangulation	25
2.3.2 Trilateration	26
2.3.3 Time of Arrival(TOA)	27
2.3.4 Time difference of Arrival(TDOA).....	28
2.3.5 Angle of Arrival (AOA).....	29
2.3.6 Fingerprint.....	30
2.4 Localisation systems	31
2.4.1 Range free localisation.....	33
2.4.2 Range based localisation	34
2.4.3 Wireless Sensor Node localisation.....	35
2.5 Summary	36

Chapter 3 LQI Characteristics and Fingerprint Localisation	38
3.1 Background	38
3.2 Received signal strength.....	39
3.3 Link Quality Indicator.....	41
3.4 Experimental conditions	42
3.4.1 Hardware	43
3.5 RSS measurements	44
3.5.1 Curve Fitting	44
3.5.2 Bi-sectioning Algorithm.....	45
3.6 Radiation Beam Patterns	47
3.7 Outliers	47
3.7.1 z-score Method.....	48
3.8 Propagation Path Loss	49
3.9 Fingerprint Localisation Method.....	50
3.9.1 Fingerprint Theory	51
3.9.2 k- NN algorithm	53
3.9.3 Weigh functions	54
3.10 Implementation.....	55
3.10.1 k-NN Experiments.....	56
3.10.2 Weighted k-NN Experiments	57
3.11 Conclusions	58
Chapter 4 Centroid & Adaptive Centroid Localisation	60
4.1 Background	60
4.2 Centroid localisation	61
4.3 Weighted Centroid localisation	62
4.4 Adaptive localisation.....	63
4.4.1 RSSI correction phase	65
4.4.2 Advanced RSSI correction Phase.....	66
4.5 Environmentally Adaptive location Algorithm.....	67
4.6 Implementation.....	69
4.6.1 Centroid localisation.....	69
4.6.2 Adaptive centroid localisation.....	71
4.6.2.1 RSSI correction phase (phase 1).....	71
4.6.2.2 Advanced RSSI correction phase (phase 2)	73
4.6.2.3 Different Indoor Topologies.....	75
4.7 Conclusions	77
Chapter 5 Localisation by triangulation	80
5.1 Background	80
5.2 LQI reception	81
5.3 Curve fitting	82
5.4 Triangulation	84
5.4.1 Triangular area formation.....	84
5.5 Weighted Centroid Localisation.....	87
5.6 Implementation.....	88
5.6.1 Position estimation by triangulation.....	88
5.6.2 WCL calculations.....	89
5.6.3 Different Test Area Shapes	90
5.7 Discussions.....	91
5.8 Conclusions	91
Chapter 6 Localisation by using reference nodes.....	93
6.1 Background	93
6.2 Reference node topology.....	94
6.3 Improved Landmarc localisation.....	96
6.3.1 Classical Landmarc	96

6.3.2 Improved Landmarc	97
6.3.3 Neighbourhood Weighted	99
6.4 External reference topology model	100
6.5 Implementation	101
6.6 Discussions.....	102
6.7 Conclusions	103
Chapter 7 Virtual Localisation	105
7.1 Background	105
7.2 Fingerprint model	106
7.3 Virtual Fingerprint	107
7.3.1 Linear Interpolation function.....	109
7.3.2 Exponential-Linear Interpolation Function	112
7.3.3 Exponential-Exponential Interpolation Function	115
7.4 Implementation.....	117
7.4.1 Linear interpolation	118
7.4.2 Exponential linear interpolation	119
7.4.3 Exponential-Exponential interpolation	120
7.5 System Evaluation	120
7.6 Conclusions	122
Chapter 8 Static & Dynamic localisation	124
8.1 Background	124
8.2 Static Segmentation.....	125
8.2.1 Fingerprint Creation Phase.....	125
8.2.2 Feature Identification Phase	126
8.2.3 Position Estimation Phase	127
8.3 Dynamic Segmentation	128
8.4 Implementation.....	131
8.4.1 Experimental Test Bed	131
8.4.2 Classical Fingerprint Approach.....	132
8.4.3 Static Segmentation.....	132
8.4.3.1 Static Segmentation with different topology	134
8.4.4 Dynamic Segmentation	136
8.4.5 Environmental effects on dynamic segments	137
8.4.6 Object Localisation in dynamic segments	138
8.5 System Evaluation	141
8.6 Conclusion	142
Chapter 9 Conclusions and Future work	143
9.1 Conclusions	143
9.2 General discussions	146
9.3 Outcomes.....	148
9.3.1 Outcome 1: Research Literature	148
9.3.2 Outcome 2:Localisation Systems	149
9.3.3 Outcome 3:LQI Characteristics and Fingerprint Localisation	149
9.3.4 Outcome 4: Optimum Weight Functions	149
9.3.5 Outcome 5: Weighted Centroid localisation	150
9.3.6 Outcome 6: Adaptive centroid localisation	150
9.3.7 Outcome 7: Triangular localisation	150
9.3.8 Outcome 8: Reference node localisation	150
9.3.9 Outcome 9: Virtual localisation	151
9.3.10 Outcome 10: Static Segmentation	151
9.3.11 Outcome 11: Dynamic Segmentation	151
9.4 Potential improvements of the research	152
References	155

TABLE OF FIGURES

Chapter 1:

Figure 1.1: satellite in orbit [3]

Figure 1.2: Active badge system [9]

Figure 1.3: Active bat system [9]

Figure 1.4: Cricket system [11]

Figure 1.5: Dolphin system [12]

Figure 1.6: Architecture of network based UWB location tracking system [20].

Figure 1.7: RFID Tag and Reader used in LANDMARC localisation system [7]

Figure 1.8: Schematic view of Wireless sensor networks [30].

Figure 1.9a: Jennic active RFID tag JN5121 [31]

Figure 1.9b: Jennic active RFID reader JN5121 [31]

Figure 1.10: Fields of Wireless sensor network applications [33]

Figure 1.11: A typical wireless sensor node (WSN) architecture [34]

Figure 1.12: Sensor nodes scattered in a sensor field [32]

Figure 1.13: The sensor network protocol stack [32]

Figure 1.14: Different network topologies specified by ZigBee [41]

Chapter 2:

Figure 2.1: triangulation technique; Tx1, Tx2 are transmitters, O is object, α , β and c are known parameters; a and b are unknown parameters

Figure 2.2: 2D trilateration technique

Figure 2.3: 3D Trilateration geometry

Figure 2.4: TOA technique

Figure 2.5: TDOA technique

Figure 2.6: AOA localisation a) Localisation with $\Delta\theta$ orientation information b) localisation without $\Delta\theta$ orientation information. [65]

Figure 2.7: Grid space for fingerprint database. B_i : transmitters, G: grid point, P: object receiver

Figure 2.8: Classification of localisation schemes [76]

Chapter 3:

Figure 3.1: Plot of P_{RX} against distance d between a transmitter and a receiver

Figure 3.2: Plot of normalised RSSI values against D distances

Figure 3.3: Recorded RSSI values against D distances between a transmitter and a receiver

Figure 3.4: Recorded LQI values from L_A , L_B , L_C , L_D transmitters against distances

Figure 3.5: Jennic receiver, JN5139 [100]

Figure 3.6: Jennic transmitter, JN5139 [100]

Figure 3.7: Plot of measured LQI values against distances for Jennic Type transmitter/receiver pair and their exponentially fitted curve

Figure 3.8: Steps of bi-sectioning method over the range $[a_1, b_1]$ [102]

Figure 3.9: bi-section algorithm used in calculations

Figure 3.10a: Tx_A radiation beam pattern

Figure 3.10b: Tx_B radiation beam pattern

Figure 3.11: Examples of outliers

Figure 3.12: An example test area with 4 transmitters and a mobile user with a grid of measurement points

Figure 3.13: Architecture of Fingerprint localisation approach [110], by using recorded LQI values

Figure 3.14: Steps of k-NN algorithm for localisation process

Figure 3.15: Block diagram of the test area with $1m \times 1m$ grid space and object point P , grid point G

Figure 3.16: Received LQI signal and database format in the server

Figure 3.17: Error plots at unknown object locations for different w_i values

Figure 3.18: 3D Average error distances versus weight functions

Chapter 4:



Figure 4.1: Graphical view of 4 transmitters with ranges and 1 object receiver,
: Transmitter node : Receiver node

Figure 4.2: Localisation system with a) $5m \times 3m$ and b) $3m \times 5m$ configurations

Figure 4.3: Algorithmic model of the localisation system

Figure 4.4: Universal (xOy) and relative ($x'By'$) coordinate systems

Figure 4.5: A block diagram of indoor test area

Figure 4.6: 3D error plots of unknown object locations with different weights

Figure 4.7: Graphical representation of error distances with respect to target locations in phase 1 and phase 2 stages

Figure 4.8: large student office

Figure 4.9: Corridor

Figure 4.10: Rest lounge

Figure 4.11: Comparison of EAL algorithm with other algorithms for large student office

Chapter 5:

Figure 5.1: Block diagram of localisation system

Figure 5.2: Plot of LQI values against d distances between Tx and Rx nodes in free space

Figure 5.3: Exponential Curve fitted on LQI values by Matlab

Figure 5.4: Test area with triangles, object P and transmitters B_i

Figure 5.5: Four triangle sub areas across the test area.

Figure 5.6: Block diagram of $B_1B_4B_3$ triangle and estimated $P'(x, y)$ point is shown inside and outside the triangle

Figure 5.7: Position of estimated object point $P'(x, y)$ with respect to triangle areas

Figure 5.8: Graphical representation of $B_2B_1B_4$ triangle and estimated $P'(x, y)$ point inside and outside the triangle

Figure 5.9: Different shaped test areas with transmitters B_i (i : number of transmitters)

Chapter 6:

Figure 6.1: Schematic view of Landmarc system. Square: Receivers, Circle: reference node transmitters, Triangle: object transmitters

Figure 6.2: Applied reference node topology. Square: A,B,C,D Receivers, Circle: T_1, T_2, T_3, T_4, T_5 reference transmitters, triangle: objects

Figure 6.3: Graphical view of reference nodes, T_1, T_2, T_3 , target object, Tgt , and weight distributions

Figure 6.4: Graphical view of the object outside 3 nearest reference nodes T_1, T_5, T_4

Chapter 7:

Figure 7.1: Grid area showing a grid point G , an object P and B_i transmitters where $i=1,2,3,4$

Figure 7.2: Physical grid space and virtual grids across each physical grid cell

Figure 7.3: Block diagram of the proposed localisation system

Figure 7.4: Linear LQI distributions are displayed along the grid cell boundaries a) B_1L_3 and B_1L_1 , b) L_4L_3 and L_4L_1 for B_1 transmitter. Each dotted arrow represents a virtual LQI value

Figure 7.5: LQI boundary values for $j=1$, $i=0$ to 5 and $i=1$, $j=0$ to 5 for k^{th} transmitter

Figure 7.6: Schematical view of Exponential LQI interpolation functions a) B_1L_1 and L_1L_4 , b) B_1L_3 and L_3L_4 cell boundaries for LQI transmissions of B_1 transmitter

Figure 7.7: Schematical view of Exponential LQI interpolation functions a) B_1L_1 and B_1L_3 , b) L_1L_4 and L_3L_4 cell boundaries for LQI transmissions of B_1 transmitter

Figure 7.8: Graphical view of exponential taper function between B_1 and L_3 together with 4 virtual grid points for B_1 transmission

Figure 7.9: Graphical view of exponential taper function between B_1 and L_3 together with 4 virtual grid points for B_2 transmission

Figure 7.10: Schematical view of Exponential LQI interpolation functions inside the grid cell $B_1L_3L_4L_1$ boundaries for LQI transmissions of B_1 transmitter

Figure 7.11: Part of the basic fingerprint database in server memory

Figure 7.12: Plot of LQI values versus distance between a receiver and a transmitter with their fitted curve

Chapter 8:

Figure 8.1: Algorithm to estimate the object locations by using static segmentation

Figure 8.2: 1st and 2nd segments across the sensing area. Grid 1 and grid 4 are the reference grids for 1st and 2nd segments respectively.

Figure 8.3: Example segments generated across the sensing area by using dynamic segmentation

Figure 8.4: Algorithm to estimate the object location by using dynamic segmentation

Figure 8.5: Sensing area, 20m x 10m with 3 segments C_1, C_2, C_3 . (grid space is 2 m)

Figure 8.6: Graphical view of estimated object locations with static segmentation, object is red dot

Figure 8.7: Experimental results of static segmentation, 20mx12m test area, object location is (8, 8)

Figure 8.8: Flow chart of the software used for static segmentation

Figure 8.9: L shaped test area with a grid space of 1mx1m. Object is at (2, 5)

Figure 8.10: Feature functions of 5 segments with 6 transmitters.

Figure 8.11: T shaped test area with a grid space of 1mx1m. Object is at (5, 3)

Figure 8.12: Feature functions of 4 segments with 6 transmitters.

Figure 8.13: Flow chart of the software used for dynamic segmentation

Figure 8.14: Object localisation by using dynamic segmentation. Object position is (4, 8), estimated average object position is (4.9, 8.4)

Figure 8.15: Object localisation by using dynamic segmentation. Object position is (14, 5), estimated average object position is (14.8, 4.3)

Figure 8.16: Feature functions of six dynamic segments in object localisation

Figure 8.17: Object localisation by using dynamic segmentation, object position is (11, 1), estimated object position is (11.3, 0.2).

Figure 8.18: Segment feature functions for dynamic segmentation, object position is (11, 1)

Figure 8.19: Object localisation by using dynamic segmentation, object position is (4, 8), estimated object position is (4.9, 7.6)

Figure 8.20: Segment feature functions for dynamic segmentation, object position is (4, 8)

TABLE OF TABLES

Chapter 1:

Table 1.1: Overview of various positioning systems [26]

Chapter 3:

Table 3.1: Examples of random x_i values and calculated z_i values where $i=10$

Table 3.2: A list of weight functions with respect to Euclidean distances

Table 3.3: Sample LQI vector r of mobile object at different locations and 4 nearest grid coordinates

Table 3.4: Examples of estimated object position coordinates and error distances

Table 3.5: Estimated object coordinates using different weight functions in table 3.2

Table 3.6: Error distances with different weight functions

Chapter 4:

Table 4.1: Average LQIs at object positions and d distances between objects and transmitters.

Table 4.2: Different weights of A, B, C, D transmitters for object location (1, 1)

Table 4.3: Sample of estimated object coordinates with different weight functions and their error calculations

Table 4.4: STD and Mean values of 100 RSSI values at object location (2, 3)

Table 4.5: q intervals of RSSI values and mean values in these intervals.

Table 4.6: Calculated adaptive parameters and adaptive RSSI values of the object.

Table 4.7: Actual and estimated d distances to transmitters from object location (2, 3)

Table 4.8: Estimated object locations and their error distances in phase 1.

Table 4.9: STD and Mean values of 100 RSSI values at object location (1, 3) in phase 2

Table 4.10: q and Q intervals, their mean and the number of RSSI values in these intervals

Table 4.11: Estimated target locations with EAL technique in phase 2

Table 4.12: Estimated object locations for large student office with EAL technique in phase 1 and 2

Table 4.13: Estimated object locations for corridor with EAL technique in phase 1 and phase 2

Table 4.14: Estimated object locations for rest lounge with EAL technique in phase 1 and phase 2

Chapter 5:

Table 5.1: A sample of Recorded LQI values and corresponding d values.

Table 5.2: $P'(x, y)$ estimated object coordinates for each triangle test area in first stage.

Table 5.3: Distances between $P'(x, y)$ and respective triangle corners.

Table 5.4: Calculated object position coordinates and their error margins in second stage.

Chapter 6:

Table 6.1: Estimated object coordinates at different locations with 3 approaches.

Table 6.2: Error calculations with 3 different approaches.

Chapter 7:

Table 7.1: LQI values at real and virtual grid points along B_1L_3 of $B_1L_3L_4L_1$ grid cell for B_1 transmitter

Table 7.2: LQI values at real and virtual grid points along B_1L_1 of $B_1L_3L_4L_1$ grid cell for B_1 transmitter

Table 7.3: LQI values for $j=1, i=0$ to 5 for B_1 transmitter in $B_1L_3L_4L_1$ grid cell

Table 7.4: LQI values for $i=1, j=0$ to 5 for B_1 transmitter in $B_1L_3L_4L_1$ grid cell

Table 7.5: LQI values at real and virtual grid points around the grid cell boundaries for B_1 transmissions where $A = \{LQI_{(a,a)}^{B_1} - LQI_{(a+5,a)}^{B_1}\}$, $B = LQI_{(a+5,a)}^{B_1}$, $E = \{LQI_{(a,a+5)}^{B_1} - LQI_{(a+5,a+5)}^{B_1}\}$, $F = LQI_{(a+5,a+5)}^{B_1}$, $C = \{LQI_{(a,a)}^{B_1} - LQI_{(a,a+5)}^{B_1}\}$, $D = LQI_{(a,a+5)}^{B_1}$, $P = \{LQI_{(a+5,a)}^{B_1} - LQI_{(a+5,a+5)}^{B_1}\}$, $R = LQI_{(a+5,a+5)}^{B_1}$

Table 7.6: Exponential taper functions parallel to B_1L_3 boundary across the grid cell where $M = (LQI_{(a,a)}^{B_1} - LQI_{(a,a+5)}^{B_1})$ and $N = (LQI_{(a+5,a)}^{B_1} - LQI_{(a+5,a+5)}^{B_1})$

Table 7.7: Estimated object position coordinates using basic fingerprint database and virtual fingerprint database with linear taper function

Table 7.8: Estimated object position coordinates using basic fingerprint database and virtual fingerprint database with exponential linear taper function

Table 7.9: Estimated object position coordinates using basic fingerprint database and virtual fingerprint database with exponential- exponential taper function

Table 7.10: Overall error calculations for basic and virtual fingerprint databases. Estimated average object coordinates are tabulated for each fingerprint technique

Chapter 8:

Table 8.1: Basic Fingerprint database with rss values at every grid point

Table 8.2: Features and segments for grid locations

Table 8.3: Examples of estimated object coordinates by using k-NN algorithms across the total sensing area with dimensions 20mx10m with grid space of 2 m.

Table 8.4: Feature functions for segment C_1, C_2, C_3 and 4 transmitters

Table 8.5: Estimated example object coordinates with static segmentation.

Table 8.6: Calculated feature functions for 3 dynamic segments F_1, F_2, F_3 across the sensing area.

Table 8.7: Estimated object coordinates and error distances with dynamic segmentation and k-NN algorithms, (Test area is 20mx10m with grid space of 2m).

Table 8.8: Dynamic segmntation results with different number of segments

Chapter 9:

Table 9.1: Localisation techniques versus achieved accuracies.

CHAPTER 1

INTRODUCTION

1.1 Overview

Much research effort is spent nowadays to locate the positions of unknown objects. Indoor positioning systems are getting used more extensively as the suitable technologies are becoming more available.

Improvements in wireless technologies and mobile computing devices helped to generate great interest in location aware systems. Location systems locate or track mobile objects for different purposes. Indoor location aware applications range from monitoring the movements of the patients in hospitals to tracking the movements of goods in a factory. Outdoor location aware applications include tracking the location of fire fighters, soldiers in a military situation and providing navigation information for travelling ordinary people.

Location detection systems can determine the position of unknown objects by using different types of information [1, 2]. Absolute positions of the objects can be defined in 2D or 3D Cartesian coordinate systems. One of the most well-known location detection system is the Global Positioning System (GPS). This is a global navigation system [3]. It provides location and time information 24 hours a day. See Figure 1.1. It is the most widely used outdoor location technology. It can detect a mobile object's position with accuracies of up to a few meters. The GPS system has several satellites orbiting around the world. Each satellite within range transmits location and time information messages to land receivers. The receiver estimates the distances from each satellite to itself by using the time of signal flights.



Figure 1.1: satellite in orbit [3]

This distance information coming from satellites allows the receiver to calculate its position by geometric trilateration. GPS is not a suitable location detection system indoors due to the fact that signals are unable to penetrate through the buildings and other obstacles.

Another outdoor localisation technology is based on cellular Networks [4]. The location of mobile terminals, cell phones, can be determined by base stations. Accuracy of location detection can be increased by improving the radio signal characteristics and the number of base stations. These location systems can often provide satisfactory estimation results for outdoor environments, however they are unsatisfactory for indoor applications due to limits on the signal propagation.

There are three main Technologies which are used for indoor location detection systems. These technologies are based on ultrasonic [5], infrared (IR) [6], and radio frequency (RF) [7, 8]. Each technology has its own advantages and disadvantages in location estimation. IR based location system is one of the earliest position detection systems [9]. A typical example is an active badge, as shown in Figure 1.2. An example of an ultrasonic based system is the active bat system, as shown in Figure 1.3, where the tracked object wears a badge which emits an ultrasonic signal periodically [10].



Figure 1.2: Active badge system [9]

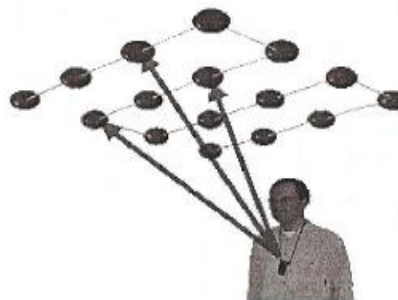


Figure 1.3: Active bat system [9]

Ultrasonic receivers with a radio link are placed in known locations in an area. They detect the signal information synchronised with transmitters and determine the object positions. However, due to characteristics of IR signals such as limited transmission range, line of sight property and negative effect of sunlight, the IR system has serious drawbacks.

Ultrasonic based technology offers low cost systems and fairly accurate location estimation. Typical examples are Cricket [11], in Figure 1.4 and Dolphin [12], in Figure 1.5, ultrasonic systems. The frequency range of their signals is limited. Dispersion of ultrasonic signals in different environments and interference from other sound sources make ultrasonic based location estimation unpopular.



Figure 1.4: Cricket system [11]

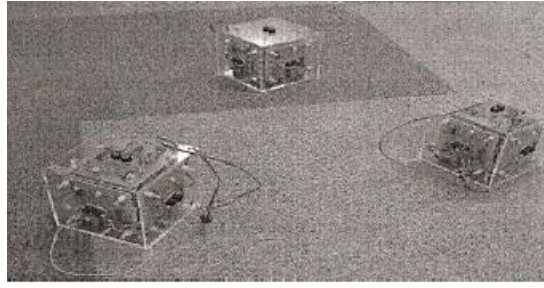


Figure 1.5: Dolphin system [12]

RF based technology is the most widely used technology in location estimation due to its many advantages such as long distance transmission, easy detection and deployment indoors [13,14]. This technology also has many disadvantages such as signal attenuation and fading, reflections from obstacles.

RF localisation systems use radio frequency signals for communication. They can be used with wireless local area networks, WLAN, and Bluetooth networks to determine object locations [15]. Sensors in the Networks detect RF signal information identified as received signal strength (RSS), signal arrival time and signal arrival angle. The location of an object can be determined by using these parameters based on triangulations with time of arrival (TOA), time difference of arrival (TDOA) and angle of arrival (AOA) techniques.

RF based technologies can be divided into wireless local area network WLAN (2.4 GHz and 5GHz band), Bluetooth (2.4 GHz band), Ultra Wideband (UWB) and Radio Frequency identification devices (RFID) [16,17]. UWB technology is similar to an infrared localisation system. UWB transceivers communicate with emitters by sending RF signals with wide bandwidth modulation [18, 19, 20]. See Figure 1.6.

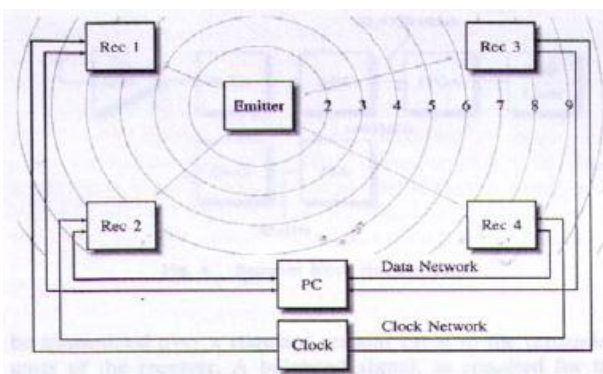


Figure 1.6: Architecture of network based UWB location tracking system [20].

The location of a transceiver is estimated by using time of flight from the UWB transceiver to a minimum 3 scanners. This technology has a wide transmission bandwidth which is

greater than 500MHz according to the Federal Communications Commission (FCC). UWB signals suffer very little loss in indoors. The only drawback is the impairment of other signals radiated from other devices.

WLAN localisation systems are also RF based localisation systems [7,8]. They use off-the-shelf wireless devices and existing WLAN infrastructure with no other extra hardware. Since WLAN is widely used in indoors, Wi-Fi enabled tags working on IEEE 802.11 standard are utilised in Wi-Fi network infrastructure. Tags communicate with Wi-Fi access points (AP) to detect RSS values. These RSS values are reported to a server and the positions of tags are calculated by using software techniques. WLAN technology has several advantages such as low costs, fast deployment and device simplicity.

RFID technology has many advantages such as being contactless and non-line-of-site, having multi object recognition ability and long transmission range. It is a widely used technology in location determination systems [21]. RFID location system is composed of RFID readers and tags [22]. Examples of an active reader and a tag are shown in Figure 1.7. They are more likely used for location detection purposes due to their on-board power utilities and the resultant long operational ranges.

The readers detect the signals from mobile tags in indoors and transfer the signal information to a server. The position of the tag is estimated by its proximity, using these signals. RFID systems must install many readers indoors to achieve higher position accuracies. There is also a trend to combine and integrate the different sensor systems and the databases to improve the accuracy of the position detection of the objects indoors [23].

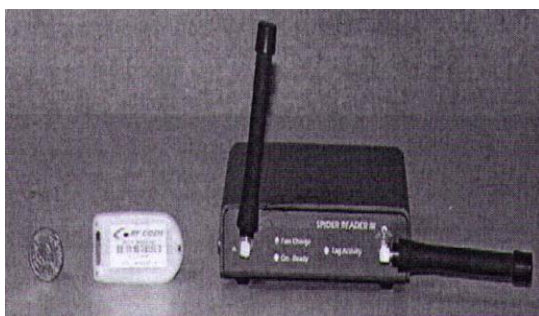


Figure 1.7: RFID Tag and Reader used in LANDMARC localisation system [7]

Large numbers of sensors are introduced in a variety of localisation schemes such as triangulation, trilateration, matching and many others. Table 1.1 is prepared to give an overview and compare various localisation systems. It can be seen that the accuracies of systems vary between 2cm and a few meters. Data repetition rates are between 1Hz and 70Hz for the RF systems. Integrated systems such as Cricket and Dolphin [11, 12] have higher

localisation accuracies. Ultrasonic and infrared technologies are often integrated with RFID techniques. Better indoor planning and positioning of advanced sensors can increase the accuracy levels [24, 25]. If accuracy and cost are the most important parameters, then the systems including ultrasonic techniques are the most desirable systems. All the systems are real time systems and the position information is produced in real time. Overview of positioning systems, (Koyuncu & Yang, 2010) [26], are given in Table 1.1.

<i>system</i>	<i>outdoor</i>	<i>indoor</i>	<i>realtime</i>	<i>accuracy</i>	<i>range</i>	<i>signal</i>	<i>Data rate</i>	<i>principle</i>	<i>cost</i>
<i>GPS</i>	+		+	1-5m	global	RF	20Hz	TOA, lateration	High
<i>Active badge</i>		+	+	7cm	5m	Infra Red	0.1Hz	TOA, lateration	moderate
<i>Active Bat</i>		+	+	9cm	50m	Ultrasound	75Hz	TOA, lateration	moderate
<i>Cricket</i>		+	+	2cm	10m	Ultrasound	1Hz	TOA, lateration	Low
<i>Dolphin</i>		+	+	2cm	Room scale	Ultrasound	20 Hz	TOA, lateration	Moderate
<i>Wave LAN</i>		+	+	3m	Room Scale	RF	4Hz	RSS, triangulate	Moderate
<i>UWB</i>		+	+	10cm	15m	RF	1Hz	TOA,	Moderate
<i>SPOT ON</i>		+	+	3m	Room scale	RF	2Hz	RSS,triangulate	Low
<i>Land Marc</i>		+	+	1-2m	50m	RF	70Hz	RSS,triangulate	moderate
<i>Radar</i>		+	+	2-3m	Room scale	RF	4Hz	RSS,triangulate	moderate
<i>Comp vision</i>		+	+	10cm	Room scale	Camera images	3.5Hz	Image process	High
<i>Cellphone</i>	+		+	50m	outdoors	RF	Tel rate	Telephone trunk	moderate
<i>INS/RFID</i>		+	+	2m	indoors	RF	100Hz	RSS/INS	moderate
<i>FPM/RFID</i>		+	+	1.7m	indoors	RF	100Hz	RSS/INS	moderate

Table 1.1: Overview of various positioning systems [26]

1.2 Wireless Sensor Networks

Recent technological developments in wireless systems and miniature embedded electronics helped the emergence of wireless sensors. They are identified as wireless sensor nodes. A wireless sensor network is constructed by a distributed collection of wireless sensor nodes [27, 28]. A wireless sensor network includes large numbers of sensor nodes and they communicate over a wireless channel [29]. They achieve distributed sensing and collaborative data processing for variety of jobs. Sensor information can be collected and analysed by using monitoring techniques [30], as shown in Figure 1.8.

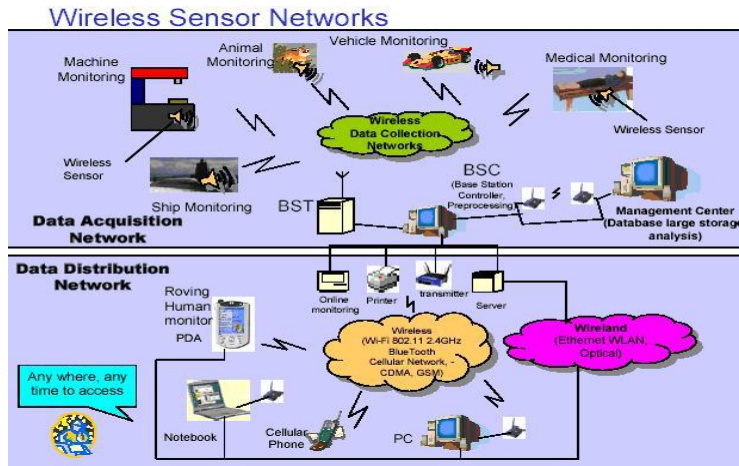


Figure 1.8: Schematic view of Wireless sensor networks [30]

Sensor nodes are small electronic devices equipped with a processor, battery, wireless transceiver for two way communications with other sensors and a memory to store information for later calculations. Typical examples of these nodes [31], which are used in this study are shown in Figures 1.9a and 1.9b.



Figure 1.9a: Jennic active RFID tag JN5121 [31]

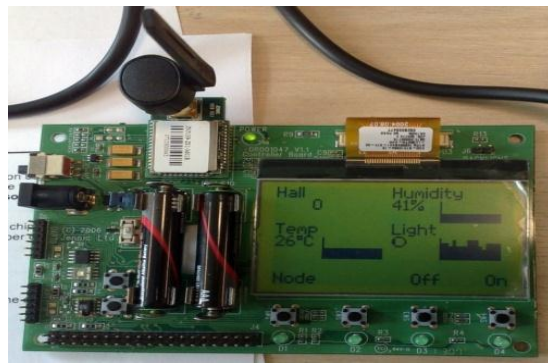


Figure 1.9b: Jennic active RFID reader JN5121 [31]

Wireless sensor networks are widely used in many applications and initial studies were started with military applications in the defence field. The Defence Advanced Research Projects Agency, (DARPA), is the pioneer in this area. Nowadays civilian applications of these networks are increasing.

Wireless sensor nodes (WSN), together with wireless sensor networks are utilised very quickly in every walk of life and the main reasons for this are presented as follows:

- WSNs are very cost effective and relatively cheap to use.
- WSNs have small sizes; they are robust and easy to apply.
- WSNs can be deployed anywhere due to their resistance to changing environmental factors.

- Wireless sensor networks can have large number of sensor nodes and they can cover large areas indoors and outdoors. This allows targets to be placed very close to sensor nodes providing high accuracy.
- WSNs can be quickly and efficiently deployed in the areas of interest which allows quick data collection.
- Data generation from multiple sensor nodes can be done simultaneously by reducing the data collection time due to their deployment density.
- In case of any node failures, WSNs can reorganise themselves with different routes and continue data reception.

1.2.1 Wireless Sensor Network applications

Wireless sensor networks may consist of different types of sensors such as magnetic, visual, infrared, acoustic, radar and RF. Consequently, different types of sensors result in different kinds of applications as identified by Akyıldız and W.Su (2001) [32]. These sensors may be monitoring a wide range of ambient conditions such as temperature, humidity, movement, lighting conditions, pressure, noise levels, or the presence and size of objects. Hence, wireless sensor network applications are categorised into military, environment, health, home and commercial areas. It is also possible to expand this classification with more categories such as space exploration, chemical processing and disaster relief operations as defined below,

- Military applications: WSNs can be an integral part of the command, control, Communication, intelligence, surveillance, reconnaissance and targeting systems. These networks are based on low cost, disposable and dense deployment of sensor nodes and their destruction during operation does not affect the operations as much as destruction of traditional sensors. This makes the Wireless Sensor Network concept a better approach for the battlefield.
- Environmental applications: WSNs are used to track the movements of birds, animals, and insects. They monitor the environmental conditions which affect crops, livestock, irrigation etc. On larger scales, earth monitoring, planetary exploration, atmospheric and meteorological conditions, forest fires, flood detection and pollution are a few of the environmental applications.
- Health applications: WSNs provide interfaces to patients to be monitored, to their diagnostics, and their drug administration in hospitals. They also allow tracking of

patients, to monitor their vital signs and follow up their wellbeing. Tele monitoring and tracking of patients and doctors inside the hospitals are other important applications.

- Home applications: WSNs can be used inside the home with sensors embedded inside home appliances. These could be vacuum cleaners, microwave ovens or refrigerators. Sensors can interact with each other and with the external network via the internet or satellites. End users can manage these devices locally or remotely. Houses thus equipped are called ‘smart houses’.
- Commercial applications: a few of these applications are monitoring product quality, managing inventories, environmental control in offices, manufacturing environments, automation ,transportation, vehicle tracking and heavy machinery.

There are many other areas where WSNs are deployed successfully. These areas can be in space control, nuclear plants or chemical processing plants where human life can be in danger. Fields of application of wireless sensor networks [33], are summarised in Figure 1.10.

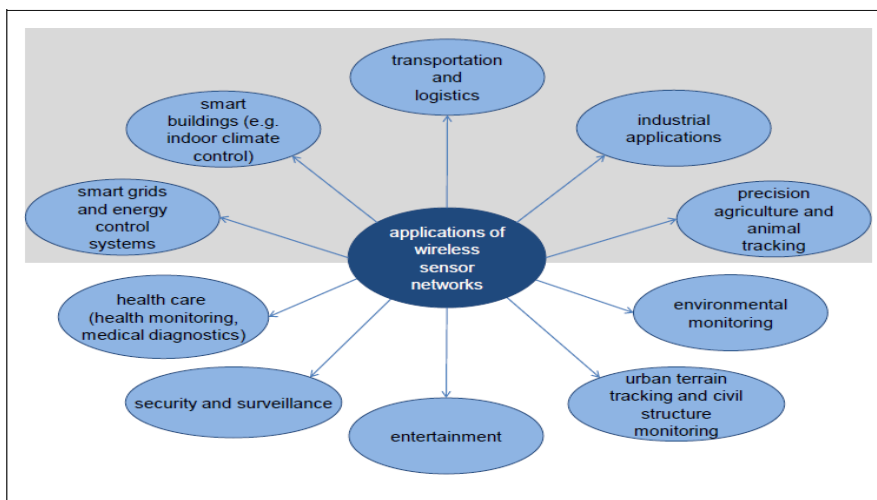


Figure 1.10: Fields of wireless sensor network applications [33]

1.2.2 Wireless sensor node architecture

A typical sensor node consists of 4 basic components as shown in Figure 1.11. These are sensor unit, processor unit (microcontroller), transceiver unit and power unit. They may also have application dependent additional components such as location finding system, and a power generator. These units are summarised [34], as follows,

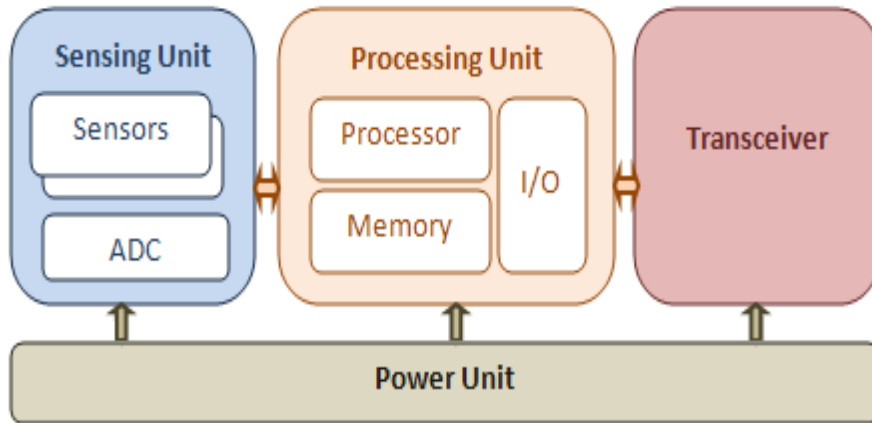


Figure 1.11: A typical wireless sensor node (WSN) architecture [34]

- a) Sensing unit: consists of two sub units, sensors and analogue to digital convertors (ADCs). A sensor is a device which measures some physical quantity and converts it into a signal to be processed by the microcontroller. There are many sensor types such as seismic, thermal, acoustic, visual, infrared etc. They can be active or passive sensors. Wireless sensor nodes may include multiple sensors. The signals are generated as analogue signals and an internal analogue to digital convertor (ADC), digitises these signals and sends them to processor unit.
- b) Processor unit: has a micro controller sub unit to manage the operations of sensors and collaborates these sensors with other internal units. It also has a storage unit and an I/O peripheral to store a small amount of data.
- c) Transceiver unit: connects the WSNs to the network. It provides transmission and reception of data with other WSNs connected to the wireless sensor network. WSNs communicate using RF transceiver and a wireless network such as Bluetooth or 802.15.4 compliant protocols, ZigBee [35] and MiWi [36].
- d) Power unit: a sensor node is supported by a power unit, a form of power storage unit. This could be a battery or a power generation unit such as a solar cell. To conserve energy, the power unit may have power conservation techniques such as dynamic voltage scaling or on-off switching.

Wireless sensor node applications may require knowledge of location with high accuracy. Hence a location finding system can use many WSNs with additional components depending on the application. For example a location finding system together with a mobile platform is deployed to carry out sensing operations in different surroundings.

1.2.3 Wireless sensor communication architecture

Sensor nodes are usually scattered in a sensor field in an orderly or disorderly form. Each of these sensor nodes collects data and sends it to an end user through a sink node. Data can be routed to an end user by a multi hop structure as shown in Figure 1.12 or collected directly by the sink node from the sensor nodes. The sink node communicates with the server at the user location through a wireless medium. The protocol stack used by the sink node and all other sensor nodes is shown in Figure 1.13.

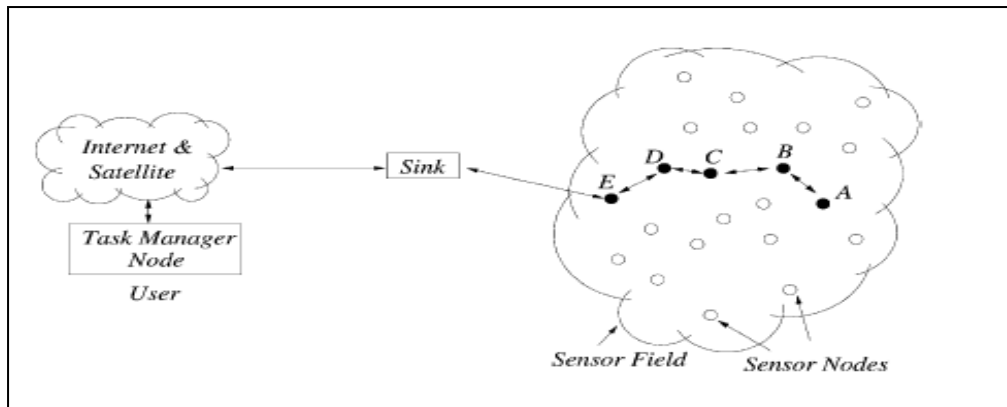


Figure 1.12: Sensor nodes scattered in a sensor field [32]

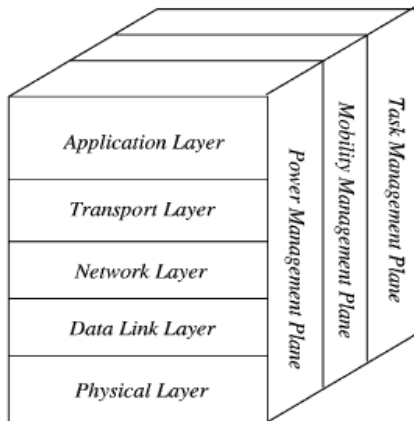


Figure 1.13: The sensor network protocol stack [32]

This protocol stack integrates data with network protocols and communicates signals efficiently throughout the wireless medium. It consists of an application layer, transport layer, network layer, data link layer, physical layer, power management plane, mobility management plane and task management plane [37].

- Application layer: depending on the sensing tasks, different types of application software can be built and used in this layer.

- Transport layer: helps to maintain the flow of data if the sensor network application requires it. It handles delays, maintains end-to-end connections and end-to-end delivery of data packets.
- Network layer: takes care of routing the data supplied by the transport layer.
- Data link layer: known as Medium Access Control (MAC). It multiplexes the data streams and provides the data frame detection and it is responsible for error control. It ensures reliable point-to-point connections in a communication network. MAC protocol establishes communication links for data transfer.
- Physical layer: addresses the needs of simple modulation, transmission and receiving techniques. It also has tasks of bit encoding, voltage determination for bit transmission and data encryption.
- Power management plane: manages how a sensor node uses the power.
- Mobility management plane: detects and registers the movements of sensor nodes so that a route back to the user is maintained and the sensor nodes can keep track of their operations.
- Task management plane: balances and schedules the sensing tasks given to a specific sensing region.

These management planes next to the layers are needed so that the sensor nodes can work together in power efficient way, route the data in the sensor network and share resources between sensor nodes. (Akyildiz et al. 2002) [32]

1.2.4 Wireless sensor network standards

A wide range of wireless data technologies exist and they are designed for different applications. Wireless technologies can be operated by a variety of standards. These standards are grouped in order of increasing range as follows:

- Wireless Personal Area Network (WPAN): this is used for short range communication between devices used by single persons. Wireless head sets are typical examples. They include standards such as Bluetooth, IEEE 802.15.4, Wireless USB and Zigbee.
- Wireless local Area Network (WLAN): also called Wi-Fi, these systems are used to provide wireless access to other systems on the local network such as computers and shared printers. WLAN offers better speeds within the local area

network. Wi-Fi 802.11a, 802.11b, 802.11g, 802.11n, 802.11ac standards are WLAN standards.

- Wireless Area Network (WAN): this is used for national coverage areas from one access point to another allowing seamless coverage for wide areas. Wi-Fi 802.11 standard is a WAN standard.

1.2.4.1 IEEE 802.15.4 standards

This is a WPAN standard. It offers the physical layer and medium access control layer (MAC) for low rate communication. It uses low cost and low power-consumption devices, (Callaway et al. 2002) [38]. The standard defines two types of network node. The first is a Full Function Device (FFD), which can serve as the coordinator of a personal area network. The second is a Reduced Function Device (RFD), which is a simple node and never acts as a coordinator [39].

1.2.4.2 ZigBee network standards

This is a wireless communication standard using low power and low data rate based on IEEE 802 standard [40]. ZigBee is built upon IEEE 802.15.4 standard, defines the network layer specifications and provides a framework for application programming. Zigbee provides low power connectivity for devices with long battery life. It does not require high data transfer rates like Bluetooth. ZigBee compliant wireless devices have a transmission range of 100 meters depending on the RF environment.

The data rate is 250kbps at 2.4GHz, 40kbps at 915 MHz and 20kbps at 868 MHz. IEEE 802.15.4 concentrates on two lower layers of protocol (physical and data link layers). On the other hand, ZigBee aims to provide the upper layers of the protocol stack (network and application layers) for interoperable data networking, security services and a range of wireless control solutions. IEEE 802.15.4 standard, hence the Zigbee standard, supports mesh, star and cluster tree type of network topologies, as seen in Figure 1.14. (Ergen, 2004) [41].

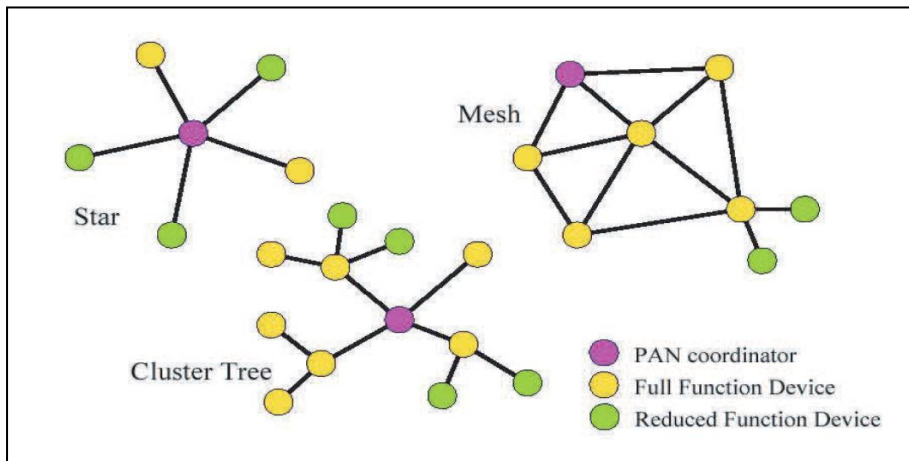


Figure 1.14: Different network topologies specified by ZigBee [41]

The star topology defines the master slave model. The master is a FFD and the end devices can be FFDs or RFDs. In mesh and tree topologies, an FFD can talk to other FFDs within its radio range forming a multi hop network. A mesh network is a true peer-to-peer topology where beacons will not be applied. ZigBee network layer defines 3 device types:

- ZigBee coordinator (ZC). There is only one ZC for every ZigBee network. It has a unique ID and it is responsible for forming the network. After forming the network it acts as a router. It is an FFD managing the whole network.
- ZigBee router (ZR). This provides routing services to network devices. They can send or receive messages. Unlike end devices they don't sleep and they stay on as long as the network is established. It is an FFD with routing capabilities.
- ZigBee End Device (ZED). This corresponds to an IEEE RFD or FFD acting as a simple end device. It is connected to ZC or ZR and does not do any routing. It communicates with the network only through their parent nodes and cannot relay messages intended for other nodes.

1.2.5 Localisation Applications

Indoor localisation systems are becoming very popular in recent years. These systems have led to new techniques in object location detection. For example, location detection of products stored in warehouses, location detection of medical personnel or equipment in a hospital, location detection of firemen in a fire, or finding tagged maintenance tools scattered all over a plant. The main progress in indoor location sensing systems has been made during the last ten years. Therefore, both the research and commercial products in this area are new. Many

people in the academic world and industry are currently involved in its research and development.

There are two main types of location information for localisation applications. These are physical location and estimated location information. Physical location is expressed in the form of coordinates and it identifies a point on a 2-D or 3-D map. Estimated location is expressed again in the form of coordinates but calculated after localisation procedures. There are four different system topologies for positioning systems (Drane et al. 1998) [42].

1. Remote positioning system: transmitter is mobile and several fixed measuring units receive the transmitter's signals. The results from all measuring units are collected, and the location of the transmitter is computed in a master station.
2. Self-positioning system: the measuring unit is mobile. This unit receives the signals from several transmitters in known locations, and has the capability to compute its location based on the measured signals.
3. Indirect remote positioning system: if a wireless data link is provided in a positioning system, it is possible to send the measurement result from a self-positioning measuring unit to a remote site, and this is called indirect remote positioning topology.
4. Indirect self-positioning system: if the measurement result is sent from a remote positioning site to a mobile unit via a wireless data link, this system is called an indirect self-positioning system.

Positioning systems enable location-awareness for mobile computers in widespread and pervasive wireless computing. By utilising location data, location-aware computers can give location-based services for mobile users. Indoor positioning systems based on wireless local area networks have been suggested as a viable solution where the global positioning system does not work well.

Instead of depending on accurate estimations of angles or distances in order to derive the object location with geometry, location-dependent characteristics of received signal strengths can be deployed to determine the object location. The advantage of this technique is that it is simple to utilise with no specialised hardware requirement. Any existing wireless local area network infrastructure can be reused for this kind of positioning system reducing the cost and excessive power consumption.

1.2.5.1 Localisation parameters

The important point in indoor positioning systems is the localisation accuracy. Throughout the literature many algorithms are developed to increase the accuracy of position detection. Due to random propagation behaviour and multi path reflections of RF signals, the localisation accuracies vary between a few centimetres and a few metres. Many hardware platforms are used with related technologies such as infrared, ultrasonic and RF to increase the localisation accuracies. On the other hand, combining these technologies causes an increase in the cost of localisation. Hence, the most important parameters which effect the localisation accuracy can be summarised as cost, power consumption, physical size, localisation time and signal accessibility These are listed in detail as follows :

1. Cost: devices used in localisation must be at manageable prices. Deployment of thousands of them must not introduce a serious financial problem.
2. Power consumption: all the devices must have long operation time. They must have on-board power sources and these power sources can be rapidly changed with new ones.
3. Physical size: the size of the transmitters and receivers must be small enough so that they can be carried for mobile operations. Advancements in electronics and miniaturisation provided small size devices and made localisation procedures easier.
4. Localisation time: unknown position detection must be carried out in the shortest possible time. Localisation procedures should not take a very long time. Advancements in electronics provide the users with required hardware for fast position detection.
5. Signal accessibility: the signals used in localisation must be easily accessible indoors. GPS signals cannot penetrate walls. Infrared and ultrasonic signals are affected and dispersed very quickly by the environmental conditions.

Finally, most suitable localisation techniques use RF signals. RF signal amplitudes are received and processed by cost effective devices. But these signals are affected by environmental factors such as obstacles. However they produce reasonable localisation accuracies indoors and outdoors.

1.3 Research objectives

The main purpose of this thesis is to develop object localisation systems with improved localisation accuracies by using Jennic wireless sensor nodes indoors. The specific research objectives with respect to this main purpose are presented as follows:

1. Study the related literature in detail to identify the previously developed localisation systems.
2. Propose and develop several localisation systems by using existing localisation systems with new approaches to improve the localisation accuracy.
3. Investigate the directional radiation behaviour of wireless sensor nodes and decide which radiation pattern will be used in designing localisation systems.
4. Calculate distances between transmitter and receiver WSNs with respect to measured LQI and RSSI values.
5. Develop enhancement procedures to eliminate outliers to reduce the random behaviour among LQI and RSSI values before any position detection.
6. Investigate weight functions with fingerprint localisation systems and determine the optimum weight function to generate the maximum localisation accuracy in position calculations.
7. Design and develop an object localisation system based on a fingerprint database with k-NN and weighted k-NN algorithms by using RSSI or LQI values.
8. Design and develop a localisation system by using weighted centroid localisation technique (WCL) and introducing bi-sectioning algorithm with RSSI or LQI values.
9. Design and develop a localisation system by using reference anchor nodes across the sensing area and introducing a weighting technique between the object and the reference nodes utilising real and Euclidean distances.
10. Design and develop a localisation system by using triangular sub areas across the sensing area and weighted centroid localisation technique (WCL) with RSSI and LQI values.
11. Design and develop a localisation technique by using environmentally adaptive centroid localisation technique with a weighted STD threshold selection mechanism introduced on received RSSI values.

12. Design and develop a localisation system based on virtual fingerprint database by using physical grid points and virtual grid data points generated with various interpolated distribution functions across the sensing area.
13. Develop a localisation system by utilising static segmentation with feature identification functions across a given sensing area. Static Segments are generated manually with ranges of received RSSI values within the fingerprint database. Localisation procedures are applied only across the object segment.
14. Develop a localisation system by utilising dynamic segmentation with feature identification functions across the sensing area. Dynamic Segments are generated automatically with dynamic ranges of RSSI values within the fingerprint database. Localisation procedures are applied only across the object segment.

1.4 Main contributions of the thesis

The contributions in this thesis cover the areas of object localisation by using Jennic wireless sensor nodes indoors. Initially an extensive literature background is researched and various localisation systems are identified. Localisation accuracy indoors was the most paramount issue throughout this research. It was observed that localisation accuracies vary between 1 metre and several metres for localisation systems using wireless sensor nodes in literature. The results of this literature survey are published in (Koyuncu & Yang, 2010) [26]. Different localisation approaches are proposed in this research and summarised here as follows:

- 1) A fingerprint localisation approach is proposed by using received LQI values from transmitters across the sensing area. Received LQI values are cleaned from outliers and filtered out for localisation calculations. Various weight functions are investigated and the weight function which gives the best localisation accuracy is determined. This weight function is utilised throughout the calculations. By using this weight function and the related fingerprint approach, a localisation error of around 0.8 meters is obtained. This approach is published in (Koyuncu & Yang, 2011) [43].
- 2) A numerical technique named bi-sectioning algorithm is developed with received LQI values to determine the object distances to wireless transmitters across the sensing area. Initially, LQI values are plotted against the distances between transmitters and receivers. Curve fitting is applied on these plots and LQI values versus distance calibration curves are generated. Object distances to transmitters are

calculated by using these calibration curves with the assistance of bi-sectioning algorithm during localisation procedures throughout the study. This technique is published in (Koyuncu & Yang, 2011) [44].

- 3) A weighted centroid localisation (WCL) approach is proposed using triangular sub areas across the sensing area indoors. LQI values, received from transmitters, at the object location are averaged out respectively. The average LQI value corresponding to each transmitter is used. Distances between the object and transmitter nodes are calculated by using bi-sectioning algorithm and best fit calibration curves. WCL is applied and (x,y) object coordinates are calculated by using trigonometric techniques for each triangular sub area. Final object coordinates are estimated by averaging all the calculated (x,y) coordinates. The proposed system offers an average localisation error of around 1 metre. This approach is published in (Koyuncu & Yang, 2011) [44].
- 4) An adaptive centroid localisation approach is proposed by using the WCL method. RSSI values received at object location are environmentally selected within certain boundaries defined by a range of STD values around the RSSI mean value. A second level adaptive localisation approach is introduced within the selected RSSI values in the first selection. A new range of RSSI values are selected by using a range of new STD values around a new RSSI mean value. Localisation procedures are applied after both stages of RSSI selection. As a result, environmental factors are introduced adaptively and proposed localisation approach generates average localisation errors of around 0.9 meters (Koyuncu & Yang, 2014) [45].
- 5) A reference anchor node approach is proposed by introducing wireless sensor nodes at known locations across the sensing area. The large number of reference nodes employed in the literature is reduced to a few nodes in this study and a new algorithm is introduced to improve the localisation accuracy. 3 nearest reference nodes and 3 closest reference nodes to nearest reference nodes are determined by using a 3-NN algorithm. Weights are utilised with respect to real distances and Euclidean distances between these reference nodes. Triangulation techniques are deployed to determine the object coordinates. The proposed system offers localisation errors of around 0.4 meters. This approach is published in (Koyuncu & Yang, 2012) [46].
- 6) A virtual fingerprint localisation approach is proposed using a virtual fingerprint database across the sensing area. Standard fingerprint localisation technique is time consuming during fingerprint preparation in off-line phase. Furthermore, the effect of

thinly distributed grid points reduces the position detection accuracy during localisation. Hence, the fingerprint database is organised into a finer database by introducing virtual grid points between physical grid points. Virtual data is generated by using various distribution functions, such as linear and exponential, among the virtual grid points. The proposed system offers localisation errors of around 1.2m less than a grid space of 4m across the sensing area. This approach is published in (Koyuncu & Yang, 2013) [47, 48].

- 7) A segmentation approach across the sensing area is introduced to reduce the search efforts for the objects. If the sensing area is large or has a non-uniform topology, the object search can be quite time consuming. In order to avoid these difficulties, the sensing area is sub divided into a number of sub areas, identified as segments, according to the area topology. Initially, the sensing area is divided manually into segments and this is identified as static segmentation. A feature function is realised by using RSSI ranges received across each static segment. Object RSSI measurements for each transmitter are compared with feature functions of all the segments. A segment whose feature function includes the object RSSI measurements is identified as an object segment and it is utilised in localisation procedures. k-NN and weighted k-NN algorithms are employed only in object segments to determine the object locations. The proposed system offers minimum localisation errors of around 1.2m where the grid space is 2m. This approach is published in (Koyuncu & Yang, 2013) [49].
- 8) A dynamic segmentation approach is introduced by determining the segments automatically across the sensing area. An overall standard deviation, (STD), of RSSI values from each transmitter is determined across the test area. A grid point on the test area boundary is selected as the reference grid point to generate dynamic segments. A Range of $\text{RSSI} \pm \text{overall STD}$ is deployed with RSSI values at that grid point for each transmitter. These ranges identify the feature function of the segment with the selected grid point. RSSI values of all the other fingerprint points are checked to see whether they are included in the feature function or not. The first segment is determined by fingerprint points whose RSSI values are included in its feature function. The same procedures are repeated and other neighbourhood segments are determined across the test area. Object RSSI values are checked with all the segment feature functions to determine the object segment. k-NN and weighted k-NN algorithms are applied to estimate the object location in the object

segment. This proposed dynamic segmentation approach offers localisation errors of around 0.9m with a grid space of 2m. This approach is published in (Koyuncu & Yang, 2013) [49].

1.5 Thesis Layout

The thesis consists of 9 chapters organised as follows:

In Chapter 1, an introduction and an historical background of the research is presented. Research objectives and the main contributions of the thesis are explained in detail. A layout plan of the thesis is given here. General information about wireless sensor networks and wireless sensor nodes are presented. Sensor architecture is defined together with IEEE 802.15.4 and ZigBee network standards. Localisation parameters are illustrated in detail. Localisation applications are given in general terms.

In Chapter 2, Brief information about object localisation techniques which inspired this research is presented. An extensive literature survey is carried out and various important localisation techniques such as triangulation, trilateration, TOA, TDOA, AOA are summarised. Localisation design considerations are overviewed and efficient localisation parameters are analysed. Different localisation concepts using wireless sensor nodes and their operational schemes in literature are investigated in great detail. These concepts and their applications together with their background information are presented to obtain efficient positioning.

In Chapter 3, a theoretical background of RSSI and LQI values is presented. Radiation beam patterns of experimental RFID devices are illustrated. Outlier removal and bi-sectioning algorithms are introduced. Propagation losses of RF signals are mentioned and ITU-R propagation model is introduced. Fingerprint based localisation approach is implemented by using LQI values. A comparative study of empirical weight functions in fingerprint localisation is carried out. The best empirical weight function for the best positioning accuracy is determined. k-NN nearest neighbourhood algorithm and weighted k-NN algorithm are utilised to estimate the object locations.

In Chapter 4, an environmentally adaptive Centroid Localisation approach, is introduced with 2 level adaptive localisation, which are static environmental threshold factors and most stable coordinate system with minimum RSS variations. Distances between object and transmitter nodes are calculated by using bi-sectioning algorithm with RSSI versus distance calibration curves. These distances are deployed with WCL technique to localise the objects.

RSSI values are adaptively adjusted to the environment. Their mean and STD values are deployed to create a range of RSSI values. Received RSSI values in \pm STD range of their mean are utilised. A static environmental factor is deployed with utilised RSSI values corresponding to the surrounding concrete walls and adaptive centroid algorithm is applied.

In Chapter 5, a triangulation approach across the sensing area using the Weighted Centroid Localisation technique is proposed. The sensing area is sub divided into triangular sections. WCL technique is applied for each triangle area by using the distance values between object and triangle corners to determine the object location. The final object location is determined by averaging the object locations calculated for each triangle.

In Chapter 6, a reference anchor node based localisation system is proposed with a new weight mechanism between transmitters and receivers. Weights are related to environmental conditions. Several reference nodes across the sensing area are utilised to calculate 3 nearest reference anchor nodes to object location by using a 3-NN algorithm. Furthermore, 3 Closest reference nodes to each previous nearest reference anchor node are selected and estimated object coordinates are recalculated. Weights are utilised with respect to real and Euclidean distances. Object distances to these nearest reference nodes are defined by using Euclidean distances and weights. A triangulation technique is deployed to determine the object coordinates.

In Chapter 7, a virtual fingerprint localisation approach is proposed. A physical fingerprint database is sub divided into a finer database by deploying linear and exponential distribution functions. These distribution functions are organised with respect to RF signal radiation directions of transmitters. The grid space across the sensing area is divided into a finite number of virtual sub spaces. Virtual grid points are generated corresponding to these sub spaces. Virtual RSSI values are calculated at these virtual grid points with respect to several linear and exponential interpolation functions. Once the new fingerprint database is constructed by using real and virtual RSSI values, localisation algorithms are deployed to calculate the object locations across the sensing area.

In Chapter 8, a segmentation localisation approach is proposed across the sensing area. Objects are searched across the specific sub areas to narrow the localisation time and effort. Two kinds of segmentation are utilised which are identified as Static and Dynamic segmentation. The theory of segment feature functions is presented. The test area is divided into sub areas, called segments, by using static and dynamic methods. A feature function is

developed for each segment. Object RSSI values are checked with feature functions of all the segments. In case of any inclusion, fingerprint localisation is carried out only within that segment.

In Chapter 9, a summary of the thesis is presented. Demonstrations of how the objectives have been achieved are illustrated. Finally, proposals for development of further research are given for the reader.

CHAPTER 2

LOCALISATION SYSTEMS

2.1 Background

In wireless sensor node applications, location sensing is one of the most important and best studied area to determine an object's locations indoors. Their power consumption aspects, long distance coverage and being immune to environmental effects make these wireless sensor nodes, (WSN), very popular among localisation devices. Localisation techniques with WSNs utilise RF signals and signal attenuation [50], takes place as the Electro-Magnetic (EM) waves travel in space [2, 51].

RSSI and LQI values are very widely used parameters to express this RF signal attenuation in order to determine the object location. Various algorithms are employed with these signal strength values to calculate the object positions. The time covered by RF signals between the transmitters and receivers is also deployed as a parameter to calculate the object location.

If ultrasound technology is used [52], time of arrival, (TOA) or time difference of arrival, (TDOA) techniques of Ultrasonic waves are utilised to localise the unknown object position. This can even be extended to the audible sound range. Another technique is based on a ranging feature which distinguishes between range free [53], and range based localisation techniques, [54]. Finally it is also possible to employ centroid [55], and distributed localisation systems, [56].

Although RSSI techniques generally perform poorly in the indoor environment without a careful area-specific training phase, the localisation accuracies can be improved by using filtering and various algorithmic methods. But it is still the cheapest solution for coarse-grain localisation. Positioning systems enable context aware computing with location awareness, [57]. In the last couple of years, location fingerprinting techniques using existing local area networks and WLAN infrastructures are widely utilised for indoor areas. Fingerprinting technique is relatively simple to deploy compared to other techniques such as angle of arrival (AOA), [58] and (TOA), [59].

In this chapter, various topics in localisation system design are overviewed. Well known basic localisation techniques are explained. Range free and range based localisations together with WSN localisation are covered and presented for the reader's attention.

2.2 Localisation Design Considerations

Localisation and positioning techniques are still being developed. Many methods and algorithms are deployed to achieve higher accuracies. In this chapter, the various issues in localisation system design which are considered in this study are presented. Designing an efficient localisation system with WSNs depends on many factors. These factors must be properly considered during the design of the localisation system. They are summarised as follows:

- a) WSNs are operated with onboard power supplies with a limited operational life. Processing, communication and sensing operations are carried out by these nodes and their operational lifetime is reduced. Hence their operational time must be indexed to their detection procedures. They should be idle when they are not detecting.
- b) WSNs are deployed in large numbers across the sensing areas. Localisation accuracies are indexed to these numbers. A larger number of nodes gives a better detection resolution. Hence these nodes must be inexpensive and easy to deploy.
- c) Cost is an important factor while deploying WSNs. The density of WSNs must be carefully thought out from cost point of view. An optimum number of WSNs must be chosen to obtain the minimum interference with each other and maximum accuracy with respect to their total cost.
- d) Localisation accuracy is an important issue for the localisation techniques. The required detection range must be carefully decided and the type of localisation system selected accordingly. Indoor localisation techniques may require accuracy of 1 metre for people while an outdoor localisation technique may have an accuracy of 5-10 metres for, say, containers in a dock yard.
- e) Environmental factors are the most important factors for any localisation technique. Various obstacles along the path of RF signals would create multiple reflections, signal interference and attenuations. These can generate false readings of RSS values during measurements. This situation in return will reduce the localisation accuracies. Many algorithms are developed to reduce the effects of these environmental factors.

- f) Signal interference between the nodes in the same network is a serious problem. It results from collisions between transmitted signal packets among the nodes. This reduces the quality of RSS reception and in return causes inaccuracies during localisation. Hence this interference problem must be reduced to an optimum level to achieve higher accuracies.
- g) Duration of signal transmission and reception between the nodes is an important constraint. Short signal packets must be used between the nodes so that battery range is extended and the cost of operational procedures is reduced.

2.3 Localisation techniques

There are many localisation systems which are designed and developed in literature. Different localisation techniques are deployed in these systems. Localisation technique is identified as the methodology which can be used to determine the final position of the unknown object. These localisation techniques can be distinguished as triangulation, trilateration, (TOA), (TDOA) and fingerprinting.

2.3.1 Triangulation

The triangulation technique [60], is the process of determining the location of an unknown point by measuring the angles to it from two known points at both ends of a fixed baseline. It utilises the trigonometric relationship between line segments and angles. The locations of two transmitters and angular directions of an unknown object from these transmitters are known. By using these two angles and the distance between the transmitters, the location of the object with respect to transmitters can be obtained as seen in Figure 2.1.

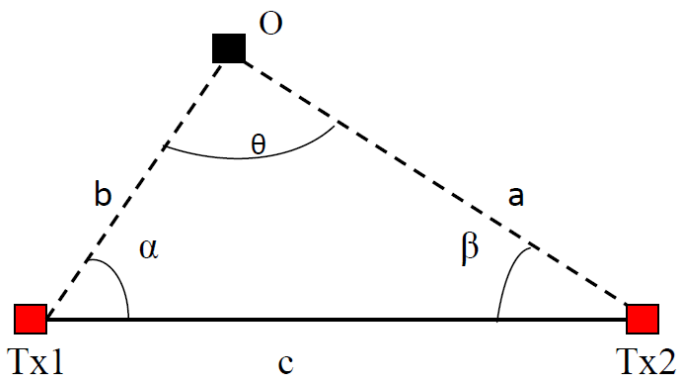


Figure 2.1: Triangulation technique; Tx1, Tx2 are transmitters, O is object, α , β and c are known parameters; a and b are unknown parameters

Triangulation equations can be expressed as;

$$\theta = \pi - (\alpha + \beta) \quad (2.1)$$

$$c = b \cos \alpha + a \cos \beta \quad (2.2)$$

$$c^2 = a^2 + b^2 - 2ab \cos \theta \quad (2.3)$$

Unknown distances a and b to transmitters from object O can be determined as;

$$a = \frac{c}{\cos \beta + \frac{\sin \beta}{\tan \alpha}} \quad \text{and} \quad b = \frac{c}{\cos \alpha + \frac{\sin \alpha}{\tan \beta}}$$

2.3.2 Trilateration

The trilateration technique [61], determines the absolute location of object points by using the geometry of spheres or circles. In 2D space the unknown object location is determined by using the distance measurements from 3 non-collinear points as shown in Figure 2.2. If the distances, radius1, radius 2 and radius 3, between the transmitter nodes and a receiver node are known, the intersection point of the circles with these radiuses defines the (x, y) coordinates of the object point X.

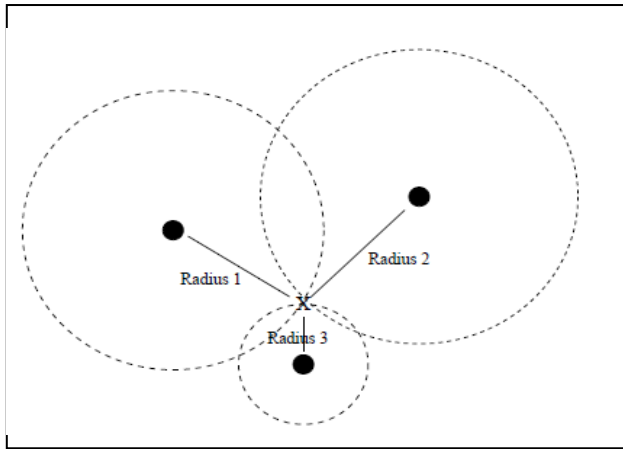


Figure 2.2: 2D trilateration technique

In 3D space, unknown object point, (x, y, z), is at the intersection of 3 sphere surfaces. Three spheres with centre points P_1, P_2, P_3 and radiuses r_1, r_2, r_3 are sufficient to determine the x, y, z unknown coordinates as seen in Figure 2.3. Equations of 3 sphere surfaces can be written as;

$$r_1^2 = x^2 + y^2 + z^2 \quad (2.4)$$

$$r_2^2 = (x - d)^2 + y^2 + z^2 \quad (2.5)$$

$$r_3^2 = (x - i)^2 + (y - j)^2 + z^2 \quad (2.6)$$

Formulation is such that centres of the spheres are on the $z=0$ plane, one centre is at the origin and another on the x axis.

By using these equations; an object point located at x,y,z coordinates which is the intersection point of 3 spheres and satisfies all three surface equations can be calculated as :

$$x = \frac{1}{2d} (r_1^2 - r_2^2 + d^2) \quad (2.7)$$

$$y = \frac{1}{2j} (r_1^2 - r_3^2 - x^2 + (x - i)^2 + j^2) \quad (2.8)$$

$$z = \pm (r_1^2 - x^2 - y^2)^{1/2} \quad (2.9)$$

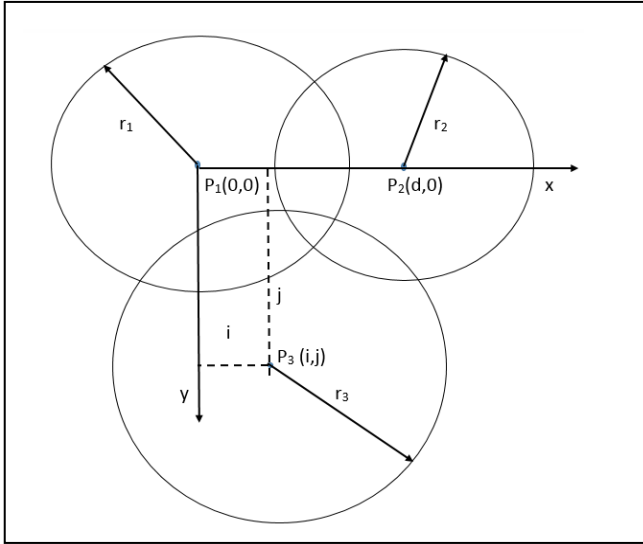


Figure 2.3: 3D Trilateration geometry

2.3.3 Time of Arrival (TOA)

TOA localisation technique uses signal transmission time and the signal arrival time [59] between receiver node and transmitter node. See Figure 2.4. The propagation time can be directly converted into distance by using the signal propagation speed. Different types of signals can be used such as RF and ultrasound. Due to the very high speed of radio signals and the resulting very short time intervals, TOA method is used mostly with ultrasonic systems.

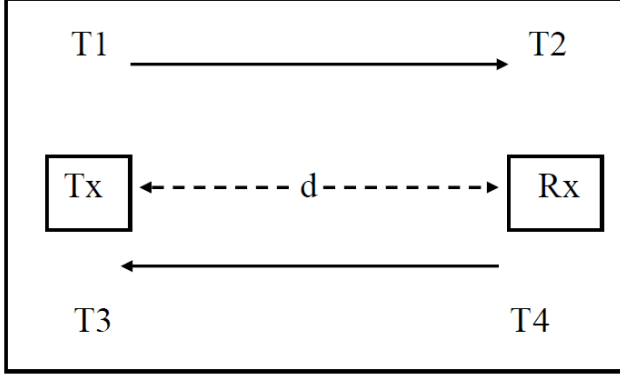


Figure 2.4: TOA technique

Assume, T_1 , T_4 are transmit times and T_2 , T_3 are receive times between transmitter T_x and receiver R_x . If the speed of the propagating signal is “ c ”, then the average distance d between the transmitter and the receiver is defined as

$$d = \frac{1}{2}[(T_3 - T_4) \cdot c + (T_2 - T_1) \cdot c] \quad (2.10)$$

Traditional TOA based systems either use synchronised clocks such as GPS [62], or uses the echoing method [63], where a node measures the round trip time of a signal transmitted to a remote node. TOA localisation has TOA measurements from 3 transmitter nodes. Trilateration is used later to determine the object’s position.

2.3.4 Time difference of Arrival (TDOA)

This technique calculates the distance based on two different signals with different speeds such as RF and ultrasound signals [11, 64]. The distance “ d ” between the transmitter and receiver node can be found by measuring the difference between the transmitting and receiving times as seen in Figure 2.5.

Distance d can be determined by the following equation.

$$d = [(T_4 - T_2) - (T_3 - T_1)] \cdot \left(\frac{v_{RF} \cdot v_{ULT}}{v_{RF} - v_{ULT}} \right) \quad (2.11)$$

where T_1 and T_3 are the transmitting times of RF and ultrasound signals, T_2 and T_4 are the reception times of the same signals. v_{RF} and v_{ULT} are the velocities of the RF and ultrasonic signals. A disadvantage of these TOA and TDOA techniques is the requirement of synchronisation between receivers and transmitters. This is difficult and costly.

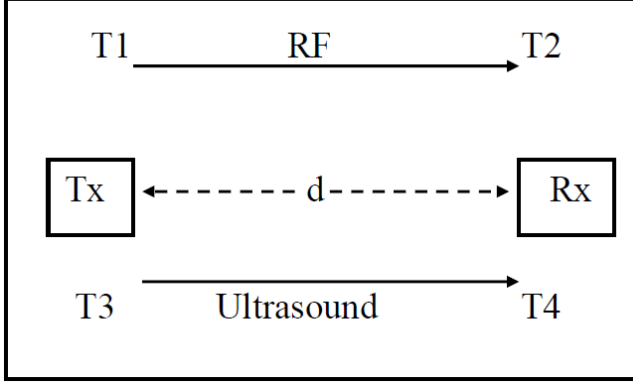


Figure 2.5: TDOA technique

2.3.5 Angle of Arrival (AOA)

Angle of arrival (AOA) on a 2D plane is defined as the angle between the propagation direction of an incident wave and some reference direction (Peng and Sichitiu, 2006) [65]. This angle is represented as degrees in a clockwise direction from the north. When the reference direction is 0° or pointing north, AOA is absolute, otherwise relative. Beacon nodes have omnidirectional antennas and unknown beacon x is capable of detecting the angles of incoming signals. The angle between reference direction 0° North and B_1B_2 line is a known angle $\Delta\theta$. As seen in Figure 2.6(a), angles $\theta_1 + \Delta\theta$ and $\theta_2 + \Delta\theta$ which are measured at x location, are the relative AOAs of the signals sent from beacons B_1 and B_2 . Hence angles $\angle xB_2B_1$ and $\angle xB_1B_2$ can be calculated and the unknown x location can be determined by using the triangulation technique as shown in Section 2.3.1.

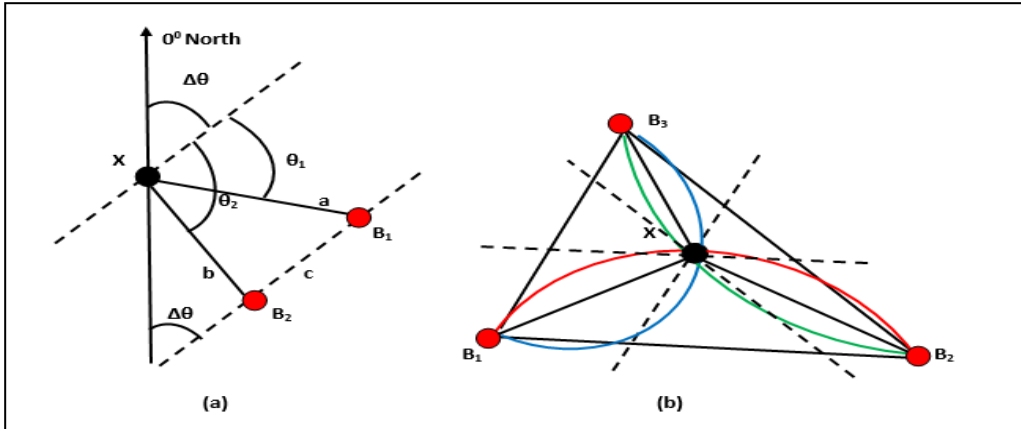


Figure 2.6: AOA localisation a) Localisation with $\Delta\theta$ orientation information b) localisation without $\Delta\theta$ orientation information [65].

When $\Delta\theta$ orientation of the unknown x is not available and the absolute AOAs cannot be obtained, AOA differences can be used instead. In Figure 2.6(b), angles $\angle B_1xB_2$, $\angle B_1xB_3$,

$\angle B_2 x B_3$ can be computed using the knowledge of relative AOAs. If two points and the chord joining them are known, a third point x from which the chord subtends a fixed angle is constrained on a circular arc as shown in Figure 2.6(b). For example, angle $\angle x B_2 B_1$ and the chord $B_1 B_2$ restrict x 's position on the arc passing through B_1 , x and B_2 . Since each chord determines one arc, the location of an unknown x is at the intersection of all arcs when three beacons are available.

2.3.6 Fingerprint

Fingerprint localisation technique utilises radio signal propagation and received signal strengths [2, 66] across a grid space. Empirical radio propagation models are used to convert the radio signal strength into distances between the transmitters and receivers. Since the signal strength changes in dynamic environments due to fading and interference, an alternative approach to estimating the object's position is employed, using RF signal strengths. Amplitudes of radio signals, radiating from transmitters, are recorded by a receiver at every grid point and stored as a database with respect to their locations. See Figure 2.7. This database is called a fingerprint database. A localisation technique which utilises this database is called fingerprint localisation.

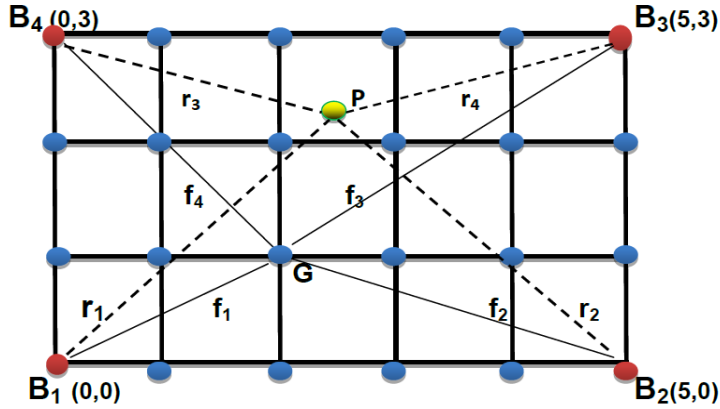


Figure 2.7: Grid space for fingerprint database. B_i : transmitters, G : grid point, P : object receiver.

In Figure 2.7, a signal vector is generated at every grid location, G , by using received radio signal strength amplitudes from the transmitters and this vector is defined as $F = \{ f_i \}$ where $i = (1, 2, 3, 4)$. An object receiver position P can be estimated by acquiring a signal vector, $P = \{ r_i \}$, where $i = (1, 2, 3, 4)$.

This signal vector is compared with known F vectors across the grid area. Fingerprinting technique can be utilised in two phases. First, in offline phase, location fingerprints are collected by performing a site survey of the received signal strengths (RSS) at grid points.

Secondly, in on-line phase, the object receiver will also sample a vector of RSS values from the transmitters and the object location is calculated by using software techniques.

A software algorithm computes the Euclidean distances between the sampled object RSS vector and each grid location fingerprint vector in the database. The coordinates associated with the fingerprint vector that provides the smallest Euclidean distance is returned as the estimate of the object position. Location accuracy is reported as the minimum distance between the real and estimated object points.

2.4 Localisation Systems:

Various localisation systems are presented in chapter 1 together with their tabulated comparisons. An overview of the localisation problem and experimental results will be provided here. The localisation problem is defined as the process of finding the current position of the objects within a specific region. Localisation using radio signals attracted attention in telecommunication and navigation. The most well known positioning system is the global positioning system (GPS) (Kaplan, 2005) [67], is a satellite based outdoor localisation system. Satellite signals are unable to penetrate buildings which make them useless indoors.

Indoor radio signal propagation is site specific and exhibits multipath effects. It has low probability of line-of-site signal propagation between the transmitter and receiver (Pahlavan & Levesque, 2005) [68]. This makes accurate indoor localisation very challenging.

For indoor localisation a number of wireless technologies are proposed such as infrared (Want et al. 1992) [6], ultrasound (Priyantha et al. 2000) [52], Wi-Fi (Bahl & Padmanabhan, 2000) [2]; (Youssef & Agrawala, 2005) [69]; UltrawideBand (UWB) (Ingram et al. 2004) [70], and more recently RFIDs (Hightower et al. 2000) [8]; (Sansanayuth et al. 2013) [71]; (Bekkali et al. 2007) [72]; (Yamano et al. 2004) [73].

Localisation techniques, in general, deploy metrics of received radio signals. The most popular received signal metrics are based on time of arrival (TOA), time difference of arrival (TDOA), angle of arrival (AOA) and received signal strength (RSS) measurements. These signal metrics are then processed by localisation algorithms to estimate the object position.

The accuracy of signal characteristics and complexity of the algorithms define the accuracy of the estimated location. Three major localisation areas can be identified depending on how the signal metrics are utilised by localisation algorithms. (Hightower & Borriello, 2001) [14]. These areas are *triangulation*, *scene analysis* and *proximity*.

- *Triangulation method:* is based on geometric properties of a triangle to estimate the object receiver position. Depending on the type of radio signal measurements, triangulation can be further sub divided into multilateration and angulation methods. In multilateration techniques, TOA, TDOA or RSS measurements from multiple wireless nodes are converted to distance estimations. In angulation techniques, AOA measurements with the help of specific antenna designs are used to determine the receiver position.
- *Scene analysis technique:* requires an offline phase to learn RSS behaviour at a specific area. This information is then stored in a database called radio map. During the online phase the receiver's unknown location is decided based on the similarity between the radio map and real time RSS measurements. Radar (Bahl & Padmanabhan, 2000) [2], Horus (Youssef and Agrawala, 2005) [69] and Compass (King et al. 2006) [74] are examples of this technique.
- *Proximity technique:* is based on detection of objects with known location. This can be done by sensors such as touch mouse (Hinckley & Sinclair, 1999) [75] or systems based on topology such as active badge location system (Want et al. 1992) [6]. The technique suffers from limited accuracy.

Location awareness is an essential service for many wireless computing scenarios. Many applications integrate location information to increase context knowledge. Widespread computing environments have specific characteristics which limit the approaches in location awareness. Processor performance and the available energy are also limited. Hence, requirements for localisation devices and the infrastructure are minimised to allow a large range of positioning scenarios.

Localisation approaches can be classified into those that are based on coordinates and those that are coordinate free (Schuhmann et al. 2008) [76], as seen in Figure 2.8. Coordinate free schemes presented by (Fekete et al. 2005) [77], focus on an abstract system of location awareness. They rely on dense sensor networks to achieve adequate accuracy and they are not cost effective. Coordinate based localisation approaches, on the other hand, are used more frequently to determine the final object coordinates across the sensing areas. These are further divided into range free and range based localisation schemes. Range-free schemes comprise of implicit distance measurements. Range based schemes use explicit distances for localisation.

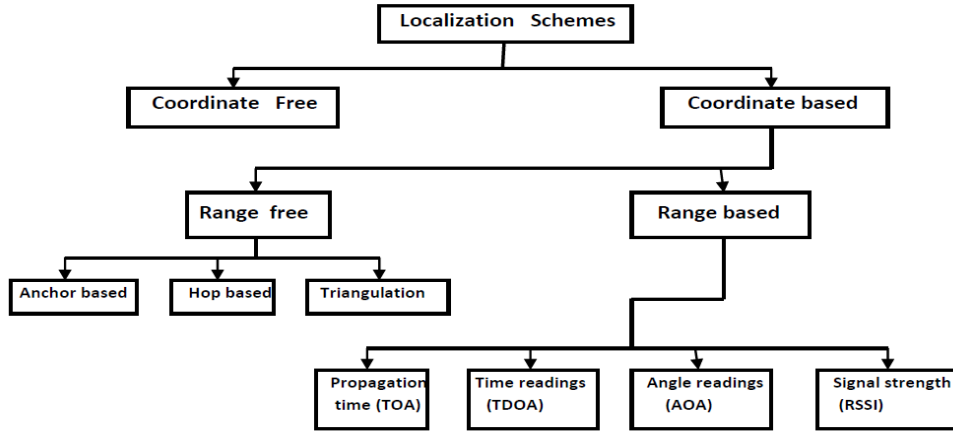


Figure 2.8: Classification of localisation schemes [76]

2.4.1 Range free localisation

Regarding range-free schemes there exist 3 main approaches:

a) Anchor based Approach:

This approach uses anchor beacons which contain 2 dimensional location information (x_i, y_i) to estimate the node positions. A node estimates its position by using special algorithms. The scheme is proposed by (Pandey et al. 2006) [78], based on the current access point (AP) capability of transmitting at different power levels. Hence a unique set of messages transmitted by various APs can be received at every location in the system. The object node is expected to transmit back the received messages to the AP which it is associated with. The location of the object is then estimated using the set of messages received from the object.

Another anchor based approach is centroid localisation, (CL), proposed by (Bulusu et al. 2000) [53]. In this approach, the unknown object calculates its position as the centroid of the coordinates of the beacon nodes where the transmissions are received from. CL only performs the averaging of beacon coordinates to localise the object, while weighted centroid localisation (WCL) uses weights to ensure improved localisation.

b) Hop based Approach :

In this type of localisation scheme, the object position is calculated based on hop distance to other nodes. As explained by (Niculesco & Nath, 2003) [79]. This scheme delivers an approximate position for all the nodes in networks where only a small number of nodes have self positioning capability. All nodes in the network, including other anchors, get the shortest

distance in hops to every anchor. This approach only works well in dense networks. It relies on flooding of messages which produces high communication overhead which is undesirable.

c) Area based approach:

Area based schemes perform location estimation by isolating the environment into triangular regions between beacon nodes as shown by (He et al. 2005) [80] and (Elnahrawy et al. 2004) [81]. The presence inside or outside of these triangular regions allows a node to narrow down the area in which it can reside.

Area based approaches normally perform particularly well in heterogeneous networks where there is a high node density. This approach is not suitable due to utilisation of a large number of nodes and the high total cost.

2.4.2 Range based localisation

Range-based schemes are subdivided into the following 3 approaches:

a) Signal propagation time localisation:

This is a time of arrival (TOA) technology and it is used as a means of obtaining range information through signal propagation time. This application is deployed by satellite navigation systems as defined by (Parkinson & Spilker, 1996) [82]. Although this approach guarantees high precision and can be globally used, it has various drawbacks such as it can only be used outdoors, it needs expensive hardware and consumes too much energy. Hence it is an inconvenient system in many situations.

b) Signal propagation time difference and arrival angle localisation:

This technology is based on measurements of time difference of arrival, [64] or the angle of arrival, [79]. TDOA estimates the distance between two communicating nodes and this is called ranging.

AOA allows nodes to estimate and map relative angles between neighbours. TDOA and AOA also utilise expensive and energy consuming hardware hence these approaches are also unsuitable for widespread usages.

c) Signal strength localisation :

This approach uses received signal strength indicator (RSSI) values of incoming transmitter beacon signals. Unlike TOA, TDOA and AOA techniques, RSSIs can be obtained reasonably cheaply by using low priced commercial hardware. RSSI techniques use theoretical and empirical models to translate the signal strength into distance estimates. Each point is mapped

to a signal strength vector, (Bahl & Padmanabhan, 2000) [2], or to a signal strength probability distribution (Youssef et al. 2003) [83] across the test areas.

This technology suffers from signal interference and multipath fading which make the range estimates inaccurate. Furthermore signal strength based approaches require special hardware such as infrared badges, cameras, tag transmitters, and readers.

Many approaches use location fingerprinting for localisation in wireless sensor networks. Two examples are given by (Youssef et al. 2003) [83] and (Bahl & Padmanabhan, 2000) [2]. This technique consists of an offline training phase and an online positioning phase. This approach needs the preconditioning of a training database for different environments.

2.4.3 Wireless sensor node localisation:

There have been great advances in wireless communication and mobile computing over the years. Radio frequency identification devices (RFID) are utilised as wireless sensor nodes for localisation purposes. They were initially developed as an automatic identification system consisting of readers, tags and servers (Want, 2006) [84].

RFID devices can be divided into two classes, active and passive. Active tags have a power source on them. Passive tags don't have any power source on them; they just back scatter the carrier signal received from the reader. Key benefits of RFIDs are their low cost and no line of sight requirement. Fast reading of multiple tags inspired the industry to develop many applications in retail, healthcare, people tracking etc. (Baudin, 2005) [85].

Applying RFID for indoor localisation is one of the main active research areas which is also utilised in this study. RFID positioning systems can be broadly divided into two groups: tag and reader localisation depending on the RFID device on the object. In tag localisation schemes, tags are deployed as reference points and localisation technique is applied to estimate the location of a tag. SpotON (Hightower et al. 2000) [8], uses RSS measurements to estimate the distance between an object tag and three readers and applies trilateration on the estimated distances. LANDMARC (Ni et al. 2003) [71] uses a scene analysis approach by using readers with different power levels and fixed location reference point tags. Readers vary their read range for all reference tags and for the object tag, k nearest reference tags are then selected and their positions are averaged out to estimate the object position.

In (Stelzer et al. 2004) [86], reference tags are synchronised with the readers. Then TDOA principles and TOA measurements relative to reference tags and the object tag are used to estimate the location of the object tag. In (Bekkali et al. 2007) [72], RSS measurements from

the reference tags are collected and a probabilistic radio map of the area is generated. Then localisation techniques are applied to estimate the object's location.

In (Lee & Lee, 2006) [87], passive tags are arranged on the floor at known positions in a square pattern. The reader receives all readable tag locations and orientations and estimates the object position by using a weighted averaging method. In (Han et al. 2007) [88], tags are arranged in a triangular pattern so that the distance in the x-direction is reduced. Estimation error is reduced from that in the square pattern.

Finally, a Bayesian approach is also proposed by (Xu & Gang, 2006) [89], to predict the position of a moving object. Using object movement probability and detected tags' locations, the reader location is determined by maximising the probability. Then the reader position is calculated by averaging the defined positions from all the tags.

2.5 Summary:

The aim of this chapter is to present today's technologies utilised in localisation techniques. Designing and implementing a localisation system is quite challenging considering the changing indoor conditions such as people's movement, interference of electronic devices, furniture alterations and the cost factor. There is no perfect localisation approach which produces the exact position of the unknown object. In this chapter, a schematical overview of the general localisation techniques is given in Figure 2.8.

The increasing demand for intelligent location-aware services in indoor spaces has generated many systems with time efficient localisation and low deployment cost. Some localisation techniques require extra hardware, such as range based and satellite system. This in return increases the cost factor.

Various techniques are used to estimate the position of the objects by using transmission times of RF signals and their signal strengths. The distances of the object from reference points are calculated with these techniques and the actual object position is calculated by using these distances. Different power level transmissions are utilised with reference tags and object tags. k nearest neighbourhood algorithms, (k- NN), are applied to estimate the nearest reference tags to object tag. Large numbers of reference tags produce interference between them and this reduces the estimation accuracy.

Other techniques such as fingerprinting techniques require an offline computation phase to produce an RF signal map across the sensing area. This in return adds extra effort and time to calculations. Some techniques deploy a large number of beacons in the sensing area. This is impractical and increases the cost. Wireless sensor nodes, namely RFIDs, are the most likely

devices which are used in position detection. Transmitter tags and receiver readers can be deployed in any formation across the sensing area and the RSS values received can be transferred to a server for processing.

These RSS measurements are affected by environmental factors and other obstacles across the sensing area. Hence the object position estimation accuracy is reduced. Nevertheless RF based systems are the most favourable systems with reasonable accuracies indoors and outdoors. They are low in cost and efficient in power usage. The future of indoor localisation lies with these RF based systems.

CHAPTER 3

LQI CHARACTERISTICS & FINGERPRINT LOCALISATION

3.1 Background

. Radio signals are based on the radiation of Electromagnetic waves in free space [90]. Signal characteristics of radio signals differ in different environments. Outdoors, it is easy to predict signal propagation behaviour due to large transmission ranges.

Indoors, the situation is different due to closed environmental conditions and the obstacles introduced along the path of the propagation. Due to indoor reflection, refraction, scattering and diffraction [91], indoor transmissions suffer from signal loss and heavy attenuation. The signal variations caused by these factors can be classified in two groups: spatial variations and temporal variations [92].

Spatial variations are generally due to signal fading [93]. Large scale fading is identified as the attenuation of the signal strength as the transmission distances increase. The small scale fading, on the other hand, is generated by the sudden changes in signal amplitudes in short distances or in short times. Multipath fading is the most important small scale fading. It causes temporal variations as well as spatial variations. Due to these signal variations, signal levels must be measured many times to obtain a consistency between them.

Indoor environments typically have many walls and obstacles which are made of different materials. Hence, the radio signals behave differently in these harsh environments and have multipath propagation. Multipath propagations result in the radio waves arriving at different times at their destination [94]. These arrived signals interfere with each other and cause reductions in signal levels. There are two identification features with RF radiation. These quantities are RSSI and LQI values. They are used to identify the transmission of the radio signal packets in space and utilised in localisation technology to determine the object locations.

The aim in this chapter is, initially, to investigate RSSI and LQI values and develop various algorithms such as bisectioning, z-score, k-NN and weighted k-NN which will be utilized throughout the study. Later on, classical fingerprint based localisation approach which is one of the basic localisation techniques in literature is introduced for reference purposes.

Fingerprint method is a preferred localisation solution to find the unknown object locations due to its low cost and the accuracies achieved with it. Fingerprint technique requires a large amount of data collection from a large number of measurement points to achieve reasonable localisation accuracies. There are two important stages in deploying fingerprint localisation. In first stage, identified as off-line phase, received signal strengths will be collected at every measurement point and they will be stored in a database. In the second stage, identified as the on-line phase, the fingerprint of the unknown object point is recorded and this fingerprint is searched for throughout the database.

Various algorithms are introduced to find the nearest measurement points to the object point across the test-bed. Fingerprint based localisation approach is studied in literature by many researchers such as (Bahl et al. 2000) [2], (Lionel et al. 2004) [7], (Kaemarungsi et al. 2004) [66] and (Alippi et al. 2005) [51]. Different algorithms are utilised in these studies and different localisation accuracies are obtained. All these systems require large numbers of measurement points and, as a result, large amounts of received signal strength data.

In this chapter, a fingerprint based approach is presented with localisation accuracies of around 1 metre. k- NN and weighted k- NN algorithms are employed throughout this study. As a main contribution in this chapter, a variety of weight mechanisms in literature is investigated together with the Euclidean distances between object and measurement points. An optimum weight function is determined to generate the best localisation accuracies.

3.2 Received signal strength

Due to complex nature of the radio signal propagation, it is difficult to determine the RSS values in a standard form. RSS distribution by a receiver at one fixed point shows a similarity to Gaussian distribution in the time domain. Signal strength values change with respect to physical surroundings and different time periods (Yin et al. 2005) [95], shows three normalised histograms of signal strength values received at an access point at different times. It can be seen that signal strength values change with time at the same point.

Incoming RSS values are measured by the sensors and these values are related to distances between transmitters and receivers. The transmitter power, (P_{TX}), is directly related to received power, (P_{RX}), at the receiver. According to Friis' free space transmission model [96], Received power can be expressed as in equation (3.1)

$$P_{RX} = P_{TX} \cdot G_{TX} \cdot G_{RX} \left(\frac{\lambda}{4\pi D} \right)^2 \quad (3.1)$$

where P_{TX} = Transmitter power , P_{RX} = Receiver power , G_{TX} = Transmitter gain , G_{RX} = Receiver gain , λ = Wave length , D = Distance between transmitter and receiver.

Received signal strength values are converted into RSSI values differently in different wireless sensor nodes as shown in equation (3.2).

$$RSSI = 10 \cdot \log \frac{P_{RX}}{P_{REF}} \text{ dBm} \quad (3.2)$$

RSSI value is the ratio of received power to a reference power (P_{REF}). Reference power is defined as the absolute value of $P_{REF}=1 \text{ mW}$.

Received power P_{RX} decreases quadratically with the distance D between a transmitter and a receiver. Theoretical plotting of P_{RX} against D is shown in Figure 3.1. RSSI, received by the receiver, increases with the decreasing D distance. The slope of the RSSI curve depends on the environmental conditions during the transmission. The relationship between RSSI and distance D can be generally expressed as:

$$RSSI = A - 20 \cdot \log D \quad (3.3)$$

$$\text{where } A = 10 \log \left[\frac{P_{TX} G_{TX} G_{RX}}{R_{REF}} \left(\frac{\lambda}{4\pi} \right)^2 \right]$$

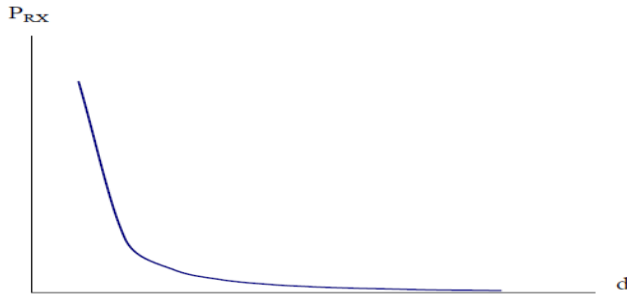


Figure 3.1: Plot of P_{RX} against distance d between a transmitter and a receiver

A desired normalised plot of RSSI values against D distances from equation (3.3) can be presented, as an example, in Figure 3.2.

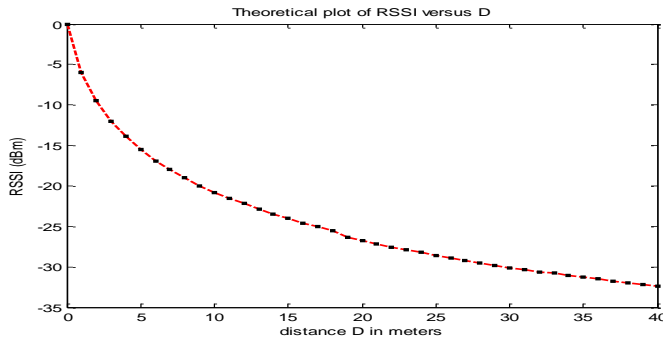


Figure 3.2: Plot of normalised RSSI values against D distances

In practical situations, radio signals are interfered with other surrounding parameters during the propagation and these interference effects reduce the signal quality significantly. Example RSSI values typically measured at a receiver point with respect to distances between a transmitter and a receiver can be seen in Figure 3.3.

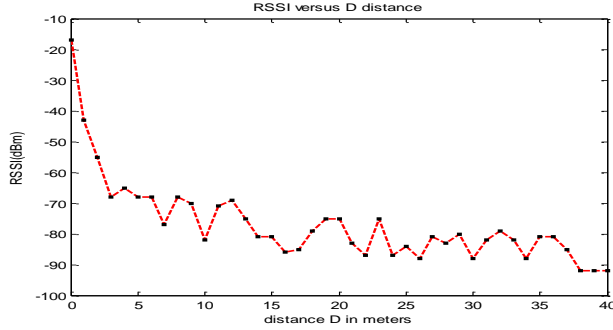


Figure 3.3: Recorded RSSI values against D distances between a transmitter and a receiver

3.3 Link Quality Indicator

During the radio signal transmissions, environmental effects reduce the quality of transmitted signal packets and in return decrease the amplitudes of RSSI values. RSSI is a measure of total energy of the received signal. There is another way to judge the signal quality by considering the signal energy and signal to noise ratio (SNR). Hence Link Quality Indicator (LQI) is introduced to define the quality of signal packets received by the receiver [97]. LQI is obtained by considering both the signal energy and SNR.

LQI represents a number of retransmissions between a transmitter and a receiver to receive one radio packet correctly by the receiver. Transmitter node transmits signal packets continuously in a loop. A receiver node receives these radio signal packets and forwards the LQI values to a server PC. Typical recordings of LQI measurements against distances, performed with four transmitters at the same location and one receiver node, are presented in Figure 3.4.

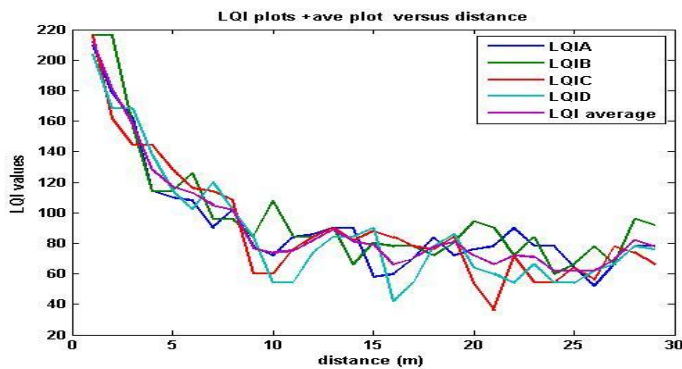


Figure 3.4: Recorded LQI values from L_A , L_B , L_C , L_D transmitters against distance

As it is observed, LQI values of incoming radio signal packets decrease with increasing distances and the resulting plot is always reproducible between any transmitter and receiver pair. Envelope functions of the plots are used to define the mathematical relationships between LQI and d distances. There are random outliers based on sudden signal fluctuations between the transmitters and receivers. These may be caused by the reflections from walls and floors and can be eliminated by using mathematical methods.

According to IEEE802.15.4 standards, LQI is an identification of RF signal strength and the quality of received signal packet [98]. It is proportional to RSSI, signal-to-noise ratio estimation or a combination of both. LQI value is generated whenever a data frame is received based on signal strength. Wireless sensor node determines the signal strength by reading the amount of gain the sensor is using to receive the frame. This gain is later converted into an 8 bit range between 0 and 255 discrete levels identified as LQI. 255 is the highest Link quality value.

The conversion between LQI and RSSI values differs for different wireless sensor nodes. In Jennic WSNs which are used in the measurements, RSSI values in dBm can be directly mapped into LQI values by using equation (3.4) [99].

$$RSSI = (LQI - 305) / 3 \text{ dBm} \quad (3.4)$$

This is valid for LQI values 0 to 255.

3.4 Experimental conditions

In this section, experimental platforms and the data collection procedures in the study are presented. Main features of the sensor devices which are used in the experiments are explained. Their radiation properties are analysed and the radiation beam patterns are displayed with polar graphs. Curve fitting procedures with recorded RSSI or LQI data are carried out to generate calibration curves of data versus distances. Distance calculations are deployed for the given relevant data by using bisection algorithm and calibration curves. Theoretical background of outlier technique is explained and it is applied with received RSS values to eliminate the sudden data variations.

ITU-R indoor propagation loss model is introduced in order to include the environmental effects during distance calculations. Its applications in determining the distances between transmitters and receivers by using RSSI values and empirical environmental loss factors are presented.

3.4.1 Hardware

JENNIC JN5139 type of WSNs are deployed [100], in the experiments. JN5139 transmitters and receivers are low cost and low power consumption wireless sensor devices. They can be used in large topographic areas for wireless localisation. Zigbee Home Sensor demo program [31], is employed to program JN5139 active devices to work as transmitters and receivers respectively. An active transmitter/ receiver pair used in this study is shown in Figure 3.5 and Figure 3.6.



Figure 3.5: Jennic receiver, JN5139 [100]



Figure 3.6: Jennic transmitter, JN5139 [100]

In the experiments, 2 types of JN5139 sensor nodes are employed. One of them is the mobile receiver node identified as the reader. The other one is the transmitter node and identified as the tag. A third one is the reference node. A number of tags are utilised as reference nodes at known positions in some of the experiments. A mobile receiver collects signal packets in the form of LQI values from stationary transmitters and reference nodes. It transfers these LQI values to a PC through a wired connection to calculate the receiver position.

ZigBee protocol [101], which is based on IEEE 802.15.4 standards in 2.4 GHz frequency band is utilised during the communication and data transmission between fixed transmitter and mobile receiver nodes.

Various indoor localisation systems are developed using received signal strengths of Jennic WSNs based on ZigBee standards in this study. The majority of the localisation systems in the literature employs wireless sensor nodes different from Jennics and their system performance evaluation is based on IEEE 802.11 standards for wireless LAN. There is insufficient investigation using ZigBee and IEEE 802.15.4 standards. This standard defines medium access control (MAC) and physical layer (PHY) protocol for low power devices. ZigBee also includes IEEE 802.15.4 standards for MAC and PHY and is suitable for wireless sensor Networks. JENNIC JN5139 wireless sensor nodes with ZigBee standards are utilised in experimental test-beds to localise the unknown object locations.

3.5 RSS measurements

Received Signal Strength measurements are conducted in various test areas including Loughborough University premises. Meeting rooms in the Computer Science department and other offices and halls are engaged at different times for experimentation. Experiments are usually carried out during evenings and weekends to avoid the interference effects of people walking around with RF signal propagation.

Received signal strength values depend on the distances between the transmitters and receivers with longer distances resulting in reduced signal strengths. Since the measurements of received signal strengths are effected by environmental conditions, recordings of signal strengths arriving from transmitters are repeated many times.

Average of signal strengths received from a transmitter at one location is taken as the measured signal strength at that location. These signal strengths can be in RSSI or LQI format depending on the type of WSNs. A typical distribution of measured LQI values against distances between a Jennic type transmitter and a receiver is presented in Figure 3.7.

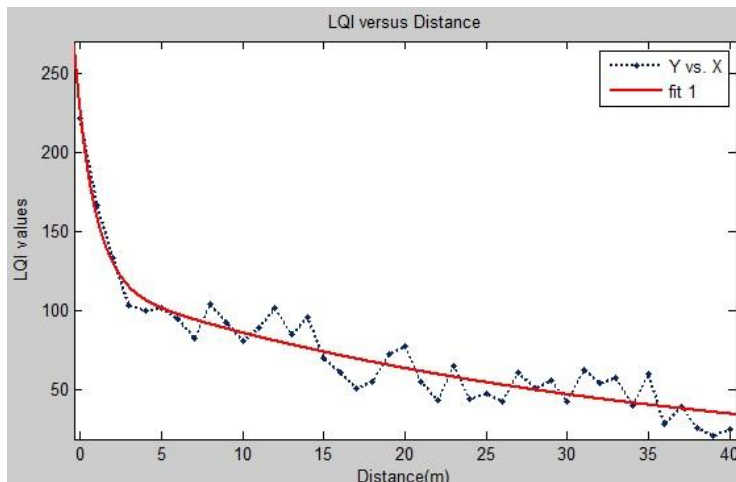


Figure 3.7: Plot of measured LQI values against distances for Jennic type transmitter receiver pair and their exponentially fitted curve

Correlation between these values and d distances can be quantised and formulated with mathematical curves by using curve fitting techniques.

3.5.1 Curve fitting

It can be observed in Figure 3.7 that the distribution of measured LQI values reflects the random behaviour of RF signals. There is a locality of randomness in the recordings. A curve fitting technique is utilised on the plot of received LQI values against d distances. An example exponentially fitted curve on the distribution of LQI values is shown in Figure 3.7.

Fitted curve equation for the received LQI data against distances between 0m and 40m in Figure 3.7 is given by the equation (3.5). This equation is generated by MATLAB with 95% confidence boundaries.

$$LQI(d) = 108.1e^{-0.8276d} + 116.2e^{-0.03035d} \quad (3.5)$$

Fitted curves are considered as the calibration curves between LQI values and **d** distances. They are utilised to determine the unknown **d** distances during experiments by using software techniques. Any LQI value measured during the experiments can easily be fitted in equation (3.5) and corresponding **d** distance can be calculated by using a software technique called a bisectioning algorithm.

3.5.2 Bi-sectioning algorithm

A numerical analysis technique is developed by using a bisectioning algorithm to determine the distances between receivers and transmitters. Bisectioning algorithm is a root finding method in mathematics [102]. The method repeatedly bisects an interval and then selects a subinterval in which a root must lie for further processing. It is also called a binary search method where the range of possible solutions is halved in each iteration [103]. This method is applied if one needs to solve the equation $F(x)$ for a real variable x . A graphical representation of a bisectioning algorithm is shown in Figure 3.8.

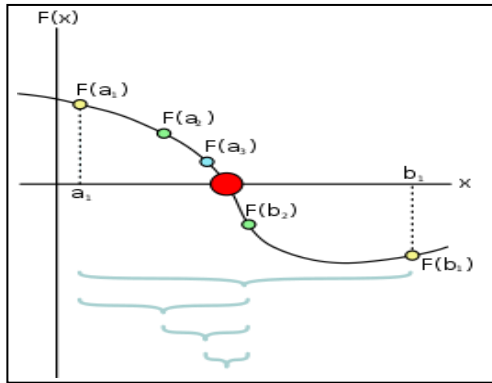


Figure 3.8: Steps of bisectioning method over the range $[a_1, b_1]$ [102]

$F(x)$ is a continuous function which is defined in an interval (a, b) as shown in Figure 3.8. $F(x)$ must have at least one root in the interval (a, b) . At each step, the method divides the interval into 2 by finding the midpoint, $c = (a+b)/2$, and the function $F(c)$ at that point.

There are two possibilities; $F(a)$ and $F(c)$ have opposite signs and bracket a root or $F(c)$ and $F(b)$ have opposite signs and bracket a root. As a result, the method selects the subinterval as a new interval to be used in the next step. The interval is reduced by 50% at each step. The process continues until the interval is sufficiently small.

Fitted curve of $F(x)$ for LQI distribution against x distance will be deployed to determine an unknown x distance for a given LQI value. Y axis displays LQI values. X axis boundaries of fitted curve are a_1 and b_1 . The middle point between a_1 and b_1 is defined by

$$x_{midnew} = \frac{1}{2}[a_1 + b_1] \quad (3.6)$$

x_{midnew} is checked with the following two statements:

$$\text{If } F(a_1) * F(x_{midnew}) < 0 \text{ then } b_1 = x_{midnew} \quad (3.7)$$

$$\text{If } F(a_1) * F(x_{midnew}) > 0 \text{ then } a_1 = x_{midnew} \quad (3.8)$$

Otherwise x_{midnew} is the resultant x value

A criteria is introduced to define the accuracy of x value:

$$\left| \frac{x_{midnew} - x_{midold}}{x_{midnew}} \right| > 0.1 \quad (3.9)$$

Procedures are repeated with correct inequality and new x_{midnew} values.

If equation (3.9) is met then the program checking continues. Otherwise the last x_{midnew} becomes x unknown distance. Program segment for bisectioning algorithm is presented in Figure 3.9.

```
public bool calc()
{
    xMidNew = (xUpper + xLower) / 2; if ((calculate(xLower) * calculate(xMidNew)) < 0)
    {
        xUpper = xMidNew;
    }
    else if ((calculate(xLower) * calculate(xMidNew)) > 0)
    {
        xLower = xMidNew;
    }
    else
    {
        valueX = xMidNew; return true;
    }
    if (iteration > 1)
    {
        if (Math.Abs((xMidNew - xMidOld) / xMidNew) > 0.1)
        {
            xMidOld = xMidNew; iteration++; return false;
        }
        else
        {
            valueX = xMidNew; return true;
        }
    }
    xMidOld = xMidNew; iteration++; return false;
}

public double calculate(double var)
{
    return ((200.1 * Math.Exp(-0.1397 * var)) + (32.54 * Math.Exp(0.0334 * var)) - Temp);
}
```

Figure 3.9: Bisection algorithm used in calculations

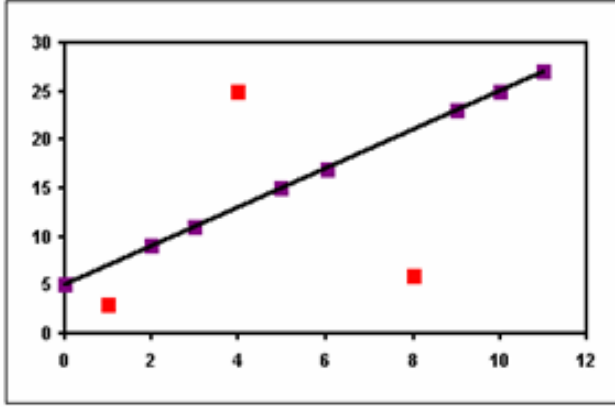


Figure 3.11: Examples of outliers

3.7.1 z-score method

In this method, mean (\bar{x}), and standard deviation (s), of the entire data set (x_i), are used to obtain a z-score, z_i , for each data point as show here;

$$z_i = \frac{(x_i - \bar{x})}{s} \quad (3.10)$$

where

$$s = \sqrt{\frac{1}{n-1} \sum_{i=1}^n (x_i - \bar{x})^2} \quad (3.11)$$

Simple z-score method is not a reliable way of defining outliers due to the fact that both mean and standard deviations are also effected by the outliers. Hence a **modified z-score** test is employed.

In this modified z-score test, z-score is determined based on outlier resistant estimators. “Median of Absolute Deviation”, (MAD), is such an estimator. It is defined as ;

$$MAD = median\{|x_i - x_m|\} \quad (3.12)$$

where x_i is the i^{th} data and x_m is the median of the data. MAD is calculated in place of standard deviation in z-score calculations. Modified z_i is given by (Augusto et al. 2010) [106] in empirical form as,

$$z_i = 0.6745x \left(\frac{x_i - x_m}{MAD} \right) \quad (3.13)$$

For example x_i data where $i=10$ is given in Table 3.1.

x_i	3.5	3.7	3.4	8.4	2.9	3.8	3.1	3.6	9.6	3.6
$ x_i - x_m $	0.1	0.1	0.2	4.8	0.7	0.2	0.5	0.0	6.0	0.0
z_{im}	-0.33	0.33	-0.66	15.9	-2.32	0.66	-1.66	0.0	19.9	0.0

Table 3.1: Examples of random x_i values and calculated z_i values where $i=10$

These random x_i numbers are listed in increasing order. Median number (x_m) is defined by $(i+1)/2 = 5.5^{\text{th}}$ data. Since there are an even number of x_i data, median x_m can be calculated as $x_m = 0.5 * (5^{\text{th}} \text{ data} + 6^{\text{th}} \text{ data}) = 3.6$.

MAD can be calculated by determining $|x_i - x_m|$ values as shown in Table 3.1. They are listed in increasing order and MAD is determined as $(i+1)/2 = 5.5^{\text{th}}$ data. Similarly, MAD becomes $0.5 * (5^{\text{th}} \text{ data} + 6^{\text{th}} \text{ data}) = 0.2$. Hence modified z_i is defined as

$$z_{im} = 0.6745 * \left(\frac{x_i - x_m}{0.2} \right) \quad (3.14)$$

Modified z_i values are also displayed in Table 3.1. Any x_i data greater than $x_m + MAD$ is labelled as an outlier. This x_i value is 3.8 and outliers are 9.6 and 8.4 which are excluded from the data set. Recorded RSSI or LQI values are organised in floating number format and in groups of 10 similar to x_i values and modified z-score outlier technique is applied to check the existence of outliers. Any outliers found are excluded and the rest of the recorded values are utilised for localisation procedures.

3.8 Propagation Path Loss

RF signal propagation is susceptible to environmental effects and the path loss introduced with RSSI and LQI values influences the localisation accuracies. There are different propagation path loss models developed in the literature [108,109]. The most popular RF propagation path loss models are:

- Free space propagation model
- Logarithmic distance path loss model
- Log-normal distribution model
- ITU-R indoor propagation model.

In practical applications, RF propagation loss is different than the theoretical models due to multipaths in the environment. In Log-normal distribution model, path loss is defined as

$$PL(d) = PL(d_0) + 10k \log\left(\frac{d}{d_0}\right) + X_G \quad (3.15)$$

where $PL(d)$ is the propagation path loss (dB) with distance d , k is path attenuation factor, X_G is the factor for random effects of shadowing and $PL(d_0)$ is the propagation loss in free space with $d_0 = 1m$. The most commonly used propagation path loss model is ITU-R indoor propagation model [108]. In this model, path loss with respect to distance is given as:

$$PL(d) = 20\text{Log}(f) + N\text{Log}(d) + L_f(n) - 28 \quad (3.16)$$

where d is the distance between transmitter and receiver (meters), N is the distance power loss coefficient, L_f is the floor penetration loss factor, n is the number of floors between a transmitter and a receiver and f is the radio frequency (MHz). Typical parameters which are used with this model in the study are $N = 30$; $n = 0$; $L_f = 15 + 4(n-1) = 11$; $f = 2400$ MHz.

Hence RSSI value received from the receiver is defined as;

$$RSSI = P + G - PL(d) \quad (3.17)$$

where P is transmitter power and G is antenna gain. Transmitter power and antenna gain values are considered from Jennic JN5139 WSN catalogues.

Distance d between a transmitter and a receiver can be calculated with equation (3.17) by substituting RSSI value received from the receiver.

3.9 Fingerprint Localisation Method

Once the received signal strength values in the form of LQI and RSSI are analyzed thoroughly and their randomness is reduced. The necessary infrastructure is organized for experimentation and fingerprint mapping localisation is carried out across a rectangular indoor test area.

Indoor fingerprint localisation technique is based on identifying the object location with received signal strengths at object position by comparing them with a pre-built radio map across the test area. A general layout of the test area is given in Figure 3.12.

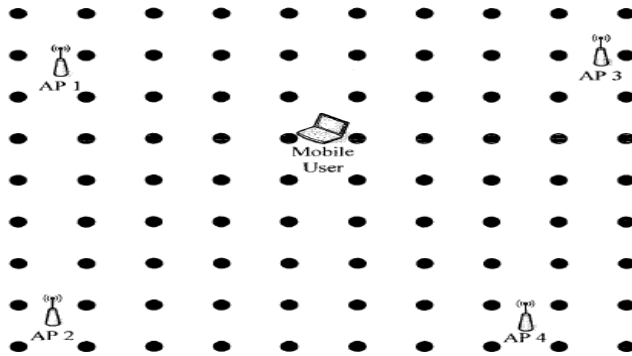


Figure 3.12: An example test area with 4 transmitters and a mobile user with a grid of measurement points

A number of measurement points is organised in a grid formation depending on the physical environment and the topology of the test area. Transmitters, located at strategic points provide RF propagation to cover the entire test area. In offline phase, at each measurement point, RSS values in RSSI or LQI format are received from all the transmitters by a receiver on each grid point and they are transferred to a distant server to build a signal location database. This database is called the radio map of the test area.

RSS values at measurement points display random behaviour and a single measurement of RSSI or LQI value can not be relied upon for localisation. Hence average value of multiple measurements over a period of time is employed as the signal fingerprint at that point. In online phase, mobile user receives RSSI or LQI values at its unknown location and transmits them to the server. These values are compared with the created radio map in offline phase in the server. A localisation algorithm is used and the probable user location is estimated by choosing minimum Euclidean distances between measured RSSI or LQI values in online phase and stored RSSI or LQI values in offline phase. A summary block diagram of fingerprint localisation approach by using LQI values [110], is presented in Figure 3.13.

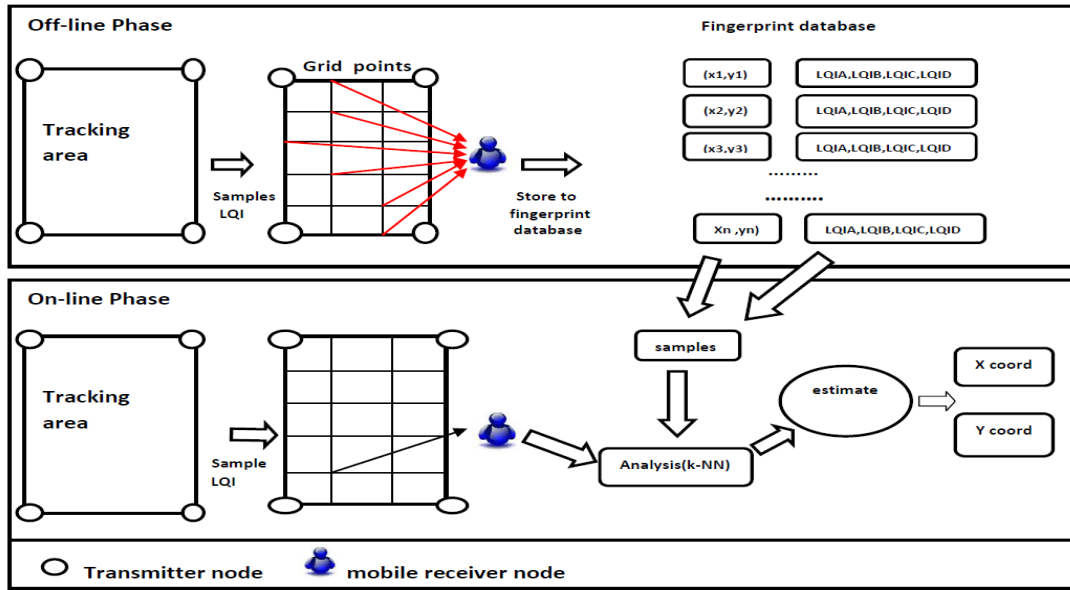


Figure 3.13: Architecture of Fingerprint localisation approach [110], by using recorded LQI values

3.9.1 Fingerprint Theory

There are two vectors which are used in the estimation of object locations. The first vector defines the signal measurements at grid points and consists of RSS values received from T_i transmitters, ($i=1, 2, 3...N$), where N is the total number of transmitters. They are recorded in the fingerprint database. This vector is identified as *location fingerprint RSS vector* and

denoted as \vec{F}_j with ($j= 1, 2, 3 \dots M$). M is the total number of grid points. Let RSS_{T_i} denote the average RSS value from T_i^{th} transmitter at j^{th} grid point. Hence, the *location fingerprint RSS vector* at j^{th} grid point is given as;

$$\vec{F}_j = (RSS_{T_1}^j, RSS_{T_2}^j, RSS_{T_3}^j, \dots, RSS_{T_N}^j)$$

The second vector consists of samples of RSS measurements from N number of T_i transmitters at a receiver on the object. This is called *sample RSS vector* and denoted as \vec{R}_k with ($k=1, 2, 3 \dots Z$) where Z is the number of object points. Hence the *sample RSS vector* at k^{th} object point is given as;

$$\vec{R}_k = (RSS_{T_1}^{'k}, RSS_{T_2}^{'k}, RSS_{T_3}^{'k}, \dots, RSS_{T_N}^{'k})$$

T_i transmitters are placed around the sensing area. The object position is estimated by comparing *location fingerprint RSS vectors* and *sample RSS vector*. \vec{R}_k vector elements are mutually independent and normally distributed. Signal distance between the *sample RSS vector* and *location fingerprint RSS vector* is used to determine the nearest measurement point for the object point. In this example, signal distance is denoted as the Euclidean distance between F_j and R_k vectors where $k=1$ corresponding to 1 object and identified as;

$$E = \left[\sum_{j=1}^M (F_j - R_1)^2 \right]^{\frac{1}{2}} \quad \text{see below for explanation} \quad (3.18)$$

F_j is the RSS vector at measurement grid point G_j and R_k is the RSS vector at object point. This technique determines the grid point corresponding to minimum signal distance between the *sample RSS vector* and the *location fingerprint RSS vector*. Hence, Euclidean distances can be illustrated for 1 object, N transmitter and M grid points as:

$$\begin{aligned} E_1 &= E(F_1, R_1) = ((RSS_{T_1}^1 - RSS_{T_1}^{'1})^2 + (RSS_{T_2}^1 - RSS_{T_2}^{'1})^2 + \dots + (RSS_{T_N}^1 - RSS_{T_N}^{'1})^2)^{\frac{1}{2}} \\ E_2 &= E(F_2, R_1) = ((RSS_{T_1}^2 - RSS_{T_1}^{'1})^2 + (RSS_{T_2}^2 - RSS_{T_2}^{'1})^2 + \dots + (RSS_{T_N}^2 - RSS_{T_N}^{'1})^2)^{\frac{1}{2}} \\ E_3 &= E(F_3, R_1) = ((RSS_{T_1}^3 - RSS_{T_1}^{'1})^2 + (RSS_{T_2}^3 - RSS_{T_2}^{'1})^2 + \dots + (RSS_{T_N}^3 - RSS_{T_N}^{'1})^2)^{\frac{1}{2}} \\ &\dots\dots\dots \\ &\dots\dots\dots \\ E_M &= E(F_M, R_1) = ((RSS_{T_1}^M - RSS_{T_1}^{'1})^2 + (RSS_{T_2}^M - RSS_{T_2}^{'1})^2 + \dots + (RSS_{T_N}^M - RSS_{T_N}^{'1})^2)^{\frac{1}{2}} \end{aligned}$$

There are M number of grid points and Euclidean distances are determined as many as M fingerprint locations and a *Euclidean vector* can be defined as;

$$\vec{E} = (E_1, E_2, E_3, E_4, \dots, E_M) \quad (3.19)$$

Euclidean distance is a signal distance and not an actual physical distance. Signal distances can only define the closeness of two locations from a radio signal point of view. Hence, minimum signal distance between two locations corresponds to the shortest physical distance between them. Euclidean distances are sorted out and stored in a database with respect to grid coordinates. Grid location corresponding to minimum Euclidean distance can be selected as the most probable close object location.

3.9.2 k-NN algorithm

Localisation accuracy can be improved by selecting a number of minimum Euclidean distances from the Euclidean database. k number of grid points in the database with smallest Euclidean distances are selected. This selection is carried out by using an algorithm called k-Nearest Neighbourhood algorithm [3, 7]. k number of grid point coordinates corresponding to k number of smallest Euclidean distances are averaged out to give a more accurate estimate of object location, (x,y), using equation (3.20).

$$(x, y)_{estimate} = \frac{1}{k} \sum_{j=1}^k (x_j, y_j) \quad (3.20)$$

(x_j,y_j) coordinates are the nearest measurement grid coordinates. The algorithm for the proposed technique is depicted in Figure 3.14.

Begin

Step(1) : AP collects LQI values (LQI_{T1}, LQI_{T2}, LQI_{T3}...LQI_{TZ}) from transmitter nodes (T₁, T₂, T₃...T_Z).

Step(2) : Averages a fixed number of LQI values at each grid point to reduce the randomness.

Step(3) : Generates a fingerprint database for averaged LQI values against grid coordinates.

Step(4) : AP collects LQI values from object point.

Step(5) : Calculates the Euclidean distance values between the object and grid points.

Step(6) : Sort the Euclidean distance values in ascending order.

Step(7) : the smallest Euclidean distance value corresponds to 1-nearest neighbour grid point of the object. The coordinates of this grid point is taken as the object coordinates

Step(8): 2 grid point coordinates corresponding to 2 smallest Euclidean distances are averaged out to give the object coordinates.

Step(9): 3 and 4 grid point coordinates corresponding to 3 and 4 smallest Euclidean distance values are averaged out to give the object coordinates.

End

Figure 3.14: Steps of k-NN algorithm for localisation process

k - NN algorithm produces a reasonable accuracy compared to grid spacing. A weighting scheme [55,111], is deployed to estimate the object location when k number of fingerprints are close to the acquired object fingerprint signature. This is identified as weighted k-NN algorithm. Many previous studies [98], include weight functions to increase the object

localisation accuracies. Weight functions depend on the real distances or Euclidean distances between the receivers and transmitters. RSS varies in indoor environment and the distances between the transmitters and receivers cannot be detected accurately by using only signal strengths and Euclidean distances. Weighting schemes are introduced to compensate these signal variations. Weight w is a function [55], depending on the distances and the characteristics of the receiver. In every localisation scenario, a different weight function can be deployed due to changing environmental conditions.

Shorter distances are usually more weighted than longer distances. Hence the weight and the distance are inversely proportional in many applications. Using concentric wave propagation with linear characteristics of receivers and transmitters, linear weight functions are deployed in localisation approaches. A weighting scheme ensures that remote transmitters can have an impact on the position determination [112]. Otherwise the approximated position moves to closest transmitter's position and positioning error increases. (x, y) coordinates of the object are determined by using w_i weight function and k -NN grid coordinates, (x_i, y_i) , as shown in equation (3.21).

$$(x, y) = \sum_{i=1}^k w_i (x_i, y_i) \quad (3.21)$$

$$\text{where } x = \sum_{i=1}^k w_i \cdot x_i \text{ and } y = \sum_{i=1}^k w_i \cdot y_i$$

w_i is the weight function of the i^{th} neighbouring grid point in k -nearest neighbourhood .

The choice of weight functions is an important factor in contributing to position accuracy. Data elements with high weight contribute more to position coordinates than the elements with low weight. When the weights are normalised they sum up to 1 as shown here;

$$\sum_{i=1}^k w_i = 1 \quad (3.22)$$

3.9.3 Weight functions

There are many weighting schemes employed during the localisation procedures with Euclidean distances in literature. Each weight function effects the localisation accuracies differently. In Landmarc system, [7], weight function w includes D^2 Euclidean distance values in the calculations. Hence, in order to stabilize the effects of shorter distances in the calculations a comparative study of empirical weight functions are carried out first time in order to increase localisation accuracies in smaller indoor areas. This study includes the Euclidean distance powers to show which weight function generates the maximum accuracy.

Different weight functions [44], obeying the previous normalisation rule, are assigned empirically in equation (3.21) in order to calculate the unknown object coordinates. Object position estimation depends on D_i Euclidean distances of k -nearest neighbours. w_i values are formulated to express this dependency with D_i values and listed in Table 3.2. These empirical weight functions can be implemented with equation (3.21) and unknown object coordinates can be calculated with different accuracy requirements. The weight function which provides the minimum error between the estimated and actual object coordinates is selected in future localisation applications.

A	B	C	D	E
$w_i = \frac{1}{k}$	$w_i = \frac{1/D_i}{\sum_{i=1}^k 1/D_i}$	$w_i = \frac{1/D_i^2}{\sum_{i=1}^k 1/D_i^2}$	$w_i = \frac{1/D_i^3}{\sum_{i=1}^k 1/D_i^3}$	$w_i = \frac{1/D_i^4}{\sum_{i=1}^k 1/D_i^4}$

Table 3.2: A list of weight functions with respect to Euclidean distances

3.10 Implementation

During experiments, fingerprint data collection are carried out in a fingerprint database in the server. Object locations are calculated by using k -NN and weighted k -NN algorithms across the test area. The ideal weight function from Table 3.2 which produces the minimum localisation error is determined during object position estimations. JN5139 active WSNs work as fixed transmitter nodes and object receiver nodes respectively [113,114].

A rectangular test area which is deployed during the experiments is on a single floor inside a building with a minimum number of obstacles. A block diagram of the test area, 15 m², with 24 grid points is shown in Figure 3.15.

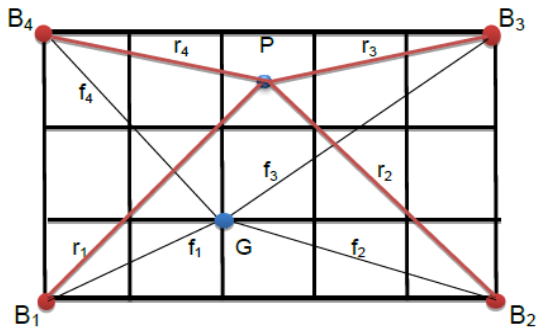


Figure 3.15: Block diagram of the test area with 1mx1m grid space and object point P, grid point G

B_i transmitters are placed at the corners of this test area. A receiver, placed on an unknown object, is positioned at an arbitrary point in the test area and interfaced to a computer. A set

of 4 LQI readings at each grid point is recorded by the receiver. Received LQI values exhibit a correlation with the receiver aerial orientation as well as its location.

Hence, the average LQI values are obtained by averaging out LQI recordings in 4 compass directions during the measurements. Received signal message format and the database format in the server are shown in Figure 3.16.

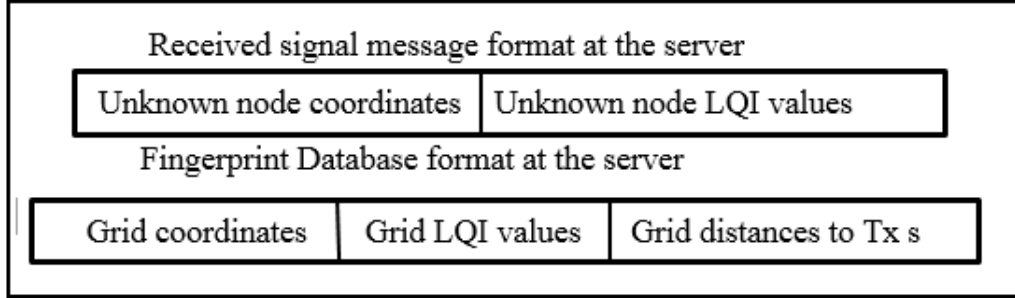


Figure 3.16: Received LQI signal and database format in the server

3.10.1 k-NN Experiments

Average LQI values are recorded for each grid point and unknown object point. Example LQI recordings of the mobile object at unknown locations across the test area and their 4 nearest Euclidean distances with coordinates are presented in Table 3.3.

Unknown (x,y) position Coordinates	LQI values at unknown object positions $r(r_1, r_2, r_3, r_4)$				4- nearest Euclidian distances(LQI)				4 Grid coordinates corresponding to 4 nearest Euclidean distances			
	r_1	r_2	r_3	r_4								
1 , 2	105	100	85	190	41.6	32.1	29	27.1	0,1	1,3	0,2	1,2
2 , 1	90	150	95	140	21.4	24.3	25.2	18.8	3,3	2,1	3,1	3,0
3 , 2	87	158	110	132	24.2	23.2	19.4	27.1	4,0	5,1	3,1	3,3
4 , 1	90	142	125	114	25.7	23.9	26.6	23.6	5,2	4,1	4,2	4,3
5 , 1	88	180	120	128	26.3	37.1	39.1	29.5	4,0	3,1	5,2	5,1

Table 3.3: Sample LQI vector r of mobile object at different locations and 4 nearest grid coordinates

k- NN algorithm is applied with fingerprint database. Estimated object locations are calculated by averaging the grid coordinates corresponding to k number of minimum Euclidean distances. Resultant average coordinates represent the object location across the test area. Location estimation error, e , is defined by a linear distance between the unknown object's estimated coordinates (x_e, y_e) and the real coordinates (x_r, y_r) . It is given by:

$$e = \sqrt{(x_e - x_r)^2 + (y_e - y_r)^2} \quad (3.23)$$

Error calculations of unknown object locations in Table 3.3 are given as an example. Localisation results of 4-NN algorithm reveal an average error of $e = 0.82m$ as shown in Table 3.4.

Unknown (x,y) object coordinates	4 Grid coordinates corresponding to 4-NN euclidean distances				Estimated (x,y) object Coordinates	Error Distance (m)
1 , 2	0,1	1,3	0,2	1,2	0.5 2.0	0.5
2 , 1	3,3	2,1	3,1	3,0	2.75 1.25	0.79
3 , 2	4,0	5,1	3,1	3,3	3.75 1.25	1.06
4 , 1	5,2	4,1	4,2	4,3	4.25 2.0	1.03
5 , 1	4,0	3,1	5,2	5,1	4.25 1.0	0.75
Average error distance (m)						0.82

Table 3.4: Examples of estimated object position coordinates and error distances

3.10.2 Weighted k-NN Experiments

w_i weight functions in Table 3.2 are calculated at each unknown object location by using 4-nearest Euclidean distances. Once w_i values are determined, coordinates of the unknown object at different positions across the test area are calculated by using equation (3.21).

An example calculation of estimated object point coordinates is given here for an unknown object point of (1, 2). 4 nearest Euclidean distance values are (41.6, 32.1, 29, 27.1) and their corresponding coordinates are {(0,1),(1,3),(0,2),(1,2)} from Table 3.3. Weight function (B) in Table 3.2 is utilised for example calculations below. w_1 , w_2 , w_3 , and w_4 weight values are calculated for 4 nearest grid coordinates. Hence estimated unknown object position coordinates (x, y) become:

$$(x, y) = 0.19 * (0,1) + 0.246 * (1,3) + 0.2725 * (0,2) + 0.291 * (1,2) = (0.54,2)$$

Weight functions in Table 3.2 are calculated for example object locations by using their Euclidean distances of k-NN grid points. Coordinates of unknown object locations are calculated by using these weight functions and they are tabulated in Table 3.5.

Unknown (x,y) Object position Coordinates	Estimated (x,y) object coordinates with different weights				
	A	B	C	D	E
1 , 2	0 , 2.0	0.5 , 2.0	0.5 , 2.0	0.6 , 2.1	0.6 , 2.11
2 , 1	2.7 , 1.2	2.7,1.2	2.7 , 1.2	2.8,1.1	2.84,1.08
3 , 2	3.7 , 1.2	3.7,1.2	3.1 , 1	3.6 , 1.1	3.64 , 1.05
4 , 1	4.2 , 2.0	4.2 , 2.0	4.2 , 2.0	4.2 , 2.0	4.22 , 2.0
5 , 1	4.2 , 1	4.2 , 0.9	4.3 , 0.8	4.3 , 0.7	4.27 , 0.62

Table 3.5: Estimated object coordinates using different weight functions in Table 3.2

Their error calculations are given in Table 3.6. It can be seen that the minimum average error distance is realised with weight function D. Hence it can be concluded that the positions of unknown objects in the test area are estimated most accurately by using weight function D in calculations.

Unknown (x,y) Object Position Coordinates	Error distance (e) between estimated and real object positions (meters) for each weight function w				
	A	B	C	D	E
1 , 2	1	0.5	0.5	0.41	0.42
2 , 1	0.728	0.728	0.728	0.80	0.843
3 , 2	1.063	1.063	1.004	1.08	1.145
4 , 1	1.019	1.019	1.019	1.019	1.0143
5 , 1	0.8	0.806	0.94	0.76	0.822
Average error	0.92	0.88	0.83	0.81	0.85

Table 3.6. Error distances with different weight functions

A 3D representations of error distances at unknown object locations are presented in Figure 3.17.

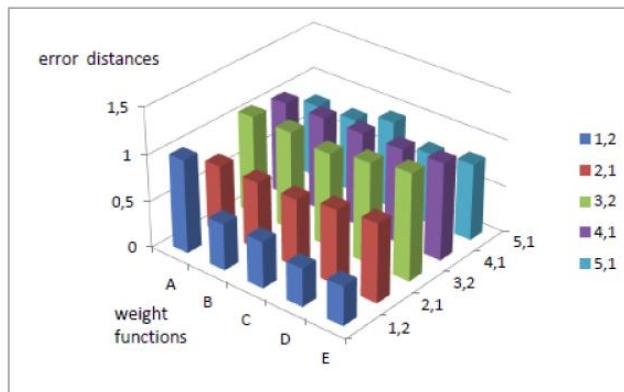


Figure 3.17: Error plots at unknown object locations for different w_i values

Finally, average error distances for different weight functions are displayed in 3D form in Figure 3.18.

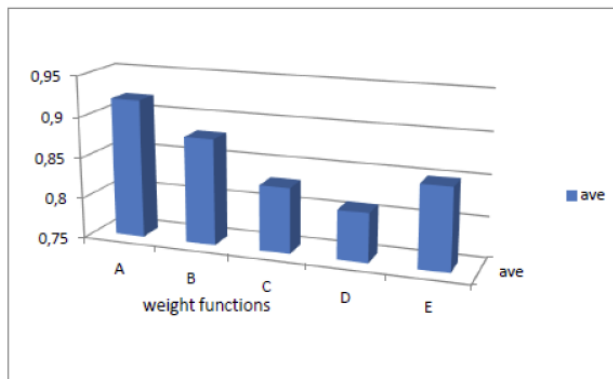


Figure 3.18: 3D Average error distances versus weight functions

3.11 Conclusions

In this chapter, Theoretical background of RSSI and LQI values are given. RSSI values define received signal strengths by the receivers. LQI values define the best quality

connectivity between the receiver and transmitter. LQI values can be considered as a metric quantity of the current quality of RSSI values.

Localisation systems are based on the distance determination between transmitters and receivers. Sudden large amplitude variations of RSSI or LQI values during the measurements are quantised as outliers and they are removed from main stream recordings by using known outlier technique such as modified z-score method.

Theoretical background of bisection algorithm is presented. This algorithm is one of the contributions in this chapter. It is a numerical analysis technique which is employed in later chapters to determine the distances between transmitters and receivers for recorded RSSI and LQI values by using their fitted calibration curves. The only condition is that these fitted curves must be monotonic curves to apply bisection algorithm. Otherwise, in non-monotonic curves, x axis values can have more than one y values.

Localisation accuracies are based on environmental effects between the transmitters and receivers. These environmental effects cause path loss problems during calculations. Various path loss models are presented. ITU indoor propagation model which is utilised in this study is given in detail. RF signal radiation behaviour of Jennic transmitter and receiver devices is investigated. It was confirmed that RF radiation is omni-directional and signal packets are transferred uniformly in all directions.

k- NN algorithm is a common algorithm used with the fingerprint localisation approach to determine relative unknown object locations. Lower values of k decrease the localisation accuracies while higher values of k do not have any significant effect on accuracies. But a weighted fingerprinting approach which introduces weight functions gives better localisation accuracies. In this study, another main contribution is to compare several empirical weight functions and to determine the best weight function in order to give the best localisation accuracies using fingerprint technique. Different weight functions are deployed with the basic fingerprint localisation approach and the one which gives the optimum localisation accuracy is determined. Weight function D which utilises the inverse 3rd order Euclidean distances is the favourite one with a localisation error less than a grid space. It gives the best localisation accuracy. Upper and lower orders do not improve the localisation accuracies.

Fingerprint localisation approach in this chapter is the basic fingerprint technique in the literature. This technique is repeated in this study to be a reference localisation for other techniques to be introduced in later chapters.

CHAPTER 4

CENTROID & ADAPTIVE CENTROID LOCALISATION

4.1 Background

Wireless sensor nodes, WSNs, are deployed in many areas to determine objects locations. Many location algorithms have been introduced over the years based on RSSs [115,116]. In many scenarios, data collected with WSNs must be coupled with environmental information to generate location information [117,118]. These nodes have limitations with size and power consumption and they must be employed within these limitations.

A number of chosen WSNs have fixed positions and are identified as transmitter beacons. The other nodes can be used to calculate their positions with the help of these beacons. There are many localisation techniques with different accuracy levels. According to (Bulusu et al. 2000) [53], location estimation is divided into two groups; course grained localisation and fine grained localisation. Course grained localisation requires a minimum amount of computation time and is called centroid localisation (CL). The localisation accuracies are around 2-5 metres. In this technique, position coordinates of all Wireless sensor nodes are known and the unknown object node is calculated as the centroid of wireless sensor node positions within the communication range.

CL algorithm can be improved by using weighted centroid localisation (WCL), [111]. WCL introduces weights to the distances between the unknown node and the other WSNs. The technique emphasises the nearest node to the unknown object node. In the classical WCL method, weights are calculated as inversely proportional to the distances between the unknown node and the other WSNs. This proportionality is identified as the attenuation factor of RF signals with the distance.

WCL technique sometimes gives incorrect position calculations indoors due to RF attenuation changes because of concrete surroundings. Adaptive WCL algorithm, AWCL, is introduced where the weights are calculated more adaptively to surroundings [119]. This

algorithm calculates the target position by using WCL but suffers from RSSI ranging errors and position errors of anchor nodes.

Hence another algorithm was developed by (W. Feng & Xiao Bi, 2009) [120], identified as adaptive cooperative location algorithm. It uses specially built nodes where the environmental factors are cooperatively adapted with RSSI values between them.

A new two level environmentally adaptive localisation algorithm (EAL) is introduced in this chapter by using simple transmitter and receiver WSNs. Environmental conditions are introduced with this new algorithm as a static threshold factor related to received RSSI values and no cooperative data processing is utilised between transmitter and receiver nodes.

RSSI values received from transmitters are filtered and outliers are removed. Remaining RSSI values have EAL algorithm applied to smooth the variations a stage further in real time. Distances between unknown receiver nodes and transmitter nodes are empirically calculated by using adaptively corrected RSSI values. Trigonometric methods are utilised to calculate the positions of the unknown objects. STD of filtered RSSI values is employed to determine an STD threshold value in each level. Environmental factors are introduced in the calculations by means of these threshold STD values in both levels for each transmitter.

To reduce these environmental affects further, a reference anchor node with a minimum received RSSI mean value is selected across the test area. Position calculations are carried out according to this reference node coordinate system and then transferred to a real Cartesian coordinate system. Origin of this coordinate system is considered as the most stable location with minimum RSSI mean and localisation procedures are carried out in this stable environment. The algorithm detects the unknown objects without any information about adaptive collaboration between nodes. Better localisation results are obtained compared to weighted centroid algorithm under similar environmental conditions. Receiver nodes detect the transmitted signals and quantise them in LQI forms. These LQI values are converted into RSSI values later and employed in the calculations.

4.2 Centroid Localisation

CL is the simplest localisation algorithm. This algorithm does not require any information about RSSI or LQI values corresponding to distances between the transmitter and object nodes. The only information required is whether the unknown object is within the range of transmitters or not. WSNs are uniformly distributed over the area of interest. Each transmitter has a circular transmission range where it can communicate with other receivers as shown in Figure 4.1.

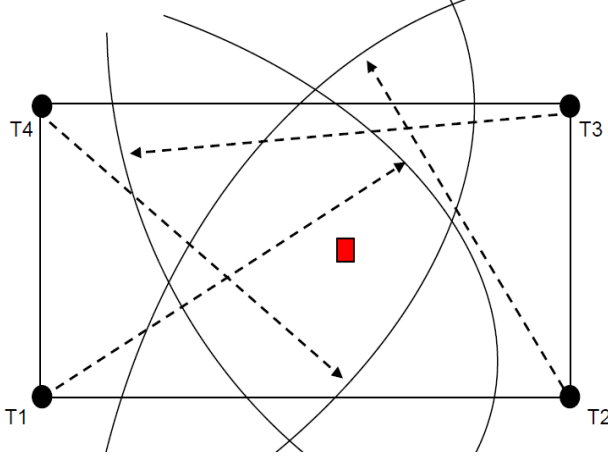


Figure 4.1: Graphical view of 4 transmitters with ranges and 1 object receiver,

● : transmitter node, ■ : receiver node

During the first phase; all the transmitters, $T_j(x,y)$, send their position information to a receiver on the unknown object within their transmission range. In second phase, receivers calculate their own positions, $P_i(x,y)$, by using centroid formation of n number of transmitter positions in range as shown in equation (4.1).

$$P_i(x, y) = \frac{1}{n} \sum_{j=1}^n T_j(x, y) \quad (4.1)$$

where i represents the unknown object and j represents the number of transmitters. Hence CL performs an averaging of transmitter coordinates to localise the unknown object location. An unknown object in one of the intersection areas will calculate its position by equation (4.1). This technique gives a large amount of errors. (Blumenthal et al. 2007) [111], showed that the accuracy depends on the ratio between transmitter distances and the communication ranges.

4.3 Weighted Centroid Localisation

Localisation accuracy with CL is very low and a new technique called weighted centroid localisation (WCL) is developed to increase the accuracy. This technique identifies the transmitters depending on their distances from the unknown object positions. The aim in this technique is to give more weight to transmitters which are nearer to the unknown object.

RSSI and LQI quantities can be employed as the distance identifiers between transmitters and receivers. These values are inversely proportional to distances between transmitters and receivers. Hence RSSI or LQI values can be employed with WCL technique.

The basic idea of WCL is to define the location of transmitters with an appropriate weight function which is based on distances between unknown objects and transmitters in range. The

weight function, w_{ij} , describes the weight for transmitter j and object node i . See Equation (4.2). The distance between the transmitter j and the object i is given by d_{ij} . k is the distance power factor.

$$w_{ij} = \frac{1}{d_{ij}^k} \quad (4.2)$$

The distance d_{ij} is raised to a higher power k in order to weight longer distances. Power factor k ensures that the remote transmitters can still have a weight effect in position determination. If k is high, the estimated object position moves towards the closest transmitters and localisation error increases. Equation (4.1) can be expanded to WCL formulation by equation (4.3).

$$P_i(x, y) = \frac{1}{\sum_{i=1}^n 1} \sum_{j=1}^n 1 \cdot B_j(x, y) \quad (4.3)$$

Weight functions are inserted instead of 1's in equation (4.3) and i object coordinates become:

$$P_i(x, y) = \frac{1}{\sum_{j=1}^n w_{ij}} \sum_{j=1}^n w_{ij} \cdot B_j(x, y) \quad (4.4)$$

Weight w_{ij} is a function with respect to distances and characteristics of receivers. Weight function changes with environmental conditions. Shorter distances have more weights than longer distances.

4.4 Adaptive Localisation

Object localisation is carried out by deploying RSSI values from transmitters. These RSSI values, hence their mean and standard deviation (STD) values, are effected from environmental conditions. A new localisation system is envisaged in this chapter to include these effects as threshold factors with RSSI values. By utilizing mean and STD values of recorded RSSI values, new ranges of smoother RSSI values are determined and used during localisation procedures. New Range of RSSI values are identified as adaptive RSSI values and the localisation technique is termed as adaptive localisation.

WSNs are utilised as transmitters and receivers during RSSI measurements. A number of transmitter nodes are strategically placed across the tracking area. In this study, RF communication between transmitters around the test area and receivers on the objects is one way communication. RF data is sent from transmitters to receivers. Block diagram of the localisation system is shown in Figure 4.2.

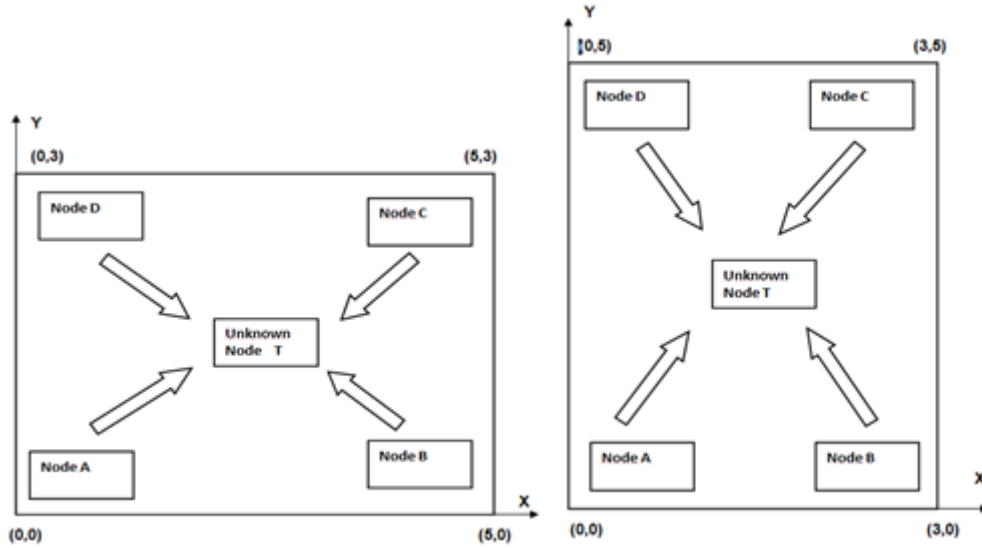


Figure 4.2: Localisation system with a) 5mx3m and b) 3mx5m configurations

Received RF signals in appropriate format are sent to a server computer by the object receiver for position calculation. The object with a receiver can stay stationary or be in motion in the indoor environment. Algorithmic model of the localisation system is presented in Figure 4.3.

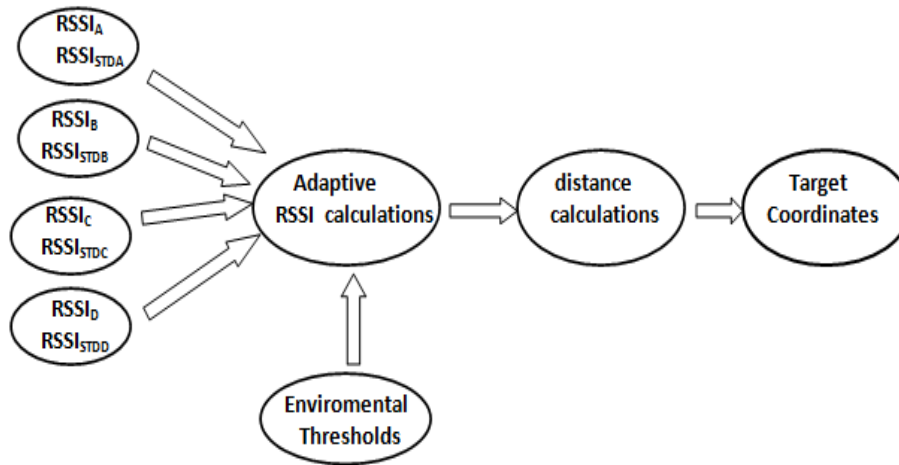


Figure 4.3: Algorithmic model of the localisation system

In the algorithmic model, there are a number of inputs consisting of RSSI values arriving from transmitters. Each input has RSSI values from a transmitter node. Standard deviations corresponding to them are also inputted into the model. The final output from the model is the coordinates of the target object.

Each data frame has N number of RSSI values with an identity number broadcast from each transmitter node. Object receiver records RSSI values of each frame and sends them to a server PC according to individual identity of the transmitters. The mean value of the received

RSSI values in one frame are defined as R_{MEAN} and the standard deviation of these RSSI values is defined as R_{STD} . R_{MEAN} is defined for N number of RSSI values as:

$$R_{MEAN} = \frac{1}{N} \sum_{p=1}^N RSSI_p \quad (4.5)$$

R_{STD} is defined for N number of RSSI values as:

$$R_{STD} = \left(\frac{1}{N} \sum_{p=1}^N (RSSI_p - R_{MEAN})^2 \right)^{1/2} \quad (4.6)$$

In order to minimise the random behavior of RSSI's, a signal interval of

$(R_{MEAN} - R_{STD} < R_{MEAN} < R_{MEAN} + R_{STD})$ is defined. RSSI measurement values within this interval are considered for localisations.

4.4.1 RSSI correction phase

If there are “q” number of (RSSI) values in $(R_{MEAN} - R_{STD} < R_{MEAN} < R_{MEAN} + R_{STD})$ interval, **m** is taken as the number of RSSI values which are less than or equal to the mean of **q** RSSI values. The average value of m number of RSSI values is given as

$$R_X = \frac{1}{m} \sum_{i=1}^m (RSSI)_i \quad (4.7)$$

where $(RSSI)_i \leq \frac{1}{q} \sum_{j=1}^q (RSSI)_j$

$(q - m)$ is the number of RSSI values whose values are greater than the mean of q RSSI values. The average value of $(q-m)$ number of RSSI values is given as

$$R_Y = \frac{1}{q - m} \sum_{i=1}^{q-m} (RSSI)_i \quad (4.8)$$

where $(RSSI)_i > \frac{1}{q} \sum_{j=1}^q (RSSI)_j$

RSSI values, received from transmitter A, at object location is expressed as

$$RSSI_A = \beta_A \cdot R_X + (1 - \beta_A) \cdot R_Y \quad (4.9)$$

where β_A is a constant and defined as the environmental factor depending on R_{STD} value of transmitter A. Similar equations can be utilised for other transmitters. An average threshold standard deviation, T_{STD} , is introduced for all the transmitter nodes in Figure 4.2 as

$$T_{STD} = \frac{1}{4}(R_{STDA} + R_{STDB} + R_{STDC} + R_{STDD}) \quad (4.10)$$

β_A is defined in terms of T_{STD} and R_{STDA} as ;

$$\beta_A = 0.5(1 + \frac{T_{STD} - R_{STDA}}{T_{STD}}) \quad \text{for } R_{STDA} \leq T_{STD} \quad (4.11)$$

$$\beta_A = 0.5(1 - \frac{R_{STDA} - T_{STD}}{T_{STD}}) \quad \text{for } R_{STDA} > T_{STD} \quad (4.12)$$

T_{STD} depends on environmental conditions since STDs depend on environmental conditions. Measured $RSSI_A$ values are identified as stable if $R_{STDA} \leq T_{STD}$. Hence β_A is calculated as $\beta_A \in (0.5, 1)$. Measured $RSSI_A$ values are identified as unstable if $R_{STDA} > T_{STD}$.

β_A is then calculated as $\beta_A \in (0, 0.5)$. By substituting β_A values in equation (4.9), adapted $RSSI_A$ values are calculated. The same procedures are applied to calculate the environmentally adapted $RSSI_B$, $RSSI_C$, $RSSI_D$ values.

Once the environmentally adaptive RSSI values are determined for an object location, distances between the object and the transmitters are estimated by using ITU-R propagation model for further procedures.

4.4.2 Advanced RSSI correction phase

A new interval of RSSI values are now identified in this phase within the selected RSSI values in phase 1 to increase the localisation accuracies further. Selected RSSI values in Phase 1 are subjected to another selection process to reduce the remaining RSSI variations a stage further.

The mean value of N number of RSSI values is R_{MEAN} and the standard deviation of these RSSI values is R_{STD} from 1st correction phase. Q number of RSSI values is selected within the q interval ($R_{MEAN} \pm R_{STD}$) from phase 1.

New Q_{MEAN} and Q_{STD} values of q number of RSSI values are calculated. There are Q number of RSSI values in the interval generated by these Q_{MEAN} and Q_{STD} values and identified as ($Q_{MEAN} - Q_{STD} < Q_{MEAN} < Q_{MEAN} + Q_{STD}$).

r is taken as the number of RSSI values which are less than or equal to the mean of Q number of RSSI values. $(Q - r)$ is the number of RSSI values whose values are more than the mean of Q values. New R_x , R_y and β_A values are redefined as;

$$R_x = \frac{1}{r} \sum_{i=1}^r (RSSI)_i \quad (4.13)$$

where $(RSSI)_i \leq \frac{1}{r} \sum_{i=1}^r (RSSI)_i$

$$R_y = \frac{1}{Q - r} \sum_{i=1}^{Q-r} (RSSI)_i \quad (4.14)$$

where $(RSSI)_i > \frac{1}{r} \sum_{i=1}^r (RSSI)_i$

A new weighted Threshold Standard Deviation, T^1_{STD} , is introduced by using Q_{STD} values and the average d distances calculated by ITU-R model at object location for all the transmitters in new $(Q_{MEAN} \pm Q_{STD})$ interval.

It is shown as ;

$$T^1_{STD} = \frac{\frac{Q_{STDA}}{d_A} + \frac{Q_{STDB}}{d_B} + \frac{Q_{STDC}}{d_C} + \frac{Q_{STDD}}{d_D}}{\frac{1}{d_A} + \frac{1}{d_B} + \frac{1}{d_C} + \frac{1}{d_D}} \quad (4.15)$$

New β_A values for transmitter A are defined in terms of T^1_{STD} and Q_{STDA} are given by

$$\beta_A = 0.5 \left(1 + \frac{T^1_{STD} - Q_{STDA}}{T^1_{STD}} \right) \quad \text{for } Q_{STDA} \leq T^1_{STD} \quad (6.16)$$

$$\beta_A = 0.5 \left(1 - \frac{Q_{STDA} - T^1_{STD}}{T^1_{STD}} \right) \quad \text{for } Q_{STDA} > T^1_{STD} \quad (6.17)$$

Adaptive $RSSI_A$ value is recalculated by substituting new β_A , R_x and R_y values in equation (4.9) for transmitter A. Finally, adaptive RSSI values for other transmitters are also calculated by using their respective β , R_x and R_y values.

4.5 Environmentally Adaptive location algorithm

In many object localisation problems with WSNs, localisation methods use simple centroid algorithm and range based RSSI algorithm. Both of these algorithms have low computation and are easy to apply with RSSI values. In environmentally adaptive location algorithm, the

transmitter node with minimum transmitted average RSSI value is selected as the reference anchor node across the test area.

A minimum average RSSI value represents the minimum RSSI amplitude recordings from a particular transmitter node. The minimum RSSI mean, corresponds to most stable RSSI values during measurements since they represent minimum RF signal energy levels.

This node is taken as the reference anchor node for stable localisation calculations and identified as the origin of the relative coordinate system. Positioning calculations are carried out with this relative coordinate system and the results are transferred to universal coordinate system to define the actual target location.

As a result, the effects of larger random variations are reduced and good positioning accuracies are obtained. Coordinates of A,B,C,D transmitter nodes and the target object node in universal coordinate system, xOy, are taken as (x_A, y_A) , (x_B, y_B) , (x_C, y_C) , (x_D, y_D) and (x_T, y_T) . If the anchor node is assumed to be B transmitter, then the coordinates of the transmitter nodes and the object node become (x'_A, y'_A) , $(0,0)$, (x'_C, y'_C) , (x'_D, y'_D) and (x'_T, y'_T) in relative coordinate system of $x'By'$. See Figure 4.4.

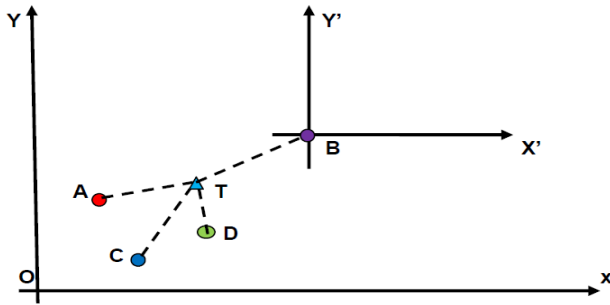


Figure 4.4: Universal (xOy) and relative (x'By') coordinate systems

The following equations are derived from the translation relationship between two coordinate systems:

$$x'_A = x_A - x_B, y'_A = y_A - y_B, x'_C = x_C - x_B, y'_C = y_C - y_B, x'_D = x_D - x_B, y'_D = y_D - y_B$$

$$x'_T = x_T - x_B, y'_T = y_T - y_B$$

Estimated distances between object T and A, C, D nodes with ITU-R model are denoted as d_A , d_C , d_D and their trigonometric equations in $(x'By')$ coordinate system are given by;

$$(x'_T - x'_A)^2 + (y'_T - y'_A)^2 = d_A^2 \quad (4.18)$$

$$(x'_T - x'_C)^2 + (y'_T - y'_C)^2 = d_C^2 \quad (4.19)$$

$$(x'_T - x'_D)^2 + (y'_T - y'_D)^2 = d_D^2 \quad (4.20)$$

x'_T and y'_T coordinates can be calculated by utilising equations (4.18), (4.19) and (4.20) as ;

$$x'_T = \frac{B_1 - B_2}{A_1 - A_2} \quad , \quad y'_T = -A_1 x'_T + B_1$$

where A and B are defined as :

$$A_1 = \frac{x'_A - x'_C}{y'_C - y'_A} \quad \text{and} \quad A_2 = \frac{x'_A - x'_D}{y'_D - y'_A}$$

$$B_1 = \frac{d_A^2 - d_C^2 + x_C'^2 - x_A'^2 + y_C'^2 - y_A'^2}{2(y'_C - y'_A)} \quad \text{and} \quad B_2 = \frac{d_A^2 - d_D^2 - x_A'^2 + x_D'^2 - y_A'^2 + y_D'^2}{2(y'_D - y'_A)}$$

Finally, (x'_T, y'_T) , can be translated to universal coordinate system to define the estimated object coordinates of (x_T, y_T) as $x_T = x'_T + x_B$ and $y_T = y'_T + y_B$.

4.6 Implementation

Initially, a simple rectangular indoor area of 5mx3m as in Figure 4.2a was deployed for experiments. Experiments are carried out in less simple indoor areas at a later stage and the results are compared. Calculations are presented in detail for 3mx5m rectangular area as in figure 4.2b and only the results are presented for other indoor areas. Test areas are not free of obstacles; there is standard room furniture surrounded by concrete walls. See Figure 4.5. Signal strengths in LQI form are received from a Jennic receiver on the object and transferred to a server PC. There are 4 transmitters at 4 corners of the test area. 100 LQI values from each transmitter are recorded by the receiver and they are converted into RSSI values in the server.

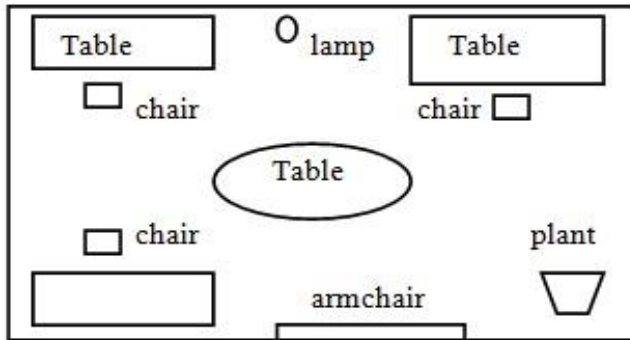


Figure 4.5 : A block diagram of indoor test area

4.6.1 Centroid localisation

Test area configuration in Figure 4.2a is used in the experiments. 100 recorded LQI values from each transmitter are stored in a database. They are averaged out to obtain a single average LQI value from each transmitter at object locations. These average LQI values are utilised and d_{ij} distances between transmitters and object locations are calculated by using bi-

sectioning algorithm. Example average LQI values and d_{ij} distances for different object locations are presented in Table 4.1. d_{ij} distances between the object and transmitters are deployed to determine the weight functions for different k values in equation (4.2). For example, the weights corresponding to unknown location (1, 1) in Table 4.1 can be calculated for different k values and displayed in Table 4.2.

object position coordinates	Ave. LQI values at unknown object positions				d_{ij} values corresponding to unknown object positions (m)			
(x , y)	LQI _A	LQI _B	LQI _C	LQI _D	d _A	d _B	d _C	d _D
1 , 1	110	120	125	150	3.43	2.65	2.34	1.71
1 , 2	105	100	95	180	4.06	4.68	5.31	1.01
2 , 1	95	145	95	137	5.31	1.71	5.31	2.03
3 , 0	95	145	93	145	5.31	1.71	5.93	1.71
3 , 2	97	151	108	132	5.31	1.71	3.43	2.03
4 , 1	92	129	121	111	5.93	2.34	2.65	3.43

Table 4.1: Average LQIs at object positions and d distances between objects and transmitters

Weights	$W_A=1/d_A^k$	$W_B=1/d_B^k$	$W_C=1/d_C^k$	$W_D=1/d_D^k$
$1/d^1$	0.29	0.37	0.42	0.58
$1/d^2$	0.08	0.14	0.18	0.34
$1/d^3$	0.02	0.05	0.07	0.19
$1/d^4$	0.01	0.02	0.03	0.11

Table 4.2: Different weights of A,B,C,D transmitters for object location (1,1)

Object coordinates, (x,y), are calculated by using equation (4.4) and d_{ij} values in Table 4.1. An example of estimated object coordinates,(x,y), for object location, (3, 0), with weight function $w=1/d$ is presented here:

$$(x, y) = \frac{\frac{1}{5.31}(0,0) + \frac{1}{1.71}(5,0) + \frac{1}{5.93}(5,3) + \frac{1}{1.71}(0,3)}{\frac{1}{5.31} + \frac{1}{1.71} + \frac{1}{5.93} + \frac{1}{1.71}} = (2.46,1.48)$$

A sample of estimated object coordinates with different weight functions are displayed in Table 4.3. Error calculations with estimated and actual object coordinates are carried out and the results are also presented in Table 4.3.

object coordinates (x , y)	Estimated object coordinates with different W_{ij} weights				Error distance, e, for each weight function at object coordinates			
	$W_1=1/d$	$W_2=1/d^2$	$W_3=1/d^3$	$W_4=1/d^4$	$e_1(W_1)$	$e_2(W_2)$	$e_3(W_3)$	$e_4(W_4)$
1 , 1	2.3, 1.8	2.1, 2.0	1.8, 2.3	1.5 ,2.5	1.52	1.48	1.52	1.58
1 , 2	1.2, 2.1	0.36, 2.7	0.08, 2.9	0.01,2.9	0.22	0.94	1.28	0.89
2 , 1	2.6 , 1.4	2.8, 1.27	3.0, 1.14	3.2, 1.02	0.72	0.84	1.03	1.2
3 , 0	2.4, 1.4	2.4, 1.4	2.4, 1.49	2.4, 1.49	1.52	1.52	1.60	1.61
3 , 2	2.8, 1.5	3.0, 1.4	3.1, 1.24	3.3, 1.1	0.53	0.6	0.77	0.95
4 , 1	3.2, 1.5	3.7, 1.5	4.0, 1.5	4.3, 1.3	0.94	0.58	0.5	0.42
Average errors					0.91m	0.99m	1.11m	1.11m

Table 4.3: Sample of estimated object coordinates with different weight functions and their error calculations

The results reveal that the minimum average error distance of 0.91m is obtained with weight function $w_1=1/d$. It is observed that the average error distance is increasing with increasing k values. 3D representations of error distances at unknown locations are given in Figure 4.6.

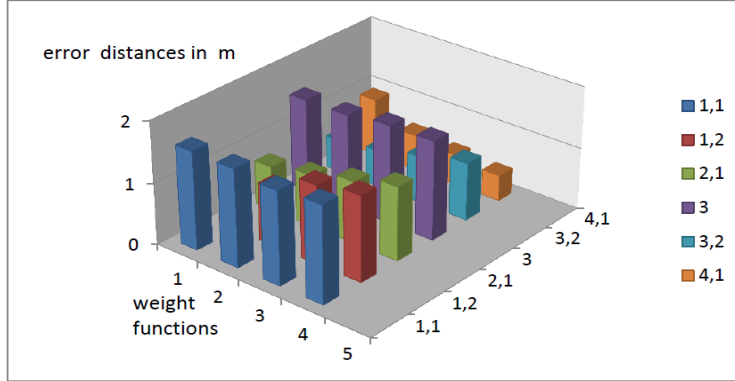


Figure 4.6: 3D error plots of unknown object locations with different weights

4.6.2 Adaptive centroid localisation

An indoor area of 3mx5m is deployed for experiments as shown in Figure 4.2b. 4 sets of 100 LQI recordings are received from 4 transmitters around the corners of the test area at object location. These recordings are converted into 4 sets of 100 RSSI values named as $RSSI_A$, $RSSI_B$, $RSSI_C$, and $RSSI_D$. The mean and standard deviation of these RSSI values are calculated and presented in Table 4.4. An example case of recordings is presented here for an object location of (2, 3).

100 RSSI (dBm) recordings from A,B,C,D TRANSMITTERS at target location							
$RSSI_A$		$RSSI_B$		$RSSI_C$		$RSSI_D$	
mean	std	mean	std	mean	std	mean	std
- 63.836	0.486	- 61.286	0.952	- 53.286	1.422	- 56.406	0.993

Table 4.4: STD and Mean values of 100 RSSI values at object location (2,3)

4.6.2.1 RSSI correction phase (phase 1)

An interval “q” is defined by ($q_{MEAN} - q_{STD} < q_{MEAN} < q_{MEAN} + q_{STD}$) around q_{MEAN} value of N number of RSSI values. RSSI values in this interval are only considered during calculations for each A, B, C, D recordings. These intervals are tabulated together with mean values of q number of RSSI values and the number of RSSI values in the intervals in Table 4.5.

Minimum mean of received RSSI values is $RSSI_A = - 63.836$ dBm as seen in Table 4.4 and the corresponding transmitter node at A (0, 0) is chosen as the reference anchor node.

transmitters	q number of RSSI	q _{mean}	q _{mean} ± q _{STD} interval
A	87	-61.286	-64.323 < q _A < -63.351
B	67	-61.378	-62.239 < q _B < -60.334
C	56	-53.630	-54.708 < q _C < -51.864
D	70	-55.866	-57.401 < q _D < -55.413

Table 4.5: q intervals of RSSI values and mean values in these intervals

Hence A(0,0) is selected as the origin of the relative coordinate system in the calculations. Rx, Ry and β values for each transmitter are calculated by using R_{STD} and T_{STD} values. Corresponding adaptive RSSI values within their q intervals are presented in Table 4.6.

Transmitters	Rx	Ry	β	Adaptive RSSI values
A	-64	-63.66	0.747	-63.9
B	-61.68	-61.06	0.505	-61.38
C	-53.72	-52.88	0.335	-53.15
D	-56.54	-55.66	0.484	-56.1

Table 4.6: Calculated adaptive parameters and adaptive RSSI values of the object

Adaptive RSSI values are substituted in ITU-R indoor propagation model and corresponding d_{estimated} values are derived. d_{actual} object distances to transmitters are tabulated against d_{estimated} values together with their error distances for an example object location (2,3) in Table 4.7.

transmitter	d _{actual} (m)	d _{estimated} (m)	Error (m)
A	3.605	d _A = 3.92	0.29
B	3.16	d _B = 3.22	0.06
C	2.2	d _C = 1.71	0.49
D	2.8	d _D = 2.15	0.65

Table 4.7: Actual and estimated d distances to transmitters from object location (2, 3)

Coordinates of transmitters and object location with respect to relative coordinate system A(0,0) are given as; (x'_B, y'_B) = (3, 0), (x'_C, y'_C) = (3, 5), (x'_D, y'_D) = (0, 5), (x'_T, y'_T) = (x_T, y_T)

Trigonometric equations to calculate x'_T and y'_T can be written as:

$$(x'_T - 3)^2 + (y'_T - 0)^2 = d_B^2$$

$$(x'_T - 3)^2 + (y'_T - 5)^2 = d_C^2$$

$$(x'_T - 0)^2 + (y'_T - 5)^2 = d_D^2$$

x'_T and y'_T can be determined as:

$$x'_T = \frac{1}{6}(d_D^2 - d_C^2 + 9) \text{ and } y'_T = \frac{1}{10}(d_B^2 - d_C^2 + 25)$$

Estimated target coordinates with respect to the relative coordinate system can be calculated as $(x'_T, y'_T) = (1.77, 3.25)$ by using d values in Table 4.7. Consequently, in the universal coordinate system target location (x_T, y_T) is $(1.77, 3.25)$. It is concluded that the proposed system estimates the object coordinates of (2,3) in the universal coordinate system as $(1.77, 3.25)$ with an error distance of 0.34 m. Other object locations are estimated by using the proposed system. Selected results with an overall average error distance are presented in Table 4.8.

Object (x,y)	Estimated object locations	Error Distance(m)
1 , 1	1.72 , 1.91	1.16
2 , 2	2.70 , 2.84	1.09
3 , 4	2.75 , 4.764	1.05
2 , 1	1.51 , 1.82	0.96
1 , 3	1.52 , 3.30	0.60
2 , 3	1.77 , 3.25	0.34
3 , 1	2.40 , 1.56	0.82
2 , 4	2.76 , 3.20	1.10
Average error		0.9

Table 4.8: Estimated object locations and their error distances in phase 1.

4.6.2.2 Advanced RSSI correction phase (phase 2)

4 sets of 100 RSSI values named as $RSSI_A$, $RSSI_B$, $RSSI_C$, and $RSSI_D$ are recorded by the server through object receiver at an example location (1, 3). The mean and STD of these RSSI values are presented in Table 4.9. Minimum mean RSSI value is $RSSI_B = -66.766$ dBm as seen in Table 4.9 and the corresponding transmitter node at coordinates B(3,0) is chosen as the reference anchor node.

100 RSSI recordings (dBm) from A,B,C,D TRANSMITTERS at target location (1, 3)							
$RSSI_A$		$RSSI_B$		$RSSI_C$		$RSSI_D$	
mean	std	mean	std	mean	std	Mean	std
- 65.83	2.32	- 66.766	5.209	- 66.613	1.997	- 62.926	3.762

Table 4.9: STD and Mean values of 100 RSSI values at object location (1, 3) in phase 2.

An interval “q” is defined by the first \pm STD around the mean of 100 RSSI value. Another interval “Q” is defined by a second \pm STD around the mean of RSSI values in “q” interval of each A, B, C, D recordings. These q and Q intervals are tabulated together with their q_{MEAN} and Q_{MEAN} values and the number of RSSI values within q and Q intervals in Table 4.10.

Similarly, R_x , R_y , β values are calculated by utilising T_{STD}^1 and Q_{STD} values. Adaptive RSSI

Tx	q number of RSSI	q _{mean} (dBm)	q _{mean} ± q _{STD} interval RSSI	Q number of RSSI	Q _{mean} (dBm)	Q _{mean} ± Q _{STD} interval RSSI
A	61	-65.97	-68.136 < q < -63.477	33	-66.19	-67.30 < Q < -64.64
B	94	-65.66	-71.976 < q < -61.557	63	-65.42	-68.108 < Q < -63.224
C	69	-67.01	-68.612 < q < -64.614	42	-67.17	-68.017 < Q < -66.02
D	84	-62.38	-66.689 < q < -59.163	59	-62.37	-64.08 < Q < -60.69

Table 4.10: q and Q intervals, their mean and the number of RSSI values in these intervals

values are calculated by using equation (4.9). $d_{\text{estimated}}$ distances between transmitters and object receiver are determined by using adaptive RSSI values and ITU-R indoor propagation model. Finally, these $d_{\text{estimated}}$ distances are employed to estimate the object positions by using trigonometric methods. Experiments are repeated in phase 2 at different object locations. Selected results and the overall average distance error are presented in Table 4.11.

Object (x,y)	Estimated target locations	Error Distance(m)
1, 1	1.55, 1.66	0.85
2, 2	2.54, 2.61	0.81
3, 4	3.71, 3.34	0.96
2, 1	1.55, 1.52	0.69
1, 3	1.55, 3.65	0.85
2, 3	1.62, 3.35	0.36
3, 1	2.50, 1.45	0.67
2, 4	2.75, 4.70	1.02
Estimated error distance		0.77m

Table 4.11: Estimated target locations with EAL technique in phase 2.

Error distances obtained in Table 4.8 for phase 1 and in Table 4.11 for phase 2 are graphically displayed in Figure 4.7 for reader's attention.

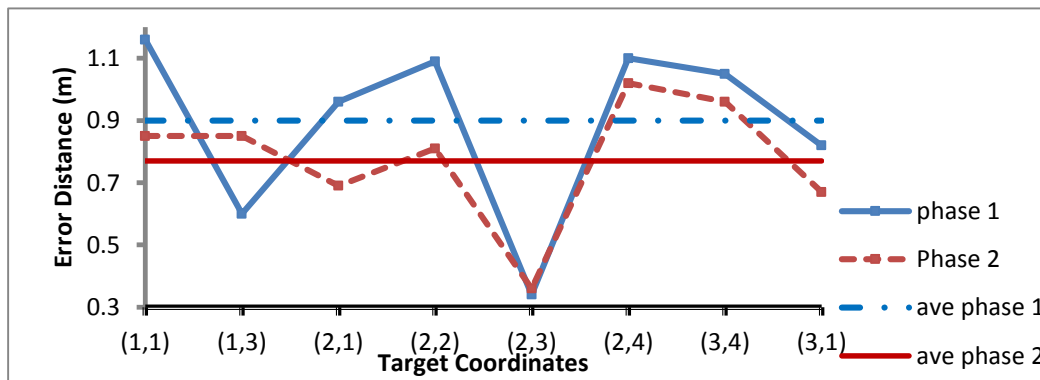


Figure 4.7: Graphical representation of error distances with respect to target locations in phase 1 and phase 2 stages

4.6.2.3 Different Indoor Topologies

Localisation experiments are repeated with EAL algorithm in other indoor areas such as a large student office, a corridor and a rest lounge. The large student office in Figure 4.8 has dimensions of 15mx8m. It contains various obstacles such as high partitions and dense furniture. The corridor is an area between offices and labs as shown in Figure 4.9. A section of it with dimensions 15mx2m is used during experiments. The rest lounge is a sitting area with complex topology and dimensions of 6mx8m as shown in Figure 4.10. It is an area where people have coffee breaks and it contains standard household furniture.

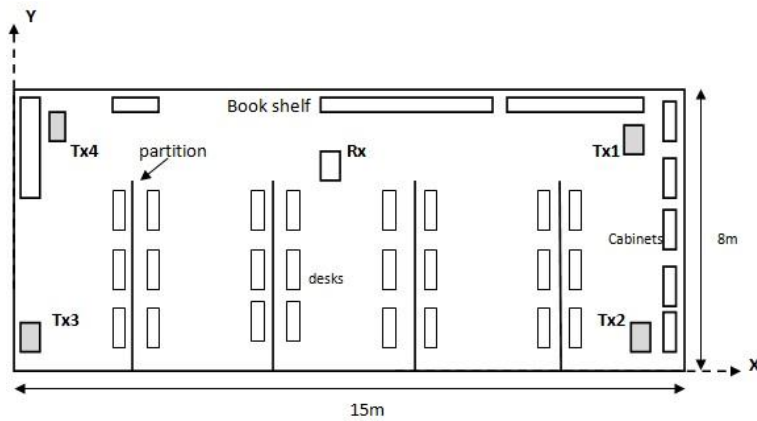


Figure 4.8: Large student office

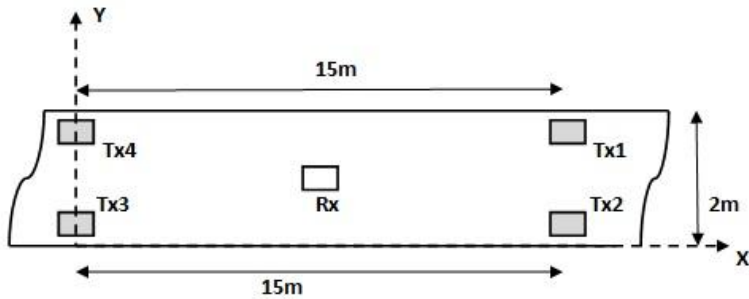


Figure 4.9: Corridor

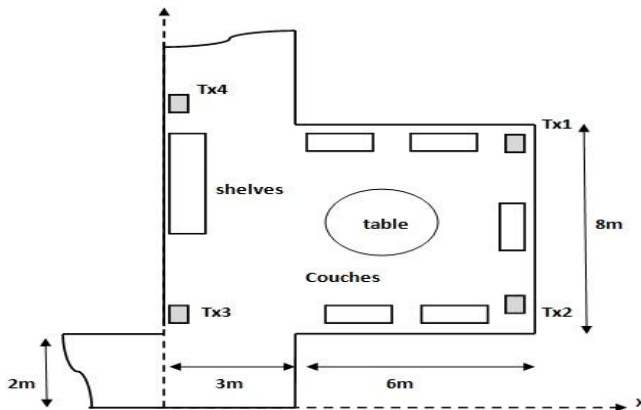


Figure 4.10: rest lounge

Experiments are repeated in these areas. 4 transmitters, Tx1 to Tx4, are strategically placed around the corners of the test areas. The object with a receiver travels around and collects LQI data at several locations to send to the server computer. LQI data is converted into RSSI data and RSSI data are adaptively corrected in phase 1 and phase 2 stages. Similarly, EAL algorithm is applied and transmitter node with minimum transmitted average RSSI value is selected as the reference anchor node across each test area. These nodes are taken as reference anchor nodes and each is identified as the origin of the relative coordinate system for each test area. Localisation calculations are carried out with these relative coordinate systems and final results are converted into the universal coordinate system in order to realise the actual target locations. A sample of estimated target locations with respect to error distances for the large student office in phase 1 and phase 2 is given in Table 4.12.

	PHASE 1		PHASE 2	
Object (x,y)	Estimated object locations	Error Distance(m)	Estimated object locations	Error Distance(m)
1 , 1	2.2 , 1.8	1.4	1.6 , 2.1	1.2
3 , 3	3.7 , 4.0	1.2	3.7 , 3.8	1.0
4 , 7	4.6 , 7.7	0.9	4.7 , 7.5	0.8
5 , 5	6.0 , 5.7	1.2	5.7 , 5.6	0.9
10 , 6	10.7 , 6.5	0.8	10.7 , 6.6	0.9
15 , 5	15.8 , 5.8	1.1	15.7 , 5.5	0.8
Average error distance		1.1m		0.91m

Table 4.12: Estimated object locations for large student office with EAL technique in phase 1 and 2

A sample of estimated object locations with respect to error distances is given in Table 4.13 for the corridor in phase 1 and phase 2. Similar object position estimations for the rest lounge are given in Table 4.14.

	PHASE 1		PHASE 2	
Object	Estimated object locations	Error	Estimated object locations	Error
1 , 1	1.8 , 1.9	1.2	2 , 1.5	1.1
3 , 3	3.9 , 3.5	1.0	3.5 , 2.2	0.9
4 , 2	4.7 , 2.8	1.0	4.6 , 2.6	0.8
5 , 1	5.7 , 0.6	0.8	4.5 , 1.5	0.7
10 , 2	10.5 , 1.2	0.9	10.5 , 2.7	0.8
12 , 1	12.6 , 1.5	0.7	12.5 , 1.4	0.6
Average error distance		0.94m		0.82m

Table 4.13: Estimated object locations for corridor with EAL technique in phase 1 and 2

	PHASE 1		PHASE 2	
Object (x,y)	Estimated object locations	Error Distance(m)	Estimated object locations	Error Distance(m)
2 , 3	2.9 , 4.0	1.3	3.0 , 3.7	1.2
3 , 5	3.6 , 6.1	1.2	3.7 , 5.9	1.1
3 , 8	3.7 , 8.9	1.1	3.6 , 8.8	1.0
4 , 6	4.8 , 6.5	0.9	4.5 , 6.7	0.8
6 , 6	7.0 , 6.6	1.1	6.8 , 7.5	0.9
7 , 6	7.7 , 6.8	1.0	7.6 , 6.5	0.7
Average error distance		1.1m		0.95m

Table 4.14: Estimated object locations for rest lounge with EAL technique in phase 1 and phase 2

It is observed that areas with uniform rectangular boundaries and fewer obstacles such as the small office room and the corridor between offices give better localisation accuracies with EAL algorithm. Average error distances are less with these indoor areas. Phase 2 results are always better than Phase 1 results. Large and complicated indoor topologies introduce higher positioning errors.

Finally, EAL algorithm is compared with other well known localisation algorithms in literature such as centroid (CL), weighted centroid (WCL), k-neighbourhood (k-NN) and weighted k-NN (W k-NN). The large student office is utilised in the experiments. A fingerprint map is constructed across the test area with a grid space of 1mx1m. Several object localisations are carried out and their average error distances are plotted with respect to algorithms. See Figure 4.11. It is observed that EAL algorithm gives better positioning accuracies compare to others across the same test area.

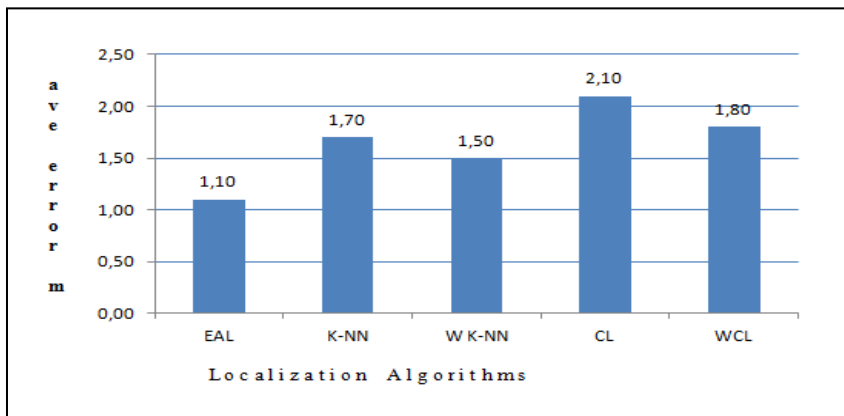


Figure 4.11: Comparison of EAL algorithm with other algorithms for large student office.

4.7 Conclusion

A novel environmentally adaptive localisation approach has been developed by using adaptive threshold factors. Random effects of the RSSI measurements were reduced in 2 phases by determining new ranges of RSSI values. Threshold factors were determined by using STD and mean values of recorded RSSI values from transmitters. Adaptive RSSI values are calculated by using these threshold factors and the RSSI values are used to calculate the estimated object distances with the ITU-R propagation model. In the literature, environmental

adaptivity is carried out with cooperation of WSNs. In this study, the originality lies with the application of static threshold factors instead of using any cooperation between WSNs. The application of 2nd phase is also an original feature. In this case, weighted threshold factor is calculated with weight functions by using distance values to transmitters. As a result, localisation accuracies are improved.

CL and its improved version WCL method are easy and cost effective methods to determine the object locations. Error distances around 1 meter are achieved with WCL method compared to error distances of 1 to 2 meters in literature with the same method. Weight functions are implemented by using d distances between transmitters and receivers.

Curve fitting on the received signal strengths and application of bi-sectioning algorithm are new implementations in WCL localisation procedures in this chapter. Bi-sectioning algorithm is applied on the fitted curve of LQI distribution at any object location to calculate the d distances between transmitters and object receivers.

An environmentally adaptive 2 phase localisation algorithm is deployed to determine the unknown object locations. This localisation algorithm has a good performance, better accuracy, stability and robustness. It is also adaptive to the concrete surroundings. In order to reduce the random variations between RSSI values, only a certain part of the recorded RSSI values are utilised in the calculations.

Mean and STD values of RSSI recordings at the object location are derived. An interval of \pm STD is defined around the mean value. This interval contains q number of RSSI values. β quantity is introduced to include the effects of indoor surroundings of the test area as environmental factors. In phase 1, β is a constant value and related to mean value of q number of RSSI values and to T_{STD} which is a static threshold STD. T_{STD} is generated as the average value of R_{STD} standard deviations of RSSI values, coming from transmitters at the object location.

This is a new concept to relate the environmental effects in the calculations in terms of T_{STD} . T_{STD} is compared with each R_{STD} corresponding to a transmitter and β value for each transmitter is calculated. These β values together with R_x and R_y values are utilised to derive the environmentally adaptive RSSI values. Adaptive RSSI values, corresponding to each transmitter, are deployed with ITU-R indoor propagation model to generate the respective d distance between each transmitter and the object receiver. Finally, trigonometric techniques are employed to calculate the object position coordinates.

In the proposed system, there is only one way communication between transmitters and receivers unlike other similar systems in literature. In phase 2, static T^1_{STD} is related to second

level Q_{STD} values in a weighted mechanism. New average distances are calculated between transmitters and object locations which are related to relevant Q_{STD} values in Q intervals.

EAL algorithm calculates the minimum RSSI mean value for each transmitter. This value is obtained as $RSSI_A$ in phase 1 and $RSSI_B$ in phase 2. Positions of these transmitters with minimum RSSI mean values are taken as the origins of relative coordinate systems. Localisation calculations are carried out with respect to these relative coordinate systems. The results are later transferred to the universal coordinate system.

Several indoor topologies are utilised to test EAL algorithms. Experimental areas are selected in the computer engineering department of Loughborough University, England. Experiments are repeated in different locations such as a small office, a large student office, a section of corridor and a rest lounge in the building.

The results show average localisation accuracy of 0.9 m in phase 1 and around 0.7 m in phase 2 for the small office. Average localisation accuracy along the corridor is 0.94m in Phase 1 and 0.82m in Phase 2. On the other hand, average localisation accuracy in the large student office is 1.1m in phase 1 and 0.91m in phase 2. Average localisation accuracy in the rest lounge is 1.1m in phase 1 and 0.95m in phase 2. In conclusion, these results reveal that EAL algorithm produces better positioning accuracies with error distances less than 1m in rectangular areas with fewer obstacles compared to indoor areas with complicated topology and denser obstacles. In areas with complex topology, EAL algorithm gives error distances just over 1m in phase 1 and just under 1m in phase 2. When EAL is compared with other algorithms across the same test area as shown in Figure 4.11, it also displays better localisation results.

Hence the technique introduced here is a simple, straight forward, cheaply implemented reliable technique which can be used in indoor localisations. Localisation procedures are not stopped at the end of phase 1. Introduction of phase 2 during localisation is justified by obtaining improved positioning accuracies compared to phase 1. The new proposed EAL technique is published in a journal [121]. Finally, the main contribution in this chapter can be identified as the application of 2 phase environmentally adaptive localisation by deploying static environmental threshold factors.

CHAPTER 5

LOCALISATION BY TRIANGULATION

5.1 Background

Wireless sensor node technology is a widely used technology to realise the object locations in different environments. It is employed for variety of indoor localisations (Lionel et al., 2004) [7]. There are many position identification systems using different technologies such as infrared [6], ultrasonic [11], Radio Frequency [8].

To define the exact coordinates of objects there is a need to measure the distances accurately between unknown object locations and known transmitter nodes. In general, RF technologies and received signal strength (RSS) values in different formats are utilised to determine the unknown locations. WSNs are strategically placed indoors and can be identified as transmitter nodes. A WSN receiver which is placed on a mobile object can receive the transmitted signal packets in the form of LQI values. These LQI values are transferred to an attached server through a wireless or wired link. They are placed in a database with respect to measurement coordinates across the test area.

Various search algorithms are utilised to compare the object LQI recordings with LQI recordings at measurement points. Any closeness between these two recordings determines the locations of object points. Search mechanism is generally applied across the total sensing area. The sensing area can be any shape or more importantly any size. Topological irregularities introduce many ambiguities in measurements. RSS data collection can be difficult and time consuming to realise. Hence, the localisation procedures take a longer time and a greater effort to determine the object locations.

k- NN, weighted k-NN, CL and WCL algorithms are a few popular algorithms for determining unknown object locations in a speedy and effective way. In order to reduce the search time and effort during object localisation procedures, an important method is introduced for deployment in the sensing area. Search areas across the sensing area can be reduced and the object search can be carried out in small sections of the sensing area.

Therefore the sensing area is divided into several sub areas in different shapes and sizes. This division is carried out according to the topology of indoor layout. Due to different architectural plans indoors, many sub areas in different shapes such as triangles, rectangles, trapezoids, can be organised. Object localisation is carried out within these sub areas. Finally, estimated object locations from these sub areas are combined together by using various trigonometric techniques to realise the unknown object location across the sensing area.

In this chapter, sensing area is divided into triangular shaped sub areas for simplicity and other shapes are unattended. Triangulation approach is introduced to calculate the object locations within triangular sub areas. Distances between unknown object and transmitter nodes are calculated by using curve fitting techniques and bi-sectioning algorithm on received LQI values. The technique offers reasonable localisation accuracies in indoor environments.

Radio signals propagate in spherical waves in free space. This propagation is slightly different indoors. A certain part of the signals are reflected back from the environment and generate a destructive effect when they arrive at destinations. Received signal amplitudes are randomised due to these effects and exhibit random behaviour. Nevertheless, free space propagation models are implemented in large indoor areas without many obstacles to determine the distances between transmitters and receivers.

Numerical techniques are employed to determine the object distances with respect to transmitters using RSS values. As the receiver gets closer to the transmitter, the signal strength increases and it decreases when it moves away from the transmitter. A weighting technique is introduced during localisation. The proposed localisation system consists of four main phases as shown in Figure 5.1.

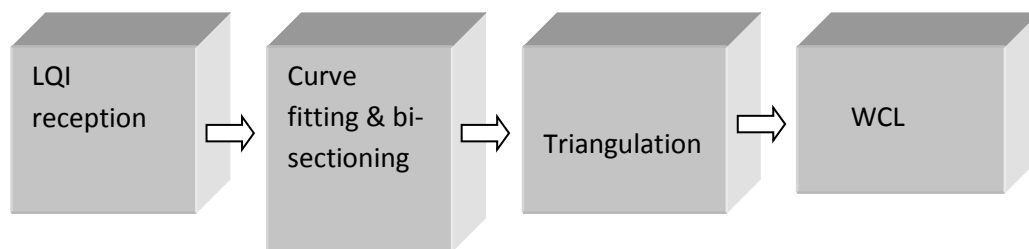


Figure 5.1: Block diagram of localisation system

5.2 LQI Reception

One way to identify the incoming radio signals is to use their RSSI values according to IEEE 802.11 standards. In many applications, RSSI has a high variance and localisation of unknown node becomes imprecise. Another method of distance determination is carried out by LQI of RF transmission. According to IEEE 802.15.4 standards, LQI is identified as the

strength of the received signal. It is proportional to RSSI and has a value between 0 to 255 (Ergen, 2004) [41]. Hence, RSSI values can be directly mapped into LQI values (Benkic et al., 2008) [132]. Transmitter nodes transmit the signal packets continuously. Mobile object receiver logs LQI of incoming signal packets and sends them to a server computer. Free space propagation model for recordings of LQI values against d distances is utilised. Reflections from surrounding minor obstacles are considered negligible. The indoor area, considered in this chapter, has a uniform layout and it is free of any major obstacles. Recorded LQI values are calibrated with respect to indoor d distances.

An example plot of LQI values arriving at a receiver node, (Rx), from a transmitter node, (Tx), with respect to distances between transmitter and receiver is presented in Figure 5.2.

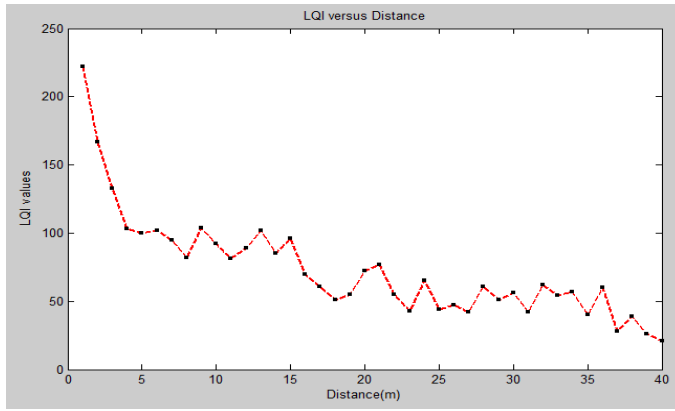


Figure 5.2: Plot of LQI values against d distances between Tx and Rx nodes in free space

During recordings, N number of LQI values where N=100 are taken at every recording point as seen in equation (5.1). The average of these values are deployed at that point in order to reduce the random effects of RF signals.

$$LQI_{AVR} = \frac{1}{N} \sum_{i=1}^N LQI_i \quad (5.1)$$

These LQI_{AVR} values are employed at every recording point in distance calculations and simply identified as “LQI values”.

5.3 Curve Fitting

The relationship between measured LQI values and distances between transmitters and receivers is an important part of the localisation. The relationship between LQI and distance d values can be expressed by using a plot of LQI versus d distances. Relationship between LQIs and d distances shows a close correlation during localisation procedures (Grossmann, 2007) [98]. A curve fitting technique is utilised to plot the curve fitted on previous example

distribution of recorded LQI values against d distances. This curve is an exponential curve fitted with 95% confidence boundaries on the recorded LQI values with MATLAB as seen in Figure 5.3.

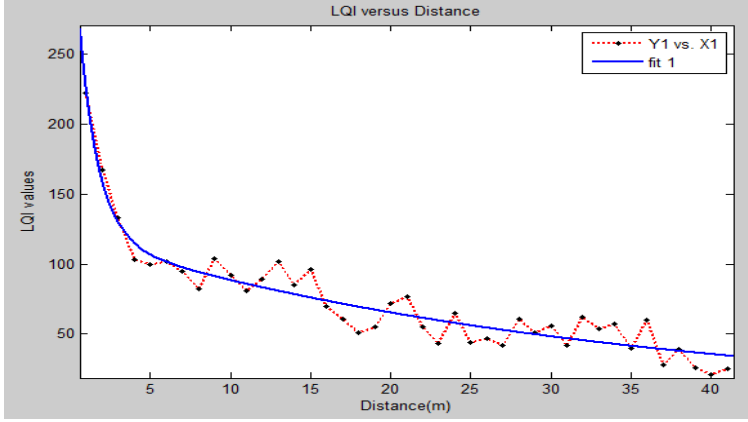


Figure 5.3: Exponential Curve fitted on LQI values by MATLAB

Fitted curve equation for the LQI data is presented in equation (5.2),

$$LQI(x) = a * \exp(b * x) + c * \exp(d * x) \quad (5.2)$$

where x is the d distance between a transmitter and a receiver and the equation constants are defined by

$$a = 247.4, \quad b = -0.827,$$

$$c = 119.8, \quad d = -0.036$$

A numerical analysis technique which is identified as a bi-sectioning algorithm is utilised to determine the distance between the unknown object receiver node and each transmitter node once its corresponding LQI value is known. This method is also called root finding method which repeatedly bisects the distance interval between transmitter and receiver.

Finally, the method selects a sub interval in which a root corresponding to an unknown distance must lie for further localisation procedures.

When an unknown LQI value is received from a transmitter and recorded in the computer, its corresponding $x=d$ value will be calculated by inserting this LQI value in equation (5.2) and applying the bi-sectioning algorithm.

Trigonometric techniques will be employed with these d values to determine the locations of the unknown object nodes. WCL technique will also be employed at a later stage to refine the calculated positions of the unknown nodes.

5.4 Triangulation

Block diagram of a rectangular test area is shown in Figure 5.4. LQI values are recorded by a receiver on the mobile object and corresponding d distance for each LQI value is calculated by using the above mentioned numerical method. Unknown object node, $P(x,y)$, could be anywhere in the test area. $P(x,y)$ is identified as the position of the mobile object and it has 4 d values (d_A, d_B, d_C, d_D) at every location corresponding to their LQI values.

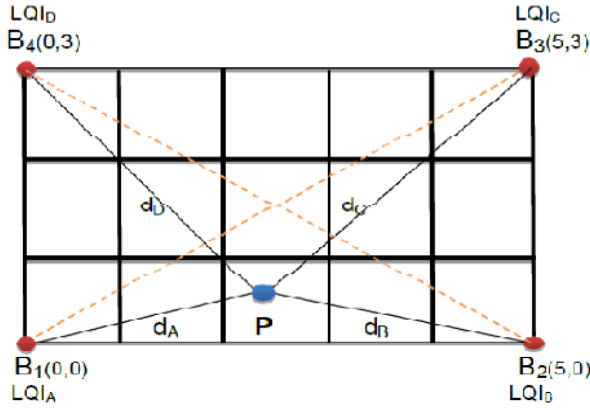


Figure 5.4: Test area with triangles, object P and transmitters B_i

Trigonometric equations corresponding to x and y coordinates of object P in $B_1B_2B_3B_4$ test area can be given by

$$x^2 + y^2 = d_A^2 \quad (5.3)$$

$$(5-x)^2 + y^2 = d_B^2 \quad (5.4)$$

$$(5-x)^2 + (3-y)^2 = d_C^2 \quad (5.5)$$

$$x^2 + (3-y)^2 = d_D^2 \quad (5.6)$$

B_1B_2 is along the x axis and B_1B_4 is along the y axis with $B_1(0, 0)$ is the coordinate centre. Trigonometric solution of these equations in terms of known d distances realises the object coordinates (x, y) . This is the first stage of object location estimation and identified as trigonometric calculation stage.

5.4.1 Triangular area Formation

The test area is divided into maximum number of sub areas in the form of triangles. The only condition is the existence of 3 transmitter nodes in each triangle at triangle corners. Coordinates of the unknown object $P(x, y)$ are calculated with respect to these triangles. There are 4 triangular sub areas in the rectangular test area which are $B_1B_2B_4$, $B_1B_2B_3$, $B_1B_3B_4$ and

$B_2B_3B_4$ as seen in Figure 5.5. The unknown object node could be in any one of these triangles. Estimated object coordinates are identified as $P'(x, y)$ in this first stage.

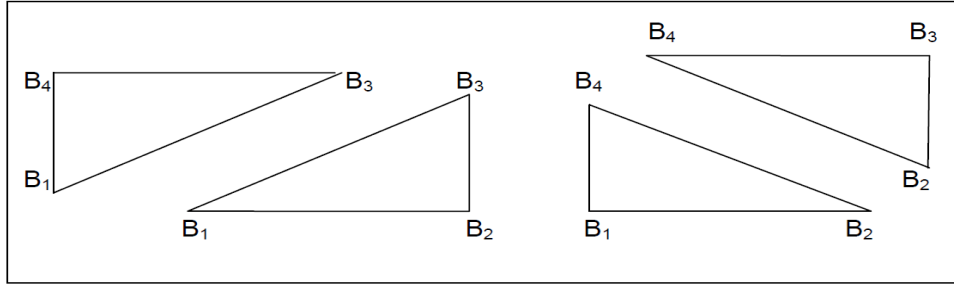


Figure 5.5: Four triangle sub areas across the test area.

$P'(x,y)$ coordinates can be inside or outside of any triangle across the test area. These coordinate equations for both cases are found to be the same as long as d values in both cases are different. A typical example can be shown for $B_1B_3B_4$ triangle in Figure 5.6. In this study object coordinates are always considered in a triangle. Because if they are outside of a triangle they will always be inside of another adjacent triangle across the test area.

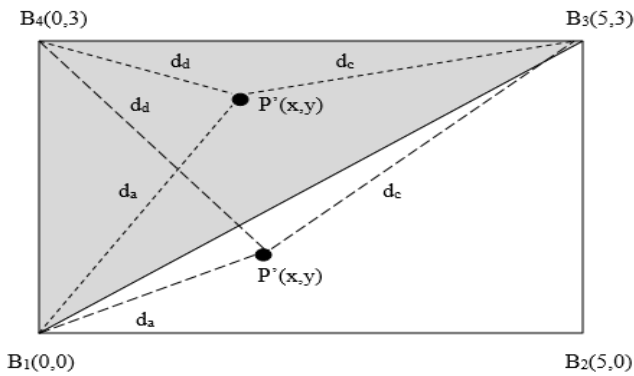


Figure 5.6: Block diagram of $B_1B_4B_3$ triangle and estimated $P'(x,y)$ point is shown inside and outside the triangle

For example, an estimated object point $P'(x, y)$ across the $B_1B_2B_3B_4$ test area can be inside $B_2B_1B_4$ and $B_1B_4B_3$ triangles as seen in Figure 5.7. But the same estimated object point is also outside the $B_2B_3B_4$ and $B_1B_2B_3$ triangles.

Estimated object location can be calculated whether it is inside or outside of any triangle. The resultant coordinates will be determined for a particular triangle. Hence, estimated object coordinates are determined for each triangle as shown here. Coordinates of $P'(x,y)$ in Figure 5.7 can be identified as follows.

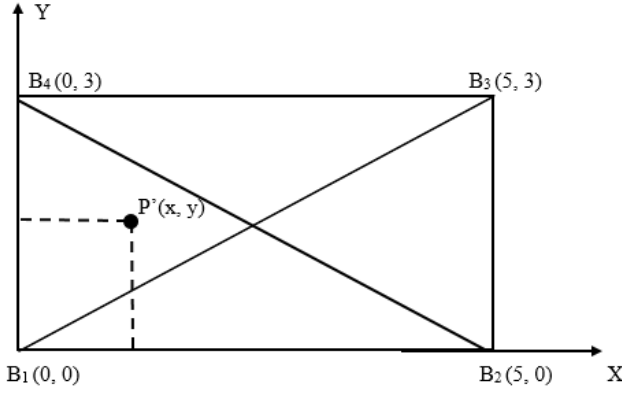


Figure 5.7: Position of estimated object point $P'(x,y)$ with respect to triangle areas

$P'_4(x,y)$ is outside $B_2B_3B_4$ triangle and calculated as:

$$P'_4(x, y) = \left(\frac{d_d^2 - d_c^2 + 25}{10}, \frac{d_b^2 - d_c^2 + 9}{6} \right) \quad (5.7)$$

$P'_3(x,y)$ is inside $B_1B_4B_3$ triangle and calculated as:

$$P'_3(x, y) = \left(\frac{d_d^2 - d_c^2 + 25}{10}, \frac{d_a^2 - d_d^2 + 9}{6} \right) \quad (5.8)$$

$P'_2(x,y)$ is outside $B_1B_2B_3$ triangle and calculated as:

$$P'_2(x, y) = \left(\frac{d_a^2 - d_b^2 + 25}{10}, \frac{d_b^2 - d_c^2 + 9}{6} \right) \quad (5.9)$$

$P'_1(x,y)$ is inside $B_2B_1B_4$ triangle and calculated as:

$$P'_1(x, y) = \left(\frac{d_a^2 - d_b^2 + 25}{10}, \frac{d_a^2 - d_d^2 + 9}{6} \right) \quad (5.10)$$

d_a, d_b, d_c, d_d distance values which are deployed here are the estimated object distances to A,B,C,D transmitters corresponding to B_1, B_2, B_3, B_4 corners of the test area while calculating $P'(x,y)$ in Figure 5.7. Hence, estimated object coordinates can be numerically calculated by substituting object's estimated d distances, (d_a, d_b, d_c, d_d) , with respect to transmitters into equations (5.7) to (5.10).

It can be concluded that unknown object location $P(x,y)$ is estimated for each triangle and these 4 estimated object locations corresponding to $P(x,y)$ are defined as $P'_1(x,y)$, $P'_2(x,y)$, $P'_3(x,y)$ and $P'_4(x,y)$.

5.5 Weighted Centroid Localisation

WCL technique is deployed to improve the localisation accuracies a stage further in the proposed system. It introduces weights in localisation procedures (Blumenthal et al. 2007) [111]. Weight function is defined by w_{ij} and it is expressed in terms of distances between the estimated object $P'(x,y)$ and transmitter nodes as given in equation (4.2). Graphical representations of an example triangle and $P'(x,y)$ estimated object point whether it is inside or outside the triangle are shown in Figure 5.8.

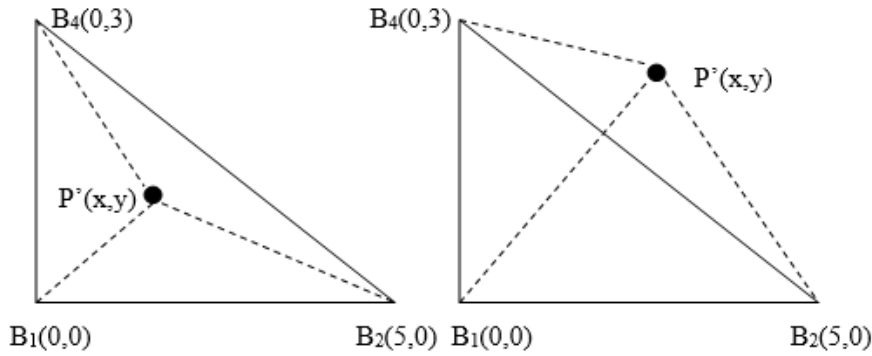


Figure 5.8: Graphical representation of $B_2B_1B_4$ triangle and estimated $P'(x, y)$ point inside and outside the triangle

Distances between $P'(x,y)$ and the corners of the corresponding triangle are calculated and utilised to derive the weights. Weighted coordinates of the estimated object locations, $P'(x,y)$, are calculated with equation (4.4). This stage is identified as second stage.

A new object location, $Q'(x,y)$, is calculated as an example by using weighted estimated object location for $B_1B_2B_4$ triangle as shown in equation (5.11).

$$Q'_1(x, y) = \frac{\frac{1}{P'B_1}(0,0) + \frac{1}{P'B_2}(5,0) + \frac{1}{P'B_4}(0,3)}{\frac{1}{P'B_1} + \frac{1}{P'B_2} + \frac{1}{P'B_4}}. \quad (5.11)$$

$P'B_1$, $P'B_2$, $P'B_3$ and $P'B_4$ are distances between the estimated object location $P'(x,y)$ and the relevant triangle corners. $Q'(x, y)$ weighted estimated object location is calculated for each triangle. Finally, resultant estimated object coordinates are calculated as the average value of 4 $Q'(x, y)$ coordinates as shown in equation (5.12).

$$Q(x, y) = \frac{1}{4} \sum_{j=1}^4 Q'_j(x, y) \quad (5.12)$$

Position error e is the distance between the actual object position $P(x, y)$ and the estimated object position $Q(x_e, y_e)$. It is expressed as

$$e = \sqrt{(x - x_e)^2 + (y - y_e)^2} \quad (5.13)$$

Positions of several unknown object locations are determined with the proposed system and their error margins with respect to actual object positions are calculated with equation (5.13).

5.6 Implementation:

JENNIC JN5139 wireless sensor nodes are deployed in the experiments. Zigbee Home Sensor demo program is utilised to program JN5139 active devices to work as fixed transmitter nodes and mobile receiver nodes. The test bed is on an empty floor with a rectangular area of 5m x 3m. Any position in the rectangular test area is implemented as an object position $P(x, y)$.

Transmitters are placed at 4 corners of the test area. The unknown object with receiver is positioned at any point in the test area and interfaced to a computer. Object receiver receives 4 LQI readings from 4 transmitters and transfers them to a database in the server. An application program, (AP), has been developed to control the entire data manipulation and calculation process.

AP measures 4 LQI values at every unknown location of the mobile object and calculates their 4 corresponding d values, (d_A , d_B , d_C , d_D) by using bisectioning algorithm and exponentially fitted curves on LQI distributions. See Table 5.1.

Unknown (x,y) position coordinates	LQI values of mobile node at unknown positions				d values calculated with bisectioning algorithm for each LQI values (m)			
	LQI _A	LQI _B	LQI _C	LQI _D	d _A	d _B	d _C	d _D
1, 1	109	115	115	140	3.43	2.97	2.97	2.03
1, 2	110	110	110	150	3.43	3.43	3.43	1.18
2, 1	113	129	111	123	3.40	2.35	3.42	2.65
3, 0	113	125	109	130	3.40	2.34	3.43	2.34
3, 2	112	140	108	120	3.41	2.03	3.43	2.66
4, 1	113	121	117	111	3.40	2.65	2.96	3.43

Table 5.1: A sample of Recorded LQI values and corresponding d values.

5.6.1 Position estimation by triangulation

This is the 1st stage of localisation. Once 4 d values are calculated for each unknown location, they are utilised to calculate the estimated object coordinates $P'_1(x, y)$, $P'_2(x, y)$, $P'_3(x, y)$, $P'_4(x, y)$ by considering 4 triangles across the test area. Equations (5.7) to (5.10) are used during the calculations and estimated object coordinates are tabulated in Table 5.2.

Unknown (x,y) position coordinat	P' ₁ , P' ₂ , P' ₃ , P' ₄ estimated positions calculated by using trigonometric methods			
	P' ₁ (x , y)	P' ₂ (x , y)	P' ₃ (x , y)	P' ₄ (x , y)
1 , 1	2.7 , 2.77	2.81 , 1.5	2.03 , 2.78	2.03 , 1.5
1 , 2	2.5 , 3.21	2.4 , 1.5	1.44 , 3.24	1.45 , 1.5
2 , 1	3.13 , 2.29	3.13 , 0.45	2.02 , 2.27	2.01 , 0.44
3 , 0	3.13 , 2.53	3.13 , 0.44	1.85 , 2.55	1.84 , 0.43
3 , 2	3.24 , 2.27	3.24 , 0.21	2.02 , 2.28	2.02 , 0.21
4 , 1	2.96 , 1.5	2.95 , 1.20	2.78 , 1.5	2.78 , 1.20

Table 5.2: P'(x,y) estimated object coordinates for each triangle test area in first stage

5.6.2 WCL Calculations:

This is the 2nd stage of localisation. Weighted centroid localisation technique is introduced with the estimated P'(x, y) points. Distances between P'(x, y) and the corners of the corresponding triangle are calculated and used in weight calculations during final recalculation of P(x, y) values. These distance values are tabulated in Table 5.3;

Unknown locations	Calculated P'(x,y) points and their distances to respective triangle corners			
	P' ₁ (2.7,2.7)	P' ₂ (2.8,1.5)	P' ₃ (2.0,2.7)	P' ₄ (2.0,1.5)
(1,1)	da=3.94	da=3.17	da=3.44	dc=3.32
	db=3.54	db=2.66	dc=2.97	db=3.32
	dd=2.8	dc=2.66	dd=2.04	dd=2.52
(1,2)	P' ₁ (2.5,3.2)	P' ₂ (2.4,1.5)	P' ₃ (1.4,3.2)	P' ₄ (1.4,1.5)
	da=4.09	da=2.91	da=3.55	dc=3.84
	db=4.09	db=2.91	dc=3.55	db=3.84
	dd=2.51	dc=2.91	dd=1.47	dd=2.09
(2,1)	P' ₁ (3.1,2.2)	P' ₂ (3.1,0.4)	P' ₃ (2.0,2.2)	P' ₄ (2.0,0.4)
	da=3.88	da=3.16	da=3.05	dc=3.92
	db=2.95	db=1.92	dc=3.05	db=3.00
	dd=3.21	dc=3.16	dd=2.14	dd=3.25
(3,0)	P' ₁ (3.1,2.5)	P' ₂ (3.1,0.4)	P' ₃ (1.8,2.5)	P' ₄ (1.8,0.4)
	da=4.04	da=3.16	da=3.16	dc=4.04
	db=3.16	db=1.92	dc=3.16	db=3.16
	dd=3.16	dc=3.16	dd=1.92	dd=3.16
(3,2)	P' ₁ (3.2,2.2)	P' ₂ (3.2,0.2)	P' ₃ (2.0,2.2)	P' ₄ (2.0,0.2)
	da=3.99	da=3.27	da=3.05	dc=4.07
	db=2.87	db=1.74	dc=3.05	db=2.98
	dd=3.34	dc=3.27	dd=2.14	dd=3.44
(4,1)	P' ₁ (2.9, 1.5)	P' ₂ (2.9,1.2)	P' ₃ (2.7,1.5)	P' ₄ (2.7,1.2)
	da=3.33	da=3.21	da=3.17	dc=2.83
	db=2.51	db=2.35	dc=2.66	db=2.50
	dd=3.33	dc=2.70	dd=3.17	dd=3.32

Table 5.3: Distances between P'(x, y) and respective triangle corners

P'(x, y) coordinates are weighted by using relevant d values in Table 5.3 and identified as Q(x, y). Each unknown object location has 4 Q(x, y) values which are obtained by using WCL technique. Hence, the average of 4 Q(x, y) values is considered as the final position coordinates of the unknown object location.

A sample of them is presented for the reader as shown in Table 5.4. Experiments are repeated with many unknown object locations. Error calculations from all unknown positions revealed an average error distance of 1.1m as shown in Table 5.4.

Unknown locations	$Q_1(x,y)$	$Q_2(x,y)$	$Q_3(x,y)$	$Q_4(x,y)$	Ave= $(Q_1+Q_2+Q_3+Q_4)/4$	Error (m)
(1, 1)	1.5, 1.1	3.5, 1.0	1.5, 2.2	3.0, 2.0	2.4, 1.6	1.5
(1, 2)	1.3, 1.3	3.3, 1.0	1.1, 2.3	2.6, 2.2	2.1, 1.7	1.3
(2, 1)	1.8, 1.0	3.6, 0.8	1.4, 2.1	3.2, 1.8	2.5, 1.4	0.6
(3, 0)	1.7, 1.0	3.6, 0.8	1.3, 2.1	3.2, 1.9	2.5, 1.5	1.5
(3, 2)	1.9, 0.9	3.7, 0.7	1.4, 2.1	3.3, 1.8	2.6, 1.4	0.7
(4, 1)	1.9, 0.9	3.5, 1.0	1.8, 2.0	3.5, 1.8	2.7, 1.4	1.3
Total average error						1.1

Table 5.4: Calculated object position coordinates and their error margins in second stage

5.6.3 Different Test Area Shapes

Other simple shape test areas besides the rectangle can be studied with triangular sub areas. Some of these test area shapes can be square, trapezoid, pentagon, circle etc. Triangular sub sections can be arranged with respect to transmitter locations in these test areas. The area between 3 transmitters is identified as a triangle sub area across the test area. The shapes of these test areas are displayed in Figure 5.9. Hence, transmitters are organised in such a way that triangle sub areas are generated across the test areas in Figure 5.9.

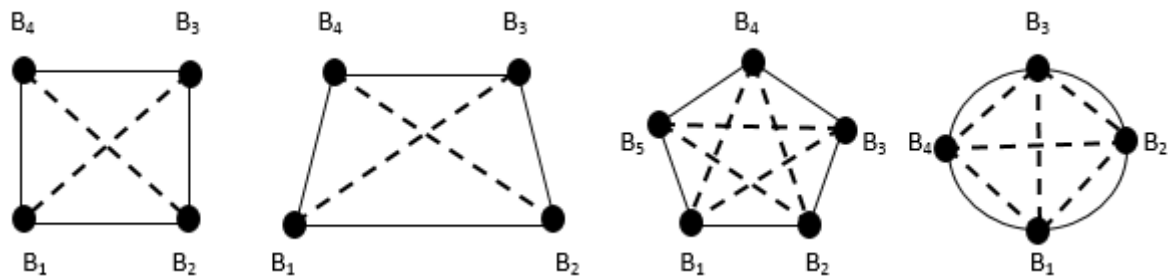


Figure 5.9: Different shaped test areas with transmitters B_i (i : number of transmitters)

Localisation procedures can be repeated with these sub areas and object coordinates can be estimated for each triangle sub area in 2 stages. Final estimated object coordinates are calculated by averaging the estimated weighted object coordinates which are obtained from all the triangle sub areas in a particular test area.

Another alternative is the segmentation of the test area. Rectangular or square sub segments can be organised across the test area according to its topology. Triangular sub areas can be arranged in segments and the triangulation technique can then be applied across each segment.

5.7 Discussions

In this chapter, a particular segmentation, identified as triangulation, was deployed across the test area. Triangle sub areas were organized with transmitter nodes at the triangle corners and these nodes must be at test area boundaries. No other shapes besides triangles are allowed in this technique. Unknown object receiver distances to transmitters were employed to calculate the estimated object coordinates $P'(x, y)$ in first stage. In second stage, these estimated object coordinates were weighted with the distances between $P'(x, y)$ and the triangle corners and the new estimated object coordinates $Q(x, y)$ were calculated. Their average gives the final estimated location of the object $P(x, y)$.

Finally, this triangular sub-sectioning method is a newly introduced technique. Test area is divided into only triangular areas and the object location estimation was carried out with respect to all the triangles not just in one sub area as in segmentation. The effects of all the other triangles are included in the calculations. The error distance was around 1m during the experiments which is approximately equal to grid spacing.

5.8 Conclusions:

Unknown object locations were determined by introducing triangle shaped sub areas across the test area. A combined triangulation and weighted approach was deployed. The test area was divided into sub areas in the shape of triangles and unknown position coordinates were calculated with respect to each triangle.

Other shapes and sizes of test areas can also be utilised indoors. But these shapes must be divided into triangle areas with a transmitter node at its corners. In this study, they are left unattended. During the first stage, each unknown object position (x, y) , is estimated 4 times for 4 triangle sub areas.

Initially, received LQI values are calibrated in free space with respect to distances between transmitter and receiver nodes. Bisection algorithm is utilised and the distances between transmitters and receivers are calculated by using the generated fitted calibration curve.

In second phase, WCL technique is employed with the estimated object coordinates in the first stage. Distances between the estimated object coordinates in first stage and the corners of respective triangles are utilised in weight calculations. Finally, estimated object coordinates are weighted with respect to estimated object distances to transmitters.

The average error distance between the unknown object locations and final estimated object locations is found to be 1.1 m. This is similar to the localisation error values mentioned in the

literature. For example in (Bal et al. 2010) [116], average accuracy is 1-2m under similar conditions indoors.

In (Sugano et al. 2006) [101], the accuracies are around 1.5-2m. The accuracies obtained in this proposed system are at the lower end of the accuracy ranges for similar localisation systems in the literature.

Finally, triangular segmentation and trigonometric methods together with WCL method produce a hybrid technique of position calculation. Realisation of this hybrid technique and determination of distances between transmitters and receivers by a numerical analysis technique are two new approaches in localisation procedures. Localisation accuracies obtained are very compatible with the results in the literature.

Hence, the triangulation technique and 2 stage localisation introduced here are the main contributions in this chapter. Object location is estimated by using distances calculated with bisectioning algorithm in 1st stage and it is re-estimated in 2nd stage by introducing a triangular weight mechanism. It is an acceptable new technique for position detection indoors. This study is published as a research paper in a journal [44].

CHAPTER 6

LOCALISATION BY USING REFERENCE NODES

6.1 Background

Localisation of wireless sensor nodes and tracking mobile targets with the help of wireless sensor networks have become two important areas in position detection technology [21, 22].

Localisation involves determining the location of a sensor node depending on other sensor nodes across the sensing area. Tracking mobile targets involves finding out the location of mobile targets based on WSNs with known positions. A number of WSNs are utilised as transmitters and receivers and some others with fixed locations are identified as reference nodes. These reference nodes assist in finding the target location together with transmitters and receivers. Hence the location of a mobile target can be detected easily by using the distributed reference (anchor) nodes without using any additional hardware.

Different algorithms are utilised with received radio signal amplitudes once they are received and stored in a database. k-Nearest Neighbourhood algorithm, (k-NN), is the most commonly used algorithm to determine the unknown target locations together with a weight mechanism between a target and reference node positions. At present, there are many types of location sensing systems each having their own strengths and limitations. RFID technology has several advantages over the others [32]. The most important advantage is their operation ability under difficult environmental conditions [33,122].

The LandMarc localisation system, developed by (Lionel et al. 2004) [7], uses a number of fixed location transmitters as reference nodes across the test area. Object transmitters move among the reference nodes, transmitters have known locations, and the receivers are strategically placed around the boundaries of the test area.

Receivers receive transmissions from object transmitters and reference node transmitters. They convert the received RF signals into a known format such as RSSI or LQI and transfer them to a local computer. Localisation algorithms are applied to these received and stored RSSI or LQI values to determine the closest reference node position to the object location.

Environmental effects interfere with the received signals and generate incorrect signal readings. In this chapter, correction procedures are introduced for these effects and distance calculations are improved during localisation.

A localisation approach based on the application of reference nodes is introduced in this chapter. The aim is to implement a system by using reference node transmitters with known locations to calculate object locations easily. Correction procedures are included to achieve high localisation accuracies. Secondly, a new weight mechanism is introduced between transmitter and receiver nodes. Weights are related to environmental conditions and by applying carefully designed weight functions object locations are calculated more accurately. Weights are generated by utilising both signal distances and real distances between transmitters and receivers. A different topology with less number of reference nodes compared to the LandMarc system is introduced. Localisation accuracies are improved by utilising a new approach of using 2 stage k-NN algorithms.

6.2 Reference Node Topology

In the classical LandMarc system, localisation accuracies are increased without introducing extra receivers (readers). Fixed location reference transmitter nodes are introduced instead to produce a location calibration. This approach helps to offset many environmental effects that contribute to signal deterioration since the reference nodes are also subject to the same effects in the environment. This is a costly approach due to the cost of extra reference transmitters. Scientists are trying to find a way to reduce the cost by reducing the number of reference transmitters with same accuracy levels.

In the LandMarc system, there are n receivers, m reference node transmitters and k number of object transmitters in the sensing area. Reference node transmitters are uniformly distributed across the sensing area and receivers are placed at locations where the transmitters can send RF signals comfortably as seen in Figure 6.1.

Transmitted signal strength vector of the reference node transmitters is

$$\vec{R}_i = (T_1, T_2, T_3, \dots, T_m) \quad \text{where } i \in (1, n)$$

\vec{R}_i is the signal strength of m reference node transmitters received by receiver i .

Transmitted signal strength vector of the object transmitter can be shown as:

$$\vec{O}_j = (S_1, S_2, S_3, \dots, S_n). \quad \text{where } j \in (1, k)$$

\vec{O}_j is the signal strength of j^{th} object transmitters received by receiver i , where $i \in (1, n)$.

Euclidean distance E with signal strengths, between \vec{O}_j and \vec{R}_i vectors is calculated. E represents the location relationship between reference node transmitters and object transmitters. Signal distance difference between the nearest reference node transmitter and object transmitter corresponds to smallest E value.

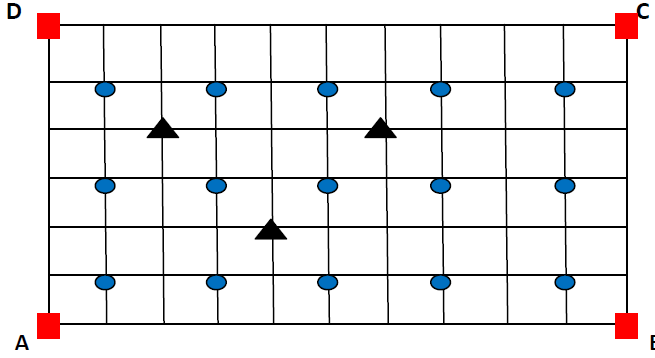


Figure 6.1: Schematic view of Landmark system. Square: Receivers, Circle: reference node transmitters, Triangle: object transmitters

Hence if there are m reference node transmitters and one object transmitter, \vec{E} vector between them can be defined as

$$\vec{E}_i = \{E_1, E_2, E_3 \dots E_m\}$$

k-NN algorithm is utilised to find the unknown object transmitter's nearest reference node neighbours by comparing different E values. Generally, 4-NN algorithm is employed in nearest neighbourhood calculations. In this study, 3-NN algorithm is preferred in order to use additional simple triangulation methods during object position calculations.

Large number of reference node transmitters introduces a large amount of signal variations, heavy computation time and an increase in equipment cost. It is ideal to reduce the number of these nodes and in return employ software techniques to reduce the localisation errors. A new reference node topology is introduced in star formation with less reference nodes as seen in Figure 6.2.

Initially, a database is generated by the received signal strengths from reference node transmitters with respect to their coordinates. Object transmitter signal strengths are compared with the database and 3 smallest Euclidean distances which correspond to the 3 nearest reference node transmitters are determined. Coordinates of these reference node transmitters are averaged out to give the estimated object coordinates as shown in equation (6.1).

$$(x, y) = \frac{1}{3} \cdot \sum_{i=1}^3 (x_i, y_i) \quad (6.1)$$

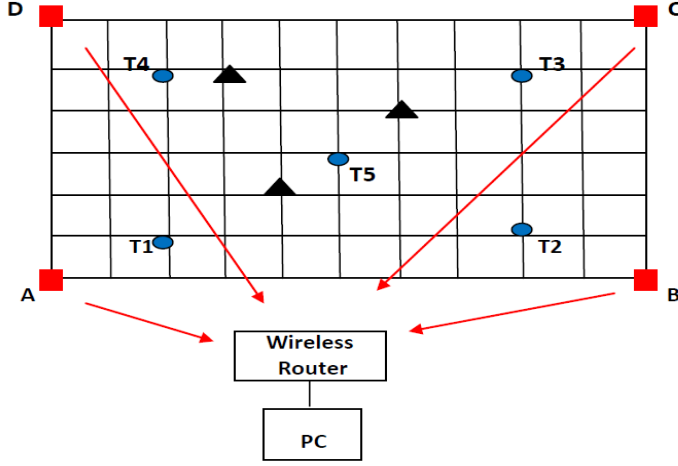


Figure 6.2: Applied reference node topology. Square: A,B,C,D Receivers, Circle: T₁,T₂,T₃,T₄,T₅ reference transmitters, triangle: objects

Introducing a weight function to i^{th} reference node transmitter is another design factor. The object transmitter has different weights depending on the 3 nearest neighbourhood reference node transmitters. Hence w_i is a function of E values for the object transmitter corresponding to the 3 nearest neighbourhood reference nodes. Empirically it is defined in equation (6.2) [44].

$$w_i = \frac{1}{\frac{E_i^3}{\sum_{i=1}^3 \frac{1}{E_i^3}}} \quad (6.2)$$

Hence, estimated object coordinates are given by

$$(x, y) = \sum_{i=1}^3 w_i(x_i, y_i) \quad (6.3)$$

6.3 Improved LandMarc Localisation

3 Localisation procedures are utilised starting from recording the received signals until the determination of object locations. In each stage different algorithms are employed to obtain the final position of the object.

6.3.1 Classical LandMarc

This stage describes the *classical LandMarc technique*. 3 nearest reference nodes to the object can be determined by using 3-NN algorithm and their coordinates are deployed to estimate the unknown object coordinates (x,y). This deployment is carried out by using weight functions shown in equation (6.2). Weight functions are applied between the object

and 3 nearest reference nodes by using Euclidean distances between them. Weighted object coordinates (x, y) are calculated accordingly with equation (6.3).

6.3.2 Improved LandMarc

In this stage the *improved LandMarc technique* is described. Each of 3 *nearest reference nodes* is considered and its 3 *trigonometrically closest reference nodes* are utilised. Consequently, each *nearest reference node* now has 3 *closest reference nodes* among the total reference nodes across the sensing area.

For example, if the *nearest reference nodes* to the unknown object in the first stage are determined as T_1 , T_4 and T_5 than the closest reference nodes of T_1 are T_2 , T_5 , T_4 in the second stage as seen in Figure 6.2. Similarly;

Closest reference nodes of T_4 are T_1 , T_5 , T_3 ,

Closest reference nodes of T_5 are T_1 , T_2 , T_3 , T_4 as a special case.

A new object coordinate estimation method can be introduced by using previously determined *closest reference nodes*. Weights are calculated by using the Euclidean distances between the nearest and closest reference nodes. If the nearest node is T_1 and its closest nodes are T_2 , T_4 and T_5 , Euclidean distances for T_1 become;

Euclidean distance between T_1 and T_2 is E_{12} ,

Euclidean distance between T_1 and T_4 is E_{14}

Euclidean distance between T_1 and T_5 is E_{15} .

Euclidean distances for other nearest nodes can also be determined similarly.

Hence the *new estimated nearest reference node* coordinates for T_1 can be expressed with a weight mechanism deploying above Euclidean distances by using equation (6.4).

$$(x', y') = \sum_{i=1}^3 w_i(x_i, y_i) \quad (6.4)$$

Similarly, this can be repeated for each reference node transmitter T_2 , T_3 , T_4 . The only exception is the *new estimated nearest reference node* coordinates for T_5 . It can be expressed as:

$$(x', y') = \sum_{i=1}^4 w_i(x_i, y_i) \quad (6.5)$$

This is because there are 4 *closest reference nodes* for the *nearest reference node* T_5 . Consequently there will be 4 Euclidean distances and 4 weights in position calculations.

New estimated nearest reference node coordinates with respect to $T_1(x_1, y_1)$ with its *closest reference nodes* $T_2(x_2, y_2)$, $T_4(x_4, y_4)$, $T_5(x_5, y_5)$ can be given as:

$$T(x'_1, y'_1) = \frac{\frac{1}{E_{12}^2}}{\frac{1}{E_{12}^2} + \frac{1}{E_{14}^2} + \frac{1}{E_{15}^2}}(x_2, y_2) + \frac{\frac{1}{E_{14}^2}}{\frac{1}{E_{12}^2} + \frac{1}{E_{14}^2} + \frac{1}{E_{15}^2}}(x_4, y_4) + \frac{\frac{1}{E_{15}^2}}{\frac{1}{E_{12}^2} + \frac{1}{E_{14}^2} + \frac{1}{E_{15}^2}}(x_5, y_5) \quad (6.6)$$

Hence, if the *nearest reference nodes* to the unknown object, determined in the first stage, are T_1 , T_4 and T_5 then the *new estimated nearest reference node* coordinates are calculated with their closest reference nodes and given as $T_1(x'_1, y'_1)$, $T_4(x'_4, y'_4)$ and $T_5(x'_5, y'_5)$.

A difference parameter, $(\Delta x, \Delta y)$, is introduced between the *nearest reference node coordinates* $T_1(x_1, y_1)$, $T_4(x_4, y_4)$, $T_5(x_5, y_5)$ in stage 1 and the *new estimated nearest reference node coordinates* $T_1(x'_1, y'_1)$, $T_4(x'_4, y'_4)$, $T_5(x'_5, y'_5)$ in stage 2. These are shown as;

$$(\Delta x_1, \Delta y_1) = (x_1, y_1) - (x'_1, y'_1)$$

$$(\Delta x_4, \Delta y_4) = (x_4, y_4) - (x'_4, y'_4)$$

$$(\Delta x_5, \Delta y_5) = (x_5, y_5) - (x'_5, y'_5)$$

These differences are considered as the variation of *nearest reference node* coordinates. Their average values are defined as:

$$(e_x, e_y) = \left\{ \frac{1}{3}(\Delta x_1 + \Delta x_2 + \Delta x_4), \frac{1}{3}(\Delta y_1 + \Delta y_2 + \Delta y_4) \right\} \quad (6.7)$$

Hence, estimated object coordinates in equation (6.1) are recalculated as

$$(x, y)_{new} = (x, y) + (e_x, e_y) \quad (6.8)$$

As the RSS measurement values which are received sequentially from object transmitter and reference node transmitters change; weights and (x', y') coordinates also change accordingly. Consequently, $(\Delta x, \Delta y)$ and (e_x, e_y) quantities have new values and new estimated object positions with small variations are generated continuously in time domain.

6.3.3 Neighbourhood Weighted

In this stage, the **neighbourhood weighted approach** is described. Object localisation is attempted by utilising the previous low density sensor node distribution across the sensing area. Localisation accuracies are proposed to be improved by using special weight functions. These weight functions are introduced to identify the environmental factors which affect the RSSI or LQI recordings.

Weight functions can be implemented in several ways. Previously, weight calculations were solely based on Euclidean distances between the sensor nodes as seen in equation (6.4). A third approach is proposed to calculate the weights between wireless sensor nodes by using real physical distances and signal Euclidean distances together.

In the proposed approach, weights are calculated between the selected reference nodes. These selected nodes are the nearest reference nodes calculated with 3-NN algorithm in section (6.3.2). If the target object is surrounded by 3 nearest reference nodes, there will be 3 different weights between these nodes as shown in Figure 6.3.

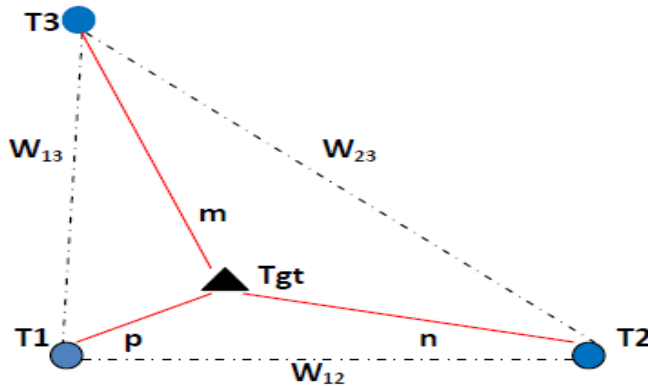


Figure 6.3: Graphical view of reference nodes, T_1 , T_2 , T_3 , target object, T_{gt} , and weight distributions

Distances between reference nodes are known and fixed. $Dist(T_i, T_j)$ refers to the real distance between two stationary *nearest reference nodes* T_i and T_j . The weight w_{ij} , between two nearest reference nodes T_i and T_j is given by

$$w_{ij} = \frac{Dist(T_i, T_j)}{Eucl(T_i, T_j)} \quad (6.9)$$

where $i \in (1, 2)$ and $j \in (2, 3)$

$Eucl(T_i, T_j)$ is the Euclidean distance between T_i and T_j reference node transmitters.

Average value of weights are introduced as the environmental factor for the related 3 *nearest reference nodes* and defined as

$$w_{AVE} = \frac{1}{3}(w_{13} + w_{23} + w_{12}) \quad (6.10)$$

Once W_{AVE} is calculated, w_{12}, w_{13}, w_{23} weight values are compared with W_{AVE} and only the ones equal to or above this value are considered. The one below is discarded and average weight value is considered instead of it in calculations.

Object location can be found by using w_{ij} weights around the object neighbourhood and Euclidean distances between the object and the relevant reference nodes. Object has 3 neighbourhood weights, w_{12}, w_{13}, w_{23} , and 3 Euclidean distances between itself and 3 nearest reference nodes.

Euclidean distances between object transmitter and reference node transmitters are determined by using these transmitters and receivers across the test area. For example, Euclidean distance between object transmitter tag, Tgt, and reference transmitter tag, T_1 , can be defined by using received signal LQI values at A,B,C,D receivers as

$$Eucl(Tgt, T_1) = \{(LQI_{Tgt} - LQI_{T_1})_A^2 + (LQI_{Tgt} - LQI_{T_1})_B^2 + (LQI_{Tgt} - LQI_{T_1})_C^2 + (LQI_{Tgt} - LQI_{T_1})_D^2\}^{\frac{1}{2}}$$

Hence real distances between the object and nearest reference nodes can be calculated by deploying the following equation;

$$Dist(Tgt, T_i) = Eucl(Tgt, T_i) \cdot \frac{(w_x + w_y)}{2} \quad (6.11)$$

$Dist(Tgt, T_i)$ refers to real distance between target object Tgt and nearest reference node T_i .

$i = (1, 2, 3)$ is the number of nearest reference node .

w_x and w_y are two neighbouring weights for any nearest reference node T_i .

3 distance values m , n and p are calculated between the object and 3 nearest reference nodes as shown in Figure 6.3. The trilateration technique is employed by using these distances and nearest reference node coordinates, and final object position coordinates, (x,y), are calculated.

6.4 External reference topology model

In the proposed approach, the object is surrounded by 3 nearest reference nodes topology as seen in Figure 6.3. The object will always be surrounded by 3 nearest reference nodes as long as it is within boundaries of T_1, T_2, T_3, T_4 . Sometimes it is possible that the target object **Tgt** can be outside T_1, T_2, T_3, T_4 boundaries and outside the 3 nearest reference nodes topology. An example case is shown in Figure 6.4.

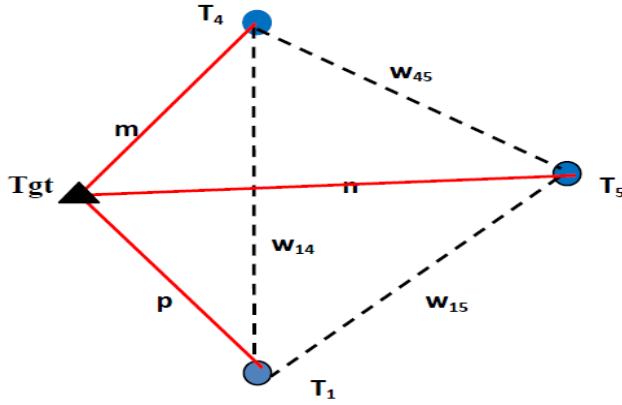


Figure 6.4: Graphical view of the object outside 3 nearest reference nodes T_1 , T_5 , T_4

Object localisation procedures will be the same as in section (6.3.2). In the new topology, nearest reference nodes to the object are taken to be T_1 , T_4 and T_5 as seen in Figure 6.4. Their closest reference nodes will be the same as in section 6.3. Weight calculations and estimated nearest reference node coordinate calculations are carried out similarly and new estimated object coordinates will be determined by equation 6.8.

6.5 Implementation

A test bed of 10mx6m in a hall, free of any major obstacles, is deployed. JN5139 wireless sensor node platforms are utilised in the experiments. These nodes offer low power consumption low processor time and low cost. They use Jennic's ZigBee network standard with rapid application development with simple programming.

Small variations are experienced while recording the received signal strength values in the form of LQI values. It is well known fact that RSS values are affected by obstacles and walls. Hence object localisation based on RSSs imposes some limitations. The test area was carefully selected so that the walls were at a distance and there were no major obstacles along the signal paths. Large numbers of RSS values are recorded at every receiver and they are averaged out. Their average values are used in the computations. 5 Transmitter tags are used as reference nodes in star formation and 4 receivers are placed at the corners of the test area. A transmitter tag is also used on the object at unknown positions as seen in Figure 6.2.

During first **LandMarc** stage, 3-NN algorithm is used and 3 nearest reference nodes are determined for each object location. Average of 3 nearest reference node coordinates gives the estimated object coordinates. In the second stage, an **improved LandMarc** localisation system is employed. Initially, 3 nearest reference nodes are determined for each object as in the first stage. Trigonometric approach is deployed, later on, to select 3 closest reference nodes for each nearest reference node.

New estimated reference node coordinates are calculated by using these closest reference nodes. The difference between the new *estimated reference node coordinates* and the *nearest reference node coordinates* are used as a correction factor for the 3-NN calculated object coordinates (x,y) in first stage.

In a hybrid weighted localisation, referred as **neighbourhood weighted** with 3-NN localisation, 3 nearest reference nodes are employed together with the physical and Euclidean distances between them.

A weight mechanism is proposed by using physical and Euclidean distances between 3 nearest reference nodes. Once the distances **m**, **n**, **p** between the object and 3 nearest reference nodes are determined, object location coordinates are calculated by using trilateration techniques. Object localisation experiments are carried out and samples of estimated object coordinates are tabulated with 3 approaches in Table 6.1.

Measurements	Coordinates (x,y)		
Object	(4 , 2)	(3 , 5)	(6 , 4)
LandMarc	(2.8 ,2.3)	(2.15, 4.76)	(4.66 , 3.05)
Improved LandMarc	(3.6 , 2.6)	(2.35, 5.42)	(5.95 , 3.12)
Neighbourhood Weighted	(4.3 , 1.84)	(2.64, 4.53)	(6.18 , 3.78)

Table 6.1: Estimated object coordinates at different locations with 3 approaches

Final estimated object location coordinates are observed to be in close agreement with actual object location coordinates. Localisation error **e** can be calculated as the distance between the actual object location and the estimated object location as seen Table 6.2.

Measurements	Error distances at object points			
Object coordinates	(4 , 2)	(3 , 5)	(6 , 4)	Average Error
LandMarc	1.23m	0.88m	1.64m	1.252 m
Improved LandMarc	0.72m	0.77m	0.88m	0.79 m
Neighbourhood	0.34m	0.59m	0.28m	0.40 m

Table 6.2: Error calculations with 3 different approaches

Results in Table 6.2 reveal that the average localisation error of LandMarc system is around 1.25 m while the average localisation errors of two new systems in the study are 0.79 m and 0.40m.

6.6 Discussions

In literature, the localisation methods using RF signals and WSNs generate positioning accuracies starting from 1 metre to several metres. Localisation techniques with higher accuracies in tens of centimetres introduce extra systems such as Ultrasonic or microwaves

next to WSN systems. This in return increases the cost factors. Hence WSNs and RF signals are utilised generally due to their cost effectiveness and convenient usage in any environment. In this study, a new reference node approach is utilized. The mathematical background is presented in the above sections. The algorithms introduced here produce impressive accuracy levels compared to other algorithms. Experimental proofs of these accuracies are given in Table 6.2.

In Classical LandMarc topology, there is a uniform distribution of n reference transmitters and it has an average localisation accuracy of 1 to 2 metres in literature. The classical LandMarc approach in this chapter uses a symmetrical star distribution of reference nodes. Localisation accuracy achieved is around 1.25m. The results are in good agreement with the classical LandMarc technique.

The improved LandMarc approach has a positioning accuracy improvement compared to existing LandMarc approach. It uses 3-NN algorithm in two stages. In the first stage 3 nearest reference nodes are selected. Every nearest node has 3 closest nodes and the object locations are estimated with respect to these closest and nearest nodes. The error distance between 2 calculations are added mathematically as a correction factor to the estimated object location coordinates by using nearest reference nodes. An accuracy level of 0.79m is achieved which is better than the classical LandMarc technique.

A second stage is introduced by using the above 3 nearest reference nodes here called the Neighbourhood Weighted approach. It uses both actual distances and Euclidean distance in hybrid form. This approach compensates for the environmental conditions through the usage of weighted RSS values. These environmental conditions are mathematically formulated with the weight functions. The accuracy level achieved with this approach is 0.4m which is quite good compared to others.

6.7 Conclusions

LandMarc localisation technique is a milestone in literature to calculate unknown object locations by using received RF signal strengths. Reference transmitter nodes are deployed in this technique to introduce known fixed locations besides the fixed receiver positions across the sensing area during calculations. Object transmitter nodes, on the other hand, have mobile positions and object localisation accuracies vary by around 1-2 metres depending on the environmental conditions.

In the study, k-NN algorithms together with weight mechanisms related to real and Euclidean distances are utilised to calculate the object coordinates. There are many different

weight mechanisms which are deployed in calculations to improve localisation accuracies. However, most of them suffer from irregular behaviour of RF signals. Many correction and smoothing techniques are applied on RSS signals to obtain better localisation accuracies.

Proposed approaches are different from localisation approaches in literature. In the second approach, 2 stage k-NN is introduced. The difference between the coordinates of nearest reference nodes in stage 1 and the new estimated nearest reference node coordinates in stage 2 are used as a mathematical correction factor in determination of nearest reference tag coordinates. Results reveal that the error distances are reduced by 37% with improved LandMarc technique from classical LandMarc technique.

In the third approach, weight calculations are based both on real distances and Euclidean distances between the reference nodes. This neighbourhood weighted approach introduces a lower localisation complexity with respect to other systems. Results revealed that the error distances are reduced by 68% with the neighbourhood technique compared to the classical LandMarc technique. Experimentation is repeated many times and large numbers of object points are tested with these approaches. Results always reveal similar accuracy levels.

Experimental results clearly define significantly improved localisation accuracies compared to classical LandMarc localisation approach. These results can be taken as the empirical proof of the accuracy improvement with the proposed method in this chapter.

A future development would be to optimise the number of reference nodes and their topology and to include the environmental factors in computations for the best possible localisation accuracies. A conference paper is published from this study [47].

CHAPTER 7

VIRTUAL LOCALISATION

7.1 Background

The localisation issue has received considerable attention in the area of wireless sensor nodes and pervasive computing of object positions [7]. There are many location systems developed by using RF technology [5, 6]. This technology utilises RSSI or LQI to track and detect object positions [10]. The read range of WSN transmitters is around 50 metres. They are located at strategic locations in sensing areas. Signal strengths in RSSI or LQI forms are received by the receivers and sent to server computers for further processing.

A fingerprint database is developed in this chapter by using the received signal strengths at predetermined multiple measurement points across the test area. These signal strengths are compared with the signal strengths received from objects at unknown positions across the test area. A number of measurement locations with nearest signal distances are determined as the nearest nodes to object locations. Weighted average value of the nearest node coordinates can be taken as the estimated unknown position coordinates.

Although the fingerprint database works well with many positioning systems, due to the random nature of RF signals and the relatively large distances between its grid points, signal receptions at grid points are affected. This has an impact on the recordings of the uniform RSSI or LQI values and the correlation between the readings are decreased.

A solution can be proposed to quantise the signal strengths between the measurement points and introduce a fingerprint database with closely recorded signal levels. This would reduce the signal strength uncertainties between the measurement points. The number of measurement points across the test area can be increased and more closely recorded signals can be obtained resulting in a larger fingerprint database. This physical increase in return takes more time and effort during measurements.

A Second approach, on the other hand, keeps the number of grid points the same and introduces virtual grid points between physical grid points without any additional time and effort. Hence, new LQI measurements are generated virtually and a new larger fingerprint

database is developed with real and virtual LQI measurements across the test area. The new approach does not utilise additional transmitters, receivers or grid measurement points. The system deploys only calculated virtual grid points which are integrated among physical grid points resulting in a larger number of LQI values across the test area [123]. In this technique, LQI measurements are carried out at grid points and recorded in a fingerprint database. Signal strengths between adjacent grid points are interpolated according to certain distribution functions. These distribution functions are named as taper functions and they are arranged according to the directions of RF radiations from transmitters. Linear and exponential taper functions are utilised in the study. The distance between the adjacent grid points are divided into an equal number of virtual grid points. Virtual distribution of LQI values at these virtual grid points are generated in linear and exponential form for each transmitter radiation. These virtual and real LQI values at virtual and real grid points produce a new fingerprint database. This fingerprint database is called a virtual fingerprint database [124]. Unknown position estimation is carried out by utilising the newly generated virtual fingerprint database and k-NN algorithm across the test area.

7.2 Fingerprint model

A number of wireless sensor transmitters and a receiver on the object are employed across the test area as shown in Figure 7.1. B_i transmitters transmit RF signals and their LQI values are recorded by the receiver on the object and receivers at grid points.

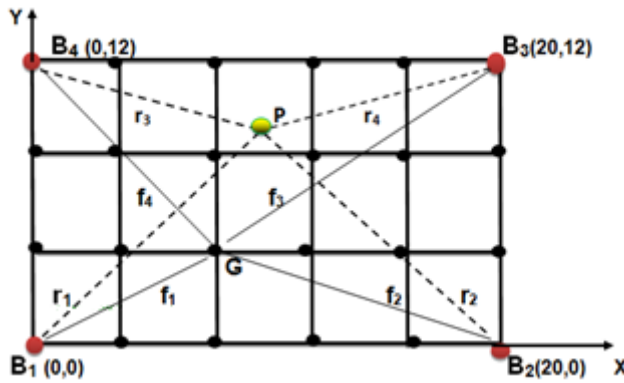


Figure 7.1: Grid area showing a grid point G, an object P and B_i transmitters where $i=1,2,3,4$

Signal distance between object location P and grid point G in the fingerprint map is calculated by using LQI values recorded at respective positions. Fingerprint vector $\vec{F} = (f_1, f_2, f_3, f_4)$, is identified as the total LQI values from B_i transmitters at a particular grid location G. Unknown object location fingerprint vector \vec{R} is the LQI values recorded at point P and denoted as $\vec{R} = (r_1, r_2, r_3, r_4)$.

The fingerprint database is prepared by collecting \vec{F} vectors from all the grid points during the off-line phase. The \vec{R} fingerprint vector at point P is also deployed and sent to PC during the on-line phase. Unknown object position coordinates (x, y), are calculated by using k-NN and weighted k-NN algorithms as explained before.

Random behaviour of received signal strengths is reduced by filtering the received signal strength amplitudes during calculations. Sudden changes among the signals occur due to movements around the test area. These changes are also eliminated by using outlier techniques.

7.3 Virtual Fingerprint

Transmitters transmit RF signals and these signals are received by a receiver on the object in the form of LQI values. A physical rectangular grid system is organised across the test area as seen in figure 7.1. These grids are organised across the test area with ample distances between them where RF radiation shows characteristics of signal variations. In order to include these effects in localisation calculations either several new LQI measurements are taken between grid points or virtual RF signal amplitudes are introduced between adjacent grid points.

Virtual RF signal amplitudes, namely virtual LQI values, are introduced at virtual grid points between adjacent grid points following a distribution function. These virtual LQI values with respect to their coordinates are identified as virtual fingerprints. The locations of virtual grid points are defined empirically between every two adjacent grid points. A physical grid system and a single expanded grid cell across the test area are displayed in Figure 7.2.

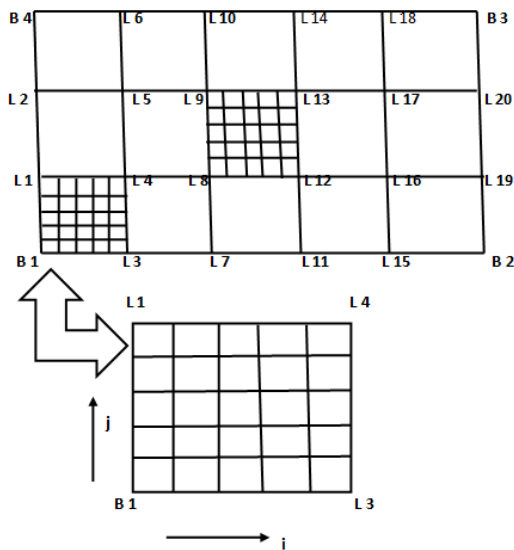


Figure 7.2: Physical grid space and virtual grids across each physical grid cell

Each physical grid cell such as ($L_8L_{12}L_{13} L_9$) is square in shape and is surrounded by 4 grid points. Each cell is further divided into n^2 square shaped virtual grid cells. n virtual grid cells between two adjacent grid points are generated. The number of physical grid points is decided according to the size of the test area. Virtual grid points, on the other hand, are selected empirically to generate the best localisation accuracies. Since the coordinates of physical grid points are defined with respect to transmitter positions, the coordinates of virtual grid points can also be easily calculated.

LQI values at adjacent grid points are utilised to generate LQI values at virtual grid points between them once LQI measurements are recorded at physical grid points, the distribution of virtual LQI values between two adjacent grid points can be determined according to any distribution function.

The distance between two adjacent grid points is divided into n sections. $n-1$ number of virtual LQI values are generated between these two adjacent grid points according to deployed taper functions. Hence the physical grid space is divided into a finer virtual grid space. Virtual LQI values at virtual grid points and the measured LQI values at grid points produce a new fingerprint database. This fingerprint database is identified as a virtual fingerprint database.

Unknown object position detection is carried out by using the newly generated virtual fingerprint database and k-NN algorithms. Virtual Euclidean distances are utilised between the object location and the virtual grid points. k number of minimum virtual Euclidean distances are selected and their weighted coordinates are averaged out to determine the object location. In conclusion, the positioning technique, employed with the virtual grid system, is the same as the physical grid system.

An overview of the proposed system is presented in a block diagram as shown in Figure 7.3. It is important that no additional wireless sensor nodes are employed across the test area. The technique introduces an increased number of LQI values due to denser virtual grid points without any extra effort. Hence, the fixed number of grid points and the fixed number of LQI data in the fingerprint database are abandoned in favour of larger the number of virtual grid points and virtual LQI data.

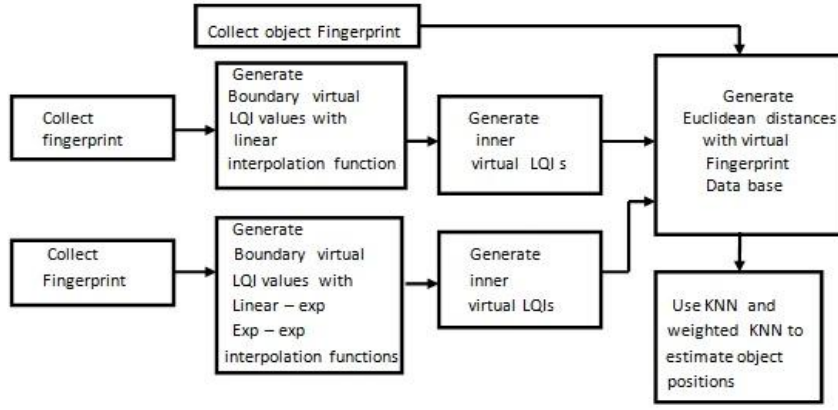


Figure 7.3: Block diagram of the proposed localisation system

7.3.1 Linear Interpolation Function

Each physical grid cell is in square shape and is further divided into $n \times n$ square shaped virtual grid cells. The proposed approach uses a linear taper function which can be identified as a linear distribution function of LQI values at virtual grid points between two adjacent physical grid points. Linear taper function is utilised to calculate the virtual LQI values in every virtual grid point. Each physical grid cell has 4 LQI values at each grid point received from 4 transmitters. An empirical value of virtual grid cell number $n=5$ is selected between two adjacent grid points. For example, LQI values received from 4 transmitters at L_3 grid point of grid cell $B_1L_3L_4L_1$ are defined as $LQI_{(5,0)}^{B1}, LQI_{(5,0)}^{B2}, LQI_{(5,0)}^{B3}, LQI_{(5,0)}^{B4}$.

Hence, $LQI_{(0,0)}^k, LQI_{(5,0)}^k, LQI_{(5,5)}^k$ and $LQI_{(0,5)}^k$ identify the LQI values at 4 corners of the grid cell $B_1L_3L_4L_1$ with respect to transmitters. Transmitters at grid cell corners are defined as the k subscripts with LQI values where $k = \{B_1, B_2, B_3, B_4\}$. Transmitter coordinates can be seen in Figure 7.2. LQI values at virtual grid points along B_1L_3 horizontal boundary of the grid cell can be interpolated linearly in terms of LQI values at B_1 and L_3 grid points as:

$$LQI_{(i,0)}^k = LQI_{(0,0)}^k + \frac{LQI_{(5,0)}^k - LQI_{(0,0)}^k}{5} \cdot i \quad (7.1)$$

$LQI_{(i,0)}^k$ defines the LQI value at i^{th} virtual grid point with respect to k^{th} transmitter. Virtual LQI values along B_1L_3 can be defined for B_1 transmitter by substituting $k=B_1$ and varying i between 0 and 5 in equation 7.1. These LQI values are displayed in Table 7.1. Virtual LQI values with respect to other transmitters can also be determined by varying k values along B_1L_3 boundary. Hence, there are 4 virtual LQI values for 4 transmitters at each i along B_1L_3 .

Grid number(i)	LQI index	LQI values	Grid types
0	$LQI_{(0,0)}^{B_1}$	$LQI_{(0,0)}^{B_1}$	B ₁ <u>real</u> grid point
1	$LQI_{(1,0)}^{B_1}$	$\frac{4}{5} LQI_{(0,0)}^{B_1} + \frac{1}{5} LQI_{(5,0)}^{B_1}$	Virtual grid point
2	$LQI_{(2,0)}^{B_1}$	$\frac{3}{5} LQI_{(0,0)}^{B_1} + \frac{2}{5} LQI_{(5,0)}^{B_1}$	Virtual grid point
3	$LQI_{(3,0)}^{B_1}$	$\frac{2}{5} LQI_{(0,0)}^{B_1} + \frac{3}{5} LQI_{(5,0)}^{B_1}$	Virtual grid point
4	$LQI_{(4,0)}^{B_1}$	$\frac{1}{5} LQI_{(0,0)}^{B_1} + \frac{4}{5} LQI_{(5,0)}^{B_1}$	Virtual grid point
5	$LQI_{(5,0)}^{B_1}$	$LQI_{(5,0)}^{B_1}$	L ₃ <u>real</u> grid point

Table 7.1: LQI values at real and virtual grid points along B₁L₃ of B₁L₃L₄L₁ grid cell for B₁ transmitter

Similarly for B₁L₁ vertical boundary of the same grid cell, LQI values at virtual grid points can be interpolated linearly in terms of LQI values at B₁ and L₁ grid points as:

$$LQI_{(0,j)}^k = LQI_{(0,0)}^k + \frac{LQI_{(0,5)}^k - LQI_{(0,0)}^k}{5} \cdot j \quad (7.2)$$

j is the number of virtual grid points. $LQI_{(0,j)}^k$ defines the LQI value at jth virtual grid point with respect to kth transmitter. Virtual LQI values along B₁L₁ can be defined for B₁ transmitter by substituting k=B₁ and j varies between 0 and 5 in equation 7.2. These LQI values are displayed in Table 7.2.

Grid number(j)	LQI index	LQI values	Grid types
0	$LQI_{(0,0)}^{B_1}$	$LQI_{(0,0)}^{B_1}$	B ₁ real grid point
1	$LQI_{(0,1)}^{B_1}$	$\frac{4}{5} LQI_{(0,0)}^{B_1} + \frac{1}{5} LQI_{(0,5)}^{B_1}$	Virtual grid point
2	$LQI_{(0,2)}^{B_1}$	$\frac{3}{5} LQI_{(0,0)}^{B_1} + \frac{2}{5} LQI_{(0,5)}^{B_1}$	Virtual grid point
3	$LQI_{(0,3)}^{B_1}$	$\frac{2}{5} LQI_{(0,0)}^{B_1} + \frac{3}{5} LQI_{(0,5)}^{B_1}$	Virtual grid point
4	$LQI_{(0,4)}^{B_1}$	$\frac{1}{5} LQI_{(0,0)}^{B_1} + \frac{4}{5} LQI_{(0,5)}^{B_1}$	Virtual grid point
5	$LQI_{(0,5)}^{B_1}$	$LQI_{(0,5)}^{B_1}$	L ₃ real grid point

Table 7.2: LQI values at real and virtual grid points along B₁L₁ of B₁L₃L₄L₁ grid cell for B₁ transmitter

k value can be varied and virtual LQI values with respect to other transmitters can be determined similarly along B₁L₁ boundary. A schematic representation of linear LQI distributions along B₁L₃ and B₁L₁ boundaries of the grid cell B₁L₃L₄L₁ for transmitter B₁, is given in Figure 7.4.

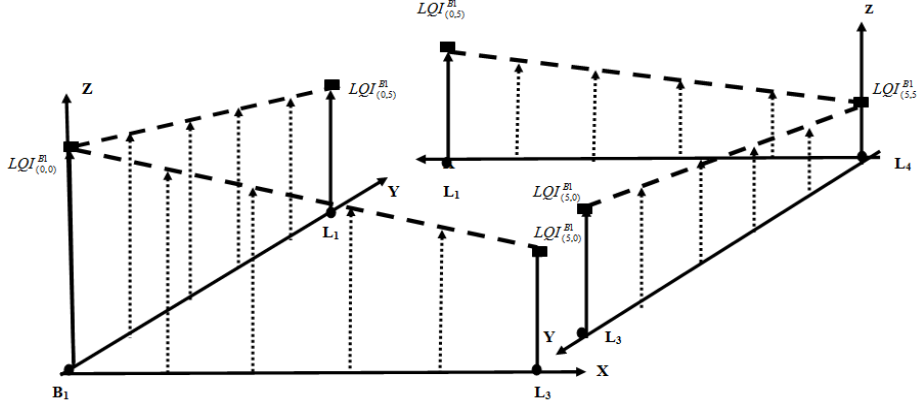


Figure 7.4: Linear LQI distributions are displayed along the grid cell boundaries a) B_1L_3 and B_1L_1 , b) L_4L_3 and L_4L_1 for B_1 transmitter. Each dotted arrow represents a virtual LQI value.

Virtual LQI values at boundaries L_1L_4 and L_3L_4 of the grid cell $B_1L_3L_4L_1$ can also be determined for B_1 transmitter similar to B_1L_3 and B_1L_1 . Once virtual LQI values for all the grid cell boundaries are determined, virtual LQI values at virtual grid points inside the grid cell can be calculated with respect to these boundary values.

For $j=1$ and i varies between 0 and 5, virtual LQI values can be calculated for k^{th} transmitter by using the following LQI boundary values.

$$LQI_{(0,0)}^k + \frac{1}{5}(LQI_{(0,5)}^k - LQI_{(0,0)}^k) \quad \text{and} \quad LQI_{(5,0)}^k + \frac{1}{5}(LQI_{(5,5)}^k - LQI_{(5,0)}^k) .$$

Similarly, for $i=1$ and j varies between 0 and 5, virtual LQI values can also be determined by using the following LQI boundary values.

$$LQI_{(0,0)}^k + \frac{1}{5}(LQI_{(5,0)}^k - LQI_{(0,0)}^k) \quad \text{and} \quad LQI_{(0,5)}^k + \frac{1}{5}(LQI_{(5,5)}^k - LQI_{(0,5)}^k) .$$

These boundary LQI values with respect to grid cells are displayed in Figure 7.5.

When $j=1$ and i varies between 0 and 5 along the horizontal line parallel to B_1L_3 , virtual LQI values can be determined as shown in Table 7.3 for B_1 transmitter.

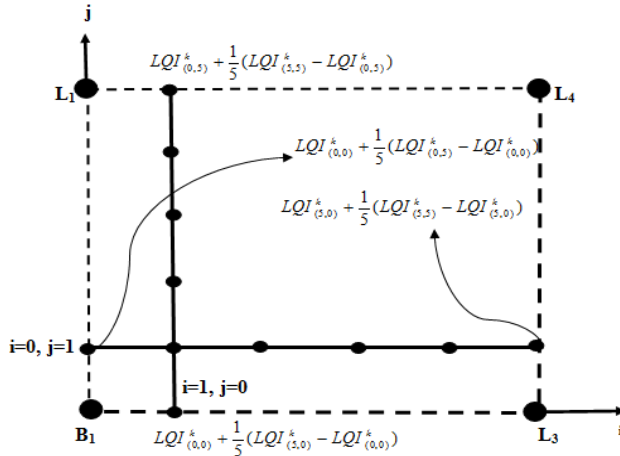


Figure 7.5: LQI boundary values for $j=1$, $i=0$ to 5 and $i=1$, $j=0$ to 5 for k^{th} transmitter

Grid No (i , j)	LQI values (horizontal to B ₁ L ₃)
0 , 1	$\frac{4}{5} LQI_{(0,0)}^{B_1} + \frac{1}{5} LQI_{(0,5)}^{B_1}$
1 , 1	$\frac{16}{25} LQI_{(0,0)}^{B_1} + \frac{4}{25} LQI_{(0,5)}^{B_1} + \frac{4}{25} LQI_{(5,0)}^{B_1} + \frac{1}{25} LQI_{(5,5)}^{B_1}$
2 , 1	$\frac{12}{25} LQI_{(0,0)}^{B_1} + \frac{3}{25} LQI_{(0,5)}^{B_1} + \frac{8}{25} LQI_{(5,0)}^{B_1} + \frac{2}{25} LQI_{(5,5)}^{B_1}$
3 , 1	$\frac{8}{25} LQI_{(0,0)}^{B_1} + \frac{2}{25} LQI_{(0,5)}^{B_1} + \frac{12}{25} LQI_{(5,0)}^{B_1} + \frac{3}{25} LQI_{(5,5)}^{B_1}$
4 , 1	$\frac{4}{25} LQI_{(0,0)}^{B_1} + \frac{1}{25} LQI_{(0,5)}^{B_1} + \frac{16}{25} LQI_{(5,0)}^{B_1} + \frac{4}{25} LQI_{(5,5)}^{B_1}$
5 , 1	$\frac{4}{5} LQI_{(5,0)}^{B_1} + \frac{1}{5} LQI_{(5,5)}^{B_1}$

Table 7.3: LQI values for j=1, i=0 to 5 for B₁ transmitter in B₁L₃L₄L₁ grid cell

Similarly, when i=1 and j varies between 0 and 5 along the vertical line parallel to B₁L₁, virtual LQI values can also be determined as shown in Table 7.4 for B₁ transmitter.

These Virtual LQI calculations will be repeated for each horizontal and vertical line along i and j directions in the grid cell. As a result, there will be 2 virtual LQI values generated for each virtual grid point (i, j). Average of two virtual LQI values is taken as the final virtual LQI value at that inner virtual grid point (i, j) for k transmitter.

Grid No (i , j)	LQI values (horizontal to B ₁ L ₄)
1 , 0	$\frac{4}{5} LQI_{(0,0)}^{B_1} + \frac{1}{5} LQI_{(5,0)}^{B_1}$
1 , 1	$\frac{16}{25} LQI_{(0,0)}^{B_1} + \frac{4}{25} LQI_{(5,0)}^{B_1} + \frac{4}{25} LQI_{(0,5)}^{B_1} + \frac{1}{25} LQI_{(5,5)}^{B_1}$
1 , 2	$\frac{12}{25} LQI_{(0,0)}^{B_1} + \frac{3}{25} LQI_{(5,0)}^{B_1} + \frac{8}{25} LQI_{(0,5)}^{B_1} + \frac{2}{25} LQI_{(5,5)}^{B_1}$
1 , 3	$\frac{8}{25} LQI_{(0,0)}^{B_1} + \frac{2}{25} LQI_{(5,0)}^{B_1} + \frac{12}{25} LQI_{(0,5)}^{B_1} + \frac{3}{25} LQI_{(5,5)}^{B_1}$
1 , 4	$\frac{4}{25} LQI_{(0,0)}^{B_1} + \frac{1}{25} LQI_{(0,5)}^{B_1} + \frac{16}{25} LQI_{(5,0)}^{B_1} + \frac{4}{25} LQI_{(5,5)}^{B_1}$
1 , 5	$\frac{4}{5} LQI_{(0,5)}^{B_1} + \frac{1}{5} LQI_{(5,5)}^{B_1}$

Table 7.4: LQI values for i=1, j=0 to 5 for B₁ transmitter in B₁L₃L₄L₁ grid cell

7.3.2 Exponential-Linear Interpolation Function

Transmitted LQI values decrease with respect to distance between a wireless sensor transmitter and a receiver. A best fit curve on the experimental LQI distribution can be shown as an exponential function in the form of $a \exp(-bx)$. This is presented in the implementation section. Due to exponential decreasing properties of LQI values between transmitters and

from B₂ transmitter at grid point L₃ is identified as $LQI_{(5,0)}^{B2}$ and this value decreases exponentially towards B₁ and L₄ grid points.

The decrease of LQI values is identified with exponential taper function between two LQI values coming from the same transmitter at 2 adjacent grid points. The taper function for LQI values, transmitted from B₁ transmitter, between B₁ and L₃ is shown in Figure 7.8 and expressed as;

$$(LQI_{(a,a)}^{B1} - LQI_{(a+5,a)}^{B1})e^{-(x-a)} + LQI_{(a+5,a)}^{B1}$$

On the other hand, exponential taper function for LQI values between B₁ and L₃, transmitted from B₂ transmitter, is shown in Figure 7.9 and expressed as;

$$(LQI_{(a+5,0)}^{B2} - LQI_{(a,a)}^{B2})e^{(x-a-5)} + LQI_{(a,a)}^{B2}$$

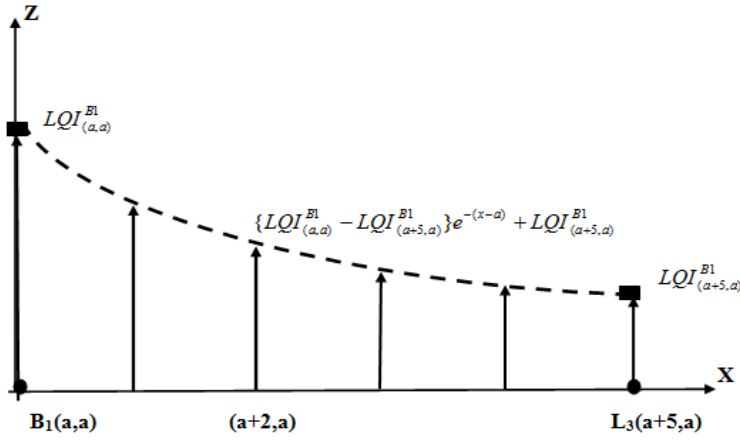


Figure 7.8: Graphical view of exponential taper function between B₁ and L₃ together with 4 virtual grid points for B₁ transmission

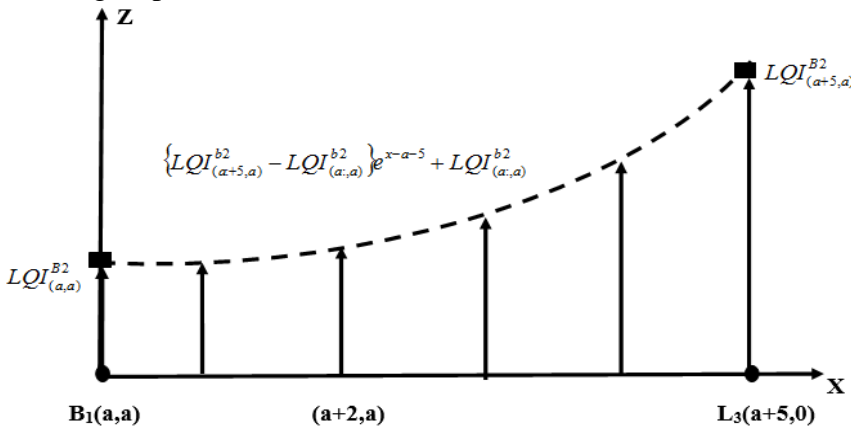


Figure 7.9: Graphical view of exponential taper function between B₁ and L₃ together with 4 virtual grid points for B₂ transmission

Virtual LQI values along B₁L₃, B₁L₁, L₁L₄ and L₃L₄ boundaries can be calculated by using exponential taper functions as shown in Figures 7.6 and 7.7. These virtual LQI values are

tabulated in Table 7.5. Each grid corner B_1 , L_1 , L_3 and L_4 is considered as the RF transmission source during calculations. Virtual grid points are located at incremental steps of 1 unit along the grid boundaries. Origin of the coordinate system is taken as (a,a) in Table 7.5.

Once the virtual LQI values are determined for one transmitter around the grid cell boundaries, other virtual LQI values can also be determined for other transmitters around the same boundaries. Boundary LQI values of a grid cell are utilised to calculate the internal virtual LQI values of the grid cell. Virtual LQI values on two cell boundaries facing opposite each other are considered and the virtual LQI values are calculated between them by using linear interpolation technique. Final virtual LQI value is derived by averaging the two resultant LQI values obtained horizontal and vertical directions

Grid locations along X	LQI values B_1L_3 Boundary	LQI values L_1L_4 Boundary	Grid locations along Y	LQI values B_1L_1 Boundary	LQI values L_3L_4 Boundary
a	$LQI_{(a,a)}^{B_1}$	$LQI_{(a,a+5)}^{B_1}$	a	$LQI_{(a,a)}^{B_1}$	$LQI_{(a+5,a)}^{B_1}$
a+1	$Ae^{-1} + B$	$Ee^{-1} + F$	a+1	$Ce^{-1} + D$	$Pe^{-1} + R$
a+2	$Ae^{-2} + B$	$Ee^{-2} + F$	a+2	$Ce^{-2} + D$	$Pe^{-2} + R$
a+3	$Ae^{-3} + B$	$Ee^{-3} + F$	a+3	$Ce^{-3} + D$	$Pe^{-3} + R$
a+4	$Ae^{-4} + B$	$Ee^{-4} + F$	a+4	$Ce^{-4} + D$	$Pe^{-4} + R$
a+5	$Ae^{-5} + B$	$Ee^{-5} + F$	a+5	$Ce^{-5} + D$	$Pe^{-5} + R$

Table 7.5: LQI values at real and virtual grid points around the grid cell boundaries for B_1 transmissions. $A = \{LQI_{(a,a)}^{B_1} - LQI_{(a+5,a)}^{B_1}\}$, $B = LQI_{(a+5,a)}^{B_1}$, $E = \{LQI_{(a,a+5)}^{B_1} - LQI_{(a+5,a+5)}^{B_1}\}$, $F = LQI_{(a+5,a+5)}^{B_1}$, $C = \{LQI_{(a,a)}^{B_1} - LQI_{(a,a+5)}^{B_1}\}$, $D = LQI_{(a,a+5)}^{B_1}$, $P = \{LQI_{(a+5,a)}^{B_1} - LQI_{(a+5,a+5)}^{B_1}\}$, $R = LQI_{(a+5,a+5)}^{B_1}$

7.3.3 Exponential – Exponential Interpolation function

Previously, exponential taper functions were utilised and virtual LQI values were calculated along the grid cell boundaries. Inside the grid cell, determination of virtual LQI values was carried out by using linear interpolation functions. Two cell boundaries facing each other were considered. Virtual LQI values at these boundaries facing each other oppositely were taken as the upper and lower limits of a linear function. Virtual LQI values were calculated along these linear functions in both x and y directions.

In this section, exponential taper functions along the two facing cell boundaries such as B_1L_3 and L_1L_4 are utilised. 2 virtual LQI values are facing opposite to each other along these two taper functions. A 3D view of these exponential functions and LQI values are displayed in Figure 7.10. Exponential taper function between $B_1(a,a)$ and $L_3(a+5,a)$ along the boundary B_1L_3 is given as

$$(LQI_{(a,a)}^{B1} - LQI_{(a+5,a)}^{B1})e^{-(x-a)} + LQI_{(a+5,a)}^{B1}$$

Similarly, exponential taper function between $L_1(a,a+5)$ and $L_4(a+5,a+5)$ along the boundary L_1L_4 parallel to B_1L_3 is given as

$$(LQI_{(a,a+5)}^{B1} - LQI_{(a+5,a+5)}^{B1})e^{-(x-a)} + LQI_{(a+5,a+5)}^{B1}$$

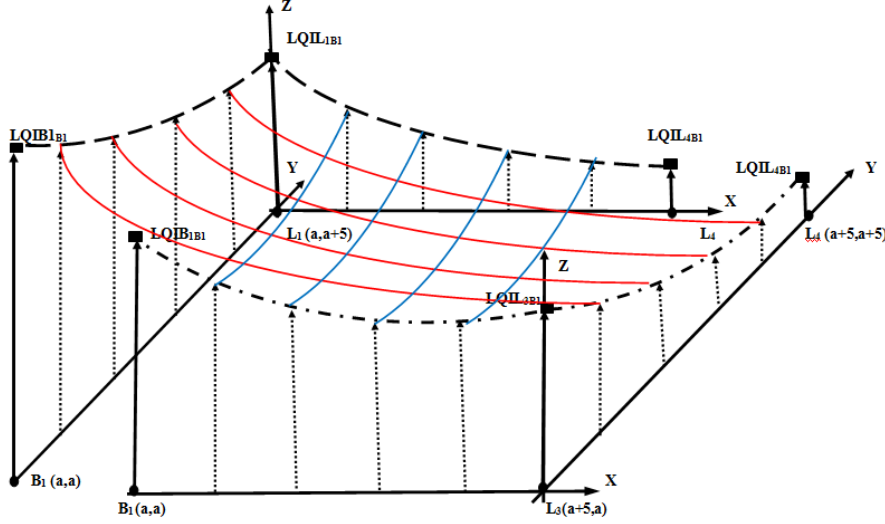


Figure 7.10: Schematic view of Exponential LQI interpolation functions inside the grid cell $B_1L_3L_4L_1$ boundaries for LQI transmissions of B_1 transmitter

Exponential taper functions along vertical B_1L_1 and L_3L_4 boundaries are also given as

$$(LQI_{(a,a)}^{B1} - LQI_{(a,a+5)}^{B1})e^{-(y-a)} + LQI_{(a,a+5)}^{B1}$$

$$(LQI_{(a+5,a)}^{B1} - LQI_{(a+5,a+5)}^{B1})e^{-(y-a)} + LQI_{(a+5,a+5)}^{B1}$$

Exponential taper function parallel to B_1L_3 across the virtual grid cell can be expressed by using the above taper function along B_1L_3 boundary. For example exponential taper functions starting at $(a, a+1)$ and $(a, a+2)$ can be expressed as in Table 7.6

Exponential taper functions at $(a,a+1)$ and $(a,a+2)$ parallel to B_1L_3	Start point
$\{[Me^{-1} + LQI_{(a,a+5)}^{B1}] - [Ne^{-1} + LQI_{(a+5,a+5)}^{B1}]\}e^{-(x-a)} + [Ne^{-1} + LQI_{(a+5,a+5)}^{B1}]$	$(a, a+1)$
$\{[Me^{-2} + LQI_{(a,a+5)}^{B1}] - [Ne^{-2} + LQI_{(a+5,a+5)}^{B1}]\}e^{-(x-a)} + [Ne^{-2} + LQI_{(a+5,a+5)}^{B1}]$	$(a, a+2)$

Table 7.6: Exponential taper functions parallel to B_1L_3 boundary across the grid cell where $M = (LQI_{(a,a)}^{B1} - LQI_{(a,a+5)}^{B1})$ and $N = (LQI_{(a+5,a)}^{B1} - LQI_{(a+5,a+5)}^{B1})$

Exponential taper functions parallel to B_1L_3 along x axis and parallel to B_1L_1 along y axis can be derived. The intersection points of these taper functions are the virtual LQI values at virtual grid points across the physical grid cell $B_1L_3L_4L_1$.

7.4 Implementation

JENNIC JN5139 wireless sensor nodes are deployed in the study. Zigbee Home Sensor program is used to program JN5139 active devices to work as both transmitter and receiver WSNs respectively [115,116]. JN5139 receiver [100], on the object is interfaced to a computer via a wired link for data transmission. A rectangular area of 12mx20m in a sports hall is selected and unknown object locations are confined in this rectangular grid area. The area was not free of obstacles. There was sports equipment lying around and people were moving around during the measurements. Wireless Sensor transmitters are placed at the corners of the rectangular area. Recordings of LQI values coming from transmitters are collected by a wireless sensor receiver sequentially placed at each grid point.

Power consumption by the sensors during the construction of the fingerprint map and computations is negligible. The wireless sensors are active devices and their onboard battery life is around 1 month. Total LQI measurements, data collection and recording of the fingerprint database takes only 1-2 hours. Construction of the database and the localisation computations take place in the server computer. Hence the only electric power used by the sensors is to transmit the LQI values.

For a grid area of 12mx20m, 24 grid points are arranged with a grid space of 4 metres. There are 96 LQI entries recorded in the fingerprint database with 4 LQI readings at each grid point from 4 transmitters. Each entry in the database includes a mapping of the grid coordinate (x,y) and 4 LQI values at that point. Wireless receiver on the object receives 4 LQI values from 4 transmitters from its 4 channels and transmits them to server computer via a wired link. There is no onboard memory at the receiver and these values are stored sequentially in an access database in the server computer. The server computer has sufficient memory space to manipulate these LQI values for position calculations. Received signal strengths can vary depending on the environmental effects. These variations are reduced by averaging 100 recorded LQI values at each measurement point for each transmitter. Averaged LQI values and the position coordinates are employed to generate the fingerprint map in the server. LQI recordings of the object receiver at unknown locations are also carried out similarly to generate object fingerprint vectors. An example basic fingerprint database is shown in Figure 7.11.

X	Y	LQIA	LQIB	LQIC	LQID
0	0	227	106	86	124
1	0	137	124	106	104
2	0	97	129	95	111
3	0	85	137	83	136
4	0	70	171	103	123
5	0	73	252	87	112
0	1	109	86	100	154
1	1	103	108	112	135
2	1	87	131	85	129
3	1	75	151	102	121
4	1	78	128	111	108
5	1	78	168	97	118
0	2	102	126	96	184
1	2	99	97	77	165
2	2	74	107	91	149
3	2	78	137	97	118
4	2	88	142	100	105
5	2	67	150	131	120
0	3	79	127	84	251
1	3	103	126	90	172
2	3	82	107	84	130
3	3	78	139	94	126
4	3	93	120	123	122
5	3	70	128	230	117

Figure 7.11: Part of the basic fingerprint database in server memory

7.4.1 Linear Interpolation

Each Grid cell is further divided into 5x5 virtual grid cells. Therefore there are a total of $15 \times 25 = 375$ virtual grid cells and $26 \times 16 = 416$ real plus virtual grid points and 416 LQI values from each transmitter across the test area.

The virtual grid space is 0.8 meters and is used as 1 unit distance in calculations. Calculated distances are multiplied by 0.8 to convert them into real distances. Initially, k-NN and weighted k-NN algorithms are utilised to determine the unknown object locations by using the basic fingerprint database with 24 grid points for comparison purposes. The same localisation algorithms are deployed with the virtual fingerprint database generated with linear taper function. Unknown object coordinates are calculated and results are presented in Table 7.7.

Unknown object	Estimated object position coordinates using basic fingerprint and virtual fingerprint (linear taper function) databases									
	1-NN X,Y		2-NN X,Y		3-NN X,Y		4-NN X,Y		Weighted 4-NN X,Y	
X Y	Basic fingerprint	Linear taper Function	Basic fingerprint	Linear taper Function	Basic fingerprint	Linear taper Function	Basic fingerprint	Linear taper Function	Basic fingerprint	Linear taper Function
2 2	1 3	0 3.8	0 3	0.3 3.5	1 2	0.3 3.7	0 4	0.4 4.1	0.9 2.9	0.5 3.6
2 3	1 4	0 5.5	1 5	0.2 4.5	0 3	0 4.7	0 4	0.1 5.2	0.5 4.5	0.2 4.5
3 5	2 4	1.1 8.0	2 3	1.3 7.6	2 6	1.2 7.1	2 3	0.9 9.0	2.1 3.3	1.4 8.6
4 4	0 12	5.8 3.2	4 8	5.2 2.4	7 9	5.4 2.4	6 7	5.3 1.6	5.8 7.31	5.8 2.0
0 8	4 12	2.4 10	4 6	2.4 9.8	5 5	2.4 9.2	4 7	1.4 9.8	4.14 7.5	2.5 9
8 8	8 12	8 6.4	8 12	8 6.6	8 9	7.2 6.4	9 9	7.2 7.1	9.8 9.2	7.2 7.4
12 8	12 12	11 6.6	12 10	10.5 6.8	11 11	10.4 7.1	10 8	10.5 6.7	10.3 8.8	10.6 6.8
4 12	8 8	5.6 12.2	6 12	4.6 13.2	5 11	4.8 13.2	6 11	5.6 13.2	6.36 10.2	5.6 13.6
8 12	8 8	6.4 14	6 8	7.4 13	5 11	6.5 13.6	5 11	6.2 14	7.01 8.8	6.6 13.8
4 16	8 12	5.4 14.4	8 10	5.6 17.6	8 12	5.7 18	7 13	4.4 16.6	7.43 12.3	5.3 17

Table 7.7: Estimated object position coordinates using basic fingerprint database and virtual fingerprint database with linear taper function

7.4.2 Exponential linear Interpolation

RF signal amplitudes decrease with the distance between transmitters and receivers. Generally, this decrease is in exponential form. Initially, wireless sensor receivers are placed in front of wireless sensor transmitters. The distance between them is increased in steps of 1 metre and RF signal amplitudes recorded by the receiver in the form of LQI values are plotted against distance. A best fit curve reveals an exponential distribution function of $a\exp(-bx)$ as seen in Figure 7.12.

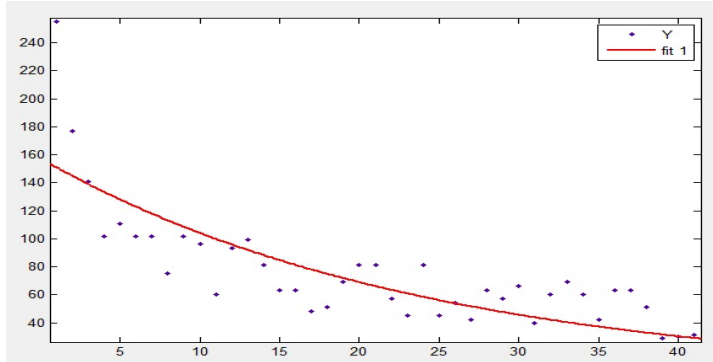


Figure 7.12: Plot of LQI values versus distance between a receiver and a transmitter with their fitted curve

In order to reflect these characteristics in a virtual world, virtual grid points are generated by using an exponential taper function between 2 adjacent grid points around grid cell boundaries. Exponential Taper functions are applied in **x** and **y** directions of grid cell boundaries and object coordinates are calculated as shown in Table 7.8.

Unknown object	Estimated object position coordinates using basic fingerprint and virtual fingerprint (Expo-linear taper function) databases									
	1-NN X,Y		2-NN X,Y		3-NN X,Y		4-NN X,Y		Weighted 4-NN X,Y	
X Y	Basic fingerprint	Expo. Linear taper function	Basic fingerprint	Expo. Linear Taper function	Basic fingerprint	Expo. Linear Taper function	Basic fingerprint	Expo. Linear Taper function	Basic fingerprint	Expo. Linear Taper function
2 2	1 3	0.9 1.3	0 3	1.2 1.4	1 2	1.0 0.9	0 4	1.3 0.9	0.9 2.9	0.9 1.3
2 3	1 4	1.2 1.3	1 5	0.8 1.4	0 3	1.3 1.2	0 4	1.2 1.5	0.5 4.5	1.4 1.6
3 5	2 4	2.2 3.5	2 3	1.8 3.7	2 6	1.7 4.1	2 3	2.6 2.7	2.1 3.3	2.1 2.8
4 4	0 12	4.5 2.4	4 8	5.3 2.4	7 9	6.4 3.1	6 7	3.2 2.2	5.8 7.31	5.3 3.2
0 8	4 12	1.7 8.6	4 6	1.3 9.6	5 5	1.6 9.3	4 7	1.4 10.0	4.14 7.5	1.7 9.1
8 8	8 12	7.1 6.7	8 12	6.5 6.6	8 9	6.6 6.8	9 9	6.8 6.7	9.8 9.2	7.3 6.2
12 8	12 12	11 7.1	12 10	10.7 6.9	11 11	10.4 6.7	10 8	11.2 6.9	10.3 8.8	10.4 6.7
4 12	8 8	4.8 10.8	6 12	5.5 10.7	5 11	5.4 13.4	6 11	5.6 11.6	6.36 10.2	4.6 13.7
8 12	8 8	7.1 10.6	6 8	6.8 10.7	5 11	6.5 10.8	5 11	6.2 10.8	7.01 8.8	6.4 13.8
4 16	8 12	5.0 14.7	8 10	4.7 14.7	8 12	5.5 17.3	7 13	5.1 14.6	7.43 12.3	5.7 14.0

Table 7.8: Estimated object position coordinates using basic fingerprint database and virtual fingerprint database with exponential linear taper function

7.4.3 Exponential-Exponential Interpolation

Exponential Taper functions are applied in **x** and **y** directions of grid cell boundaries as before. Previously, virtual LQI values at virtual grid points inside the grid cell are calculated by linear interpolation along **x** and **y** directions.

In this case, virtual LQI values at virtual grid points inside the grid cell are calculated by using exponential interpolation along **x** and **y** directions as shown in Figure 9.10. A virtual database is developed by using these newly generated virtual LQI values. Object positions are calculated with this virtual database and shown in Table 7.9.

Unknown object	Estimated object position coordinates using basic fingerprint and virtual fingerprint (Expo-Expo taper function) databases									
	1-NN X,Y		2-NN X,Y		3-NN X,Y		4-NN X,Y		Weighted 4-NN X,Y	
X Y	Basic finger print	Expo. Expo taper function	Basic finger print	Expo. Expo. Taper function	Basic finger print	Expo. Expo. Taper function	Basic finger print	Expo. Expo. Taper function	Basic finger print	Expo. expo Taper function
2 2	1 3	1.3 1.5	0 3	1.5 1.5	1 2	1.3 1.2	0 4	1 1.2	0.9 2.9	1 1.5
2 3	1 4	1.3 2.3	1 5	1.2 2.2	0 3	1.5 1.8	0 4	1.5 1.8	0.5 4.5	1.2 1.9
3 5	2 4	2.2 3.2	2 3	2 4.1	2 6	2.5 4	2 3	2.4 3.5	2.1 3.3	2.1 3.2
4 4	0 12	4.7 3.1	4 8	5 3.1	7 9	5.4 3	6 7	3 3.2	5.8 7.31	5 3.1
0 8	4 12	0.7 8.8	4 6	1 9	5 5	1 8.6	4 7	1 9	4.14 7.5	1 9
8 8	8 12	7.0 6.9	8 12	6.6 7	8 9	7 7	9 9	7 7.2	9.8 9.2	7 7.2
12 8	12 12	11.2 7.0	12 10	11 7.1	11 11	11 7	10 8	11 7	10.3 8.8	11 7
4 12	8 8	4.6 11	6 12	4.5 11	5 11	4.7 13	6 11	4.7 11	6.36 10.2	4.5 13
8 12	8 8	7.0 11	6 8	7 11.2	5 11	7.2 11	5 11	7 11	7.01 8.8	7 13.5
4 16	8 12	4.7 15	8 10	5.2 15	8 12	4.5 17	7 13	5 15	7.43 12.3	5 15

Table 7.9: Estimated object position coordinates using basic fingerprint database and virtual fingerprint database with exponential-exponential taper function

Location estimation error, e , is defined by the linear distance between unknown object coordinates (x_t, y_t) and their estimated coordinates (x_e, y_e) . Error calculation results between actual and estimated average object coordinates are tabulated in Table 7.10. It can be concluded that the best localisation results are achieved with exponential-exponential interpolation function.

7.5 System Evaluation

The virtual localisation approach is a novel localisation technique which is introduced in this chapter. Its mathematical analysis is given in detail in section 7.3. It is a well known fact that if the number of grid points is increased in a fingerprint map, localisation accuracies are also improved as a result. Unfortunately, increasing the grid numbers and the signal measurements at these grids is rather time consuming and costly. Therefore, the idea of creating virtual grid points and virtual measurements at these grid points across the fingerprint map is employed in this study.

Object	Error calculations between object and average estimated object positions							
X Y	Basic fingerprint	Error (m)	Virtual Fingerprint (Linear taper)	Error (m)	Virtual Fingerprint (Exp.Lin taper)	Error (m)	Virtual Fingerprint (Exp. Exp taper)	Error (m)
2 2	0.5 3	1.8	0.3 3.8	2.5	1.0 1.2	1.3	1.2 1.3	1
2 3	0.5 4.1	1.9	0.1 4.9	2.7	1.2 1.4	1.8	1.3 2	1.2
3 5	1.5 2.8	2.7	1.2 8.0	3.5	2.0 3.3	2.0	2.2 3	2.1
4 4	4.5 8.6	4.6	5.5 2.3	2.3	4.9 2.6	1.6	4.6 3.1	1
0 8	4.2 7.5	4.2	2.2 12.1	4.7	1.5 9.3	1.5	0.9 8.8	1.2
8 8	8.5 10.2	2.2	7.5 6.8	1.3	6.8 6.6	1.8	6.9 7	1.4
12 8	11.1 9.9	2.0	10.6 6.8	1.8	10.7 6.8	1.8	11 7	1.4
4 12	6.3 10.4	2.8	5.2 13.1	1.6	5.3 12.2	1.3	4.6 11.8	0.6
8 12	6.2 9.4	3.1	6.6 13.6	2.1	6.5 11.3	1.7	7 11.5	1.1
4 16	7.6 11.8	5.5	5.2 16.7	1.4	5.6 15.0	1.9	4.8 15.4	1
Total ave error(m)		3.1		2.4		1.7		1.2

Table 7.10: Overall error calculations for basic and virtual fingerprint databases. Estimated average object coordinates are tabulated for each fingerprint technique

There is only one virtual technique worth mentioning in the literature, where a linear distribution of LQI values are employed across the virtual grid space (Y. Zhao et al. 2007) [125]. In this technique several virtual reference nodes are introduced in classical Landmarc system and an elimination technique is used to eliminate most unlikely reference nodes. It is a different technique than the one used in this study. The technique introduced in this chapter uses all the grid points to introduce virtual grid points across the total test area and not several virtual reference grid points. Furthermore LQI distributions are in linear and exponential forms across the total virtual grid space.

The proposed positioning system uses a number of transmitters and a receiver as in basic fingerprint localisation systems. The originality lies in the introduction of virtual grid points with specific LQI interpolation functions between the physical grid points. Initially, localisation with classical fingerprint mapping technique is deployed and localisation accuracies of approximately 1 grid space are obtained in general. The number of physical fingerprint points is increased across the sensing area and the localisation accuracies are improved compared to coarse distribution of fingerprint points.

The key idea of the proposed approach is to obtain more accurate object localisation by keeping the same fingerprint map but increasing the number of grid points. One solution to increase the positioning accuracy is to add more grid points which will be more labour intensive and time consuming. A better solution will be to simulate a larger number of grid points by introducing virtual grid points and keeping the same number of real grid points.

The proposed system has the following advantages. Firstly, the hardware cost is the same as fingerprint localisation systems. Secondly, the number of measurement points corresponding to grid points in the test area is unchanged and only extra virtual grid points are

introduced between these grid points. Hence less time and effort is spent during the off line phase. Both real and virtual grid points are used together to generate a new denser fingerprint database for location determination.

Shortcomings of the virtual grids are their numbers across the sensing area. In theory, higher grid densities give greater localisation accuracies. In practice, there is a trade off between localisation accuracies and the number of virtual grid points. In the study, optimum localisation accuracies are obtained with 4 virtual grid points between two adjacent real grid points. This is obtained by dividing the distance between two adjacent real grid points into $n=5$ equal sections. During calculations, a total number of 416 grid points are deployed. 24 of them are real and 392 of them are virtual. If the number of virtual grid points is changed by making $n>5$ or $n<5$, a deterioration is observed in localisation accuracies. This is confirmed by experimental results.

Once the virtual grid space is determined, LQI values at physical grid points are interpolated between the virtual grids by introducing different interpolation functions. Finally, the virtual fingerprint database is compared with the unknown fingerprint signatures of the objects to determine the object locations. Experimental results of the object localisation with virtual fingerprint map reveal that the localisation accuracies are better compared to using physical fingerprint map.

7.6 Conclusions

In general, basic fingerprint localisation systems, in literature, generate localisation errors of around 1 grid space. In this study, classical fingerprint approach is utilised to compare with the proposed approaches. Fingerprint approach has an average localisation error of 3.1 metres which is slightly less than grid spacing of 4 metres. Application of taper functions and introducing virtual LQI values between grid points produce better localisation accuracies.

Linear interpolation technique has an average localisation error of 2.4 metres where the LQI values are linearly distributed between the virtual grid points. Exponential-linear interpolation technique, has an average error of 1.7metres. Virtual LQI distribution is exponential along the grid cell boundaries and linear within the grid cell. Exponential-exponential interpolation technique on the other hand, has an average error of 1.2 metres and virtual LQI distributions are exponential both along the grid cell boundaries and inside the grid cell. Exponential-exponential interpolation technique gives the minimum error of the 3 proposed approaches.

In this study, the main contribution is the localisation by using virtual fingerprinting. Position detection is implemented in the confined area of a sports hall. But the same technique can be generalised in any indoor area. Environmental conditions affect the LQI reception by the receivers. Although signal amplitude randomness is introduced among the LQI values, these random signal amplitudes decrease with respect to distance and it is still a valid physical condition. The fitted curves on these decreasing LQI distributions can be in linear or exponential format. These curves are taken as examples in virtual LQI distributions across the virtual fingerprint map.

Hence there is no relationship between the randomness of LQI values and the virtual grid points. Furthermore, signal filtering is employed to reduce the random effects on the recorded LQI values during measurements at physical grid points. It is observed that the proposed approaches improve localisation accuracies in large indoor areas. In future studies, different indoor areas will be tested with this new technique. A conference and a journal paper are published from this study [47,48].

CHAPTER 8

STATIC & DYNAMIC SEGMENTATION

8.1 Background

Fingerprint based localisation approach utilises a number of grid points across the indoor sensing area. RF signal strengths are measured at every grid point arriving from the surrounding transmitters and a fingerprint map is generated. Received signal strengths from the object position are compared with the signal strengths at grid positions across the fingerprint map. Minimum signal distances between the transmitters and object positions are selected and deployed in object position identification.

During these procedures, the total sensing area is utilised and all the recordings at grid points are checked against the signal strengths arriving from the object position. This takes a lot of computation time and effort to estimate the object location. To reduce the computation time and effort and to speed up the position estimation, localisation calculations are concentrated in selected sub areas across the sensing area. Each sub area is termed a segment, and division of the test area into segments is called segmentation [126]. The idea of segmentation is introduced to search for the object location in a localised way. In identification of sub areas, there are basically two kinds of segmentation defined as static and dynamic segmentation.

In static segmentation, the sensing area is divided manually into a number of segments according to area topology. A unique feature function is identified for each segment with respect to signal strengths received across that sub area [127,128]. This feature function displays an RSSI interval for each transmitter across the relevant segment. An *object location vector* is compared with the feature functions of the segments and the feature function which includes the *object location vector* is determined. The segment whose feature function contains the *object location vector* is identified as the object segment. Localisation algorithms are utilised to estimate the unknown object location in the object segment.

In dynamic segmentation, segments are determined automatically across the entire test area. Segment feature functions are realised similarly by selecting a range of RSSI values for each transmitter. Standard deviation of received RSSI values at each fingerprint point is utilised for each transmitter. \pm average STD_T interval for each transmitter across the total sensing area is employed to determine the feature functions of the segments.

A fingerprint point on the sensing area boundary is chosen as the reference point and its $RSSI \pm$ average STD_T interval for each transmitter is utilised to determine the other fingerprint points in its segment. Fingerprint points with the majority of their RSSI values in $RSSI \pm$ average STD_T intervals of reference point are considered to be in the reference point segment. Once the reference point segment boundary is determined, another fingerprint point is selected adjacent to its borderline and similar operation is carried out with the fingerprint points outside the previous segment. These operations are repeated and several segments are generated automatically across the sensing area. Once the segment boundaries are determined, *object location vector* is compared with segment feature functions. A segment is selected as an object segment which contains the *object location vector* at the start of object localisation. Unknown object location is determined by using localisation algorithms across the object segment. During the object localisation procedures there are 3 phases; Creation of a basic fingerprint database, a feature identification phase and a position estimation phase.

8.2 Static Segmentation

8.2.1 Fingerprint Creation Phase

Wireless sensor transmitters are strategically placed indoors around the sensing area. A receiver at each grid point receives the signal packets from transmitter nodes and sends them to the server PC to establish the fingerprint map during offline phase. The unknown object receiver also receives the broadcasted signal packets and measures the signal strength values of each received packet and sends them to the server PC during the online phase.

Segment determination takes place during an intermediate phase between offline and online phases since offline phase is used to collect fingerprint data and online phase is used to calculate the object locations. It is also possible to join the data collection and segment determination phases under offline phase.

RSS values received at grid points are also sent to the server PC and arranged in a database with respect to T transmitters as shown in Table 8.1. Assume that there are H number of T transmitters and N number of grid points.

Grid number	Grid locations (xi , yi)	RSS values
1	x ₁ , y ₁	rss ¹ _{T1} , rss ¹ _{T2} , rss ¹ _{T3} , , rss ¹ _{TH}
2	x ₂ , y ₂	rss ² _{T1} , rss ² _{T2} , rss ² _{T3} , , rss ² _{TH}
3	x ₃ , y ₃	rss ³ _{T1} , rss ³ _{T2} , rss ³ _{T3} , , rss ³ _{TH}
4	x ₄ , y ₄	rss ⁴ _{T1} , rss ⁴ _{T2} , rss ⁴ _{T3} , , rss ⁴ _{TH}
..
..
..
N	x _N , y _N	rss ^N _{T1} , rss ^N _{T2} , rss ^N _{T3} , , rss ^N _{TH}

Table 8.1: Basic Fingerprint database with **rss** values at every grid point

8.2.2 Feature Identification Phase

In each segment, a unique feature is assigned based on RSSI values collected at grid points from transmitter nodes {T₁,T₂,T₃,.....T_H} . There are A_m segments where m=1,2,3,4,...M, M is the total number of segments. Each segment has a feature F_A. These can be tabulated in Table 8.2.

Segment Number	Grid locations (xi , yi)	Corresponding segments	Features
1	(x ₁ , y ₁) (x _p , y _p)	A ₁	F _{A1}
2	(x _{p+1} , y _{p+1}) (x _q , y _q)	A ₂	F _{A2}
3	(x _{q+1} , y _{q+1}) (x _t , y _t)	A ₃	F _{A3}
...
...
M	(x _{r+1} , y _{r+1}) (x _N , y _N)	A _M	F _{AM}

Table 8.2: Features and segments for grid locations.

p , q , t and r in Table 8.2 represent the number of grid points across each segment. A unique feature function is identified for each segment. Each feature function, F_{Am}, is a set of categories for segment A_m based on RSSI values received from transmitters T_j= {T₁,T₂,T₃,T₄,.....,T_H}. It can be expressed as:

$$F_{A_m} = \{S_{T_1}, S_{T_2}, S_{T_3} S_{T_H} \} \quad (8.1)$$

S_{T_j} is the range of RSSI values for transmitter T_j.

Each range is defined by an interval of RSSI values around the mean of received RSSI values from each transmitter T_j across a particular segment. This can be shown as:

$$RSSI_{lower} < RSSI_{T_j} mean < RSSI_{upper}$$

There are m different segments and m different feature functions one for each segment. Each feature function has feature ranges for all the transmitters. For example if $R = \{r_1, r_2, r_3, \dots, r_z\}$ represents the grid points in a given segment A_m , then there is a set of features F_{A_m} that distinguishes segment A_m from other segments. Hence, S_{T_j} is considered as the range of RSSI values for transmitter T_j at grid point R in a segment A_m . An example can be given as $-70dBm < S_{T_j} < -60dBm$.

8.2.3 Position Estimation Phase

In this phase, the object location is estimated. Each segment has a feature function identified by RSSI ranges for all the transmitters. Segments are manually organized in rectangular shapes according to the topology of the sensing area. RSSI ranges for transmitters are determined as the identifying features of each segment. Mean, $(mean_{A_m T_j})$, and STD, $(std_{A_m T_j})$, of RSSI values for each transmitter across each segment is calculated.

A typical feature function F_{A_m} of segment A_m is defined by the individual ranges of RSSI values for T_j transmitters (ie. $j=4$). It is shown as;

$$F_{A_m} = \begin{Bmatrix} S_{T_1} \\ S_{T_2} \\ S_{T_3} \\ S_{T_4} \end{Bmatrix} = \begin{Bmatrix} mean_{A_m T_1} - std_{A_m T_1} < RSSI_{T_1} < mean_{A_m T_1} + std_{A_m T_1}, \\ mean_{A_m T_2} - std_{A_m T_2} < RSSI_{T_2} < mean_{A_m T_2} + std_{A_m T_2}, \\ mean_{A_m T_3} - std_{A_m T_3} < RSSI_{T_3} < mean_{A_m T_3} + std_{A_m T_3}, \\ mean_{A_m T_4} - std_{A_m T_4} < RSSI_{T_4} < mean_{A_m T_4} + std_{A_m T_4} \end{Bmatrix} \quad (8.2)$$

Object location vector, $O_j = \{RSSI'_{T_1}, RSSI'_{T_2}, \dots, RSSI'_{T_H}\}$, received from transmitters $T = \{T_1, T_2, T_3, T_4, \dots, T_H\}$, is recorded at object location. Elements of *object location vector* are ranged with feature functions of the segments.

If the elements of O_j are in the related ranges of the feature function of a specific segment, then that segment is identified as the object segment where the object is located.

Once the object segment is determined, *object location vector* and the *fingerprint location vectors* in the object segment are utilised to determine the object location by using k-NN and weighted k-NN algorithms. Software algorithm for the object localisation by using static segmentation is shown in Figure 8.1.

Begin

Step(1) : Object receiver collects RSSI values ,($rss_{i_{T_1}}, rss_{i_{T_2}}, rss_{i_{T_3}}, \dots, rss_{i_{T_H}}$), from transmitter nodes ($T_1, T_2, T_3 \dots T_H$) .

Step(2) : Find the correct segment by comparing collected object RSSI values and segment unique feature functions.

$$F_{A_m} = \{S_{T_1}, S_{T_2}, S_{T_3} \dots \dots \dots S_{T_H}\}$$

Step(3) : Calculate Eucliden distances between the RSSI values at grid points and the object RSSI values in the selected segment .

Step(4) : Sort the Euclidean distance values in ascending order.

Step(5) : Select k smallest Euclidean distances and their corresponding grid points.

Step(6) : Calculate the estimated object point by using k -NN and weighted k -NN algorithm.

End

Figure 8.1: Algorithm to estimate the object locations by using static segmentation

8.3 Dynamic Segmentation

Fingerprint localisation approach utilises the total sensing area while static segmentation reduces the number of grid points during the object localisation and a lesser number of *fingerprint location vectors* are utilised across the relevant segment. Unique feature function is assigned to each segment representing the RSSI ranges for all the transmitters across that segment.

Dynamic segmentation also utilises segments across the sensing area. But segments are selected automatically. A sequential method is introduced to determine the segments. RSSI ranges of transmitters at a selected reference grid point are compared with RSSI values at other grid points. Initially, a fingerprint database is constructed by using *fingerprint location vectors* at grid points across the sensing area. Mean and STD of recorded RSSI values for each transmitter across the total sensing area are calculated by using *fingerprint location vectors* at grid points.

A reference grid point is selected manually as the starting point of sequential checking with other grid points. RSSI values received at this reference point from all the T_j transmitters are utilised to introduce a reference feature function. Feature ranges of reference feature function are defined by $RSSI_{REF_{T_j}} \pm STD_{T_j}$ and shown as;

$$R_{T_j} = \{r_{T_1}, r_{T_2}, r_{T_3} \dots \dots \dots r_{T_H}\} \quad (8.3)$$

where

$$R_{T_j} = \begin{Bmatrix} r_{T_1} \\ r_{T_2} \\ r_{T_3} \\ \dots \\ \dots \\ r_{T_H} \end{Bmatrix} = \begin{Bmatrix} RSSI_{REF_{T_1}} \pm STD_{T_1} \\ RSSI_{REF_{T_2}} \pm STD_{T_2} \\ RSSI_{REF_{T_3}} \pm STD_{T_3} \\ \dots \\ \dots \\ RSSI_{REF_{T_H}} \pm STD_{T_H} \end{Bmatrix} \quad (8.4)$$

fingerprint location vector at each grid point can be identified by

$$F_J = \{RSSI_{T_1}^J, RSSI_{T_2}^J, RSSI_{T_3}^J, \dots, RSSI_{T_H}^J\} \quad (8.5)$$

where J represents the grid number.

Each *fingerprint location vector*, F_J , is compared with the elements of *reference feature function*, R_{T_j} , and checked whether $F_J \in R_{T_j}$.

If the 75% elements of F_J are in R_{T_j} ranges then the grid point with particular *fingerprint location vector* is considered to be in the same segment with reference grid point.

Grid points with F_J vectors satisfying $F_J \in R_{T_j}$ condition are selected and defined as the first segment S_1 across the sensing area. An example selection is presented in Figure 8.2.

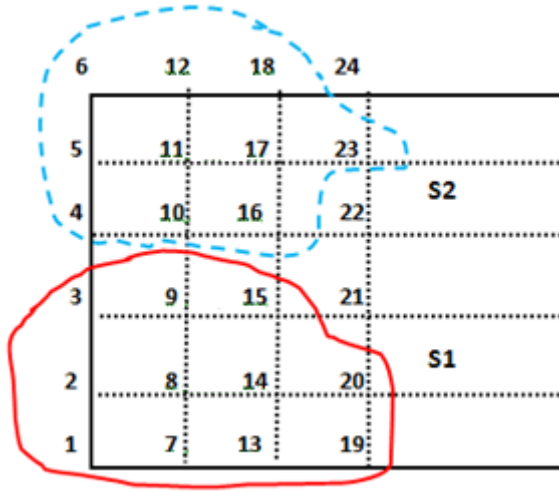


Figure 8.2: 1st and 2nd segments across the sensing area. Grid 1 and grid 4 are the reference grids for 1st and 2nd segments respectively.

If n_1 numbers of grid points are selected among N number of grid points, they are identified as first segment S_1 and stored in a database S_1 . Hence $(N-n_1)$ numbers of grid points are subjected to selection of the next segment.

A random grid point adjacent to S_1 segment is selected as a new reference grid point and a new *reference feature function*, R'_{T_j} , is generated as ;

$$R'_{T_j} = \{r'_{T_1}, r'_{T_2}, r'_{T_3} \dots r'_{T_H}\} \quad (8.6)$$

where

$$R'_{T_j} = \begin{Bmatrix} r'_{T_1} \\ r'_{T_2} \\ r'_{T_3} \\ \dots \\ \dots \\ r'_{T_H} \end{Bmatrix} = \begin{Bmatrix} RSSI'_{REF_{T_1}} \pm STD_{T_1} \\ RSSI'_{REF_{T_2}} \pm STD_{T_2} \\ RSSI'_{REF_{T_3}} \pm STD_{T_3} \\ \dots \\ \dots \\ RSSI'_{REF_{T_H}} \pm STD_{T_H} \end{Bmatrix} \quad (8.7)$$

Similarly, each element of *reference feature function*, R'_{T_j} , and F_j *fingerprint location vector* elements of $(N-n_1)$ grid points are compared with each other. Grid points with F_j vectors satisfying $F_j \in R'_{T_j}$ condition are selected and identified as the second segment S_2 across the sensing area. If the number of grid points is n_2 in segment S_2 , the same procedure is repeated for $\{N-(n_1+n_2)\}$ grid points to find the next segment. Segments which are generated with this sequential method across the total sensing area are presented schematically in Figure 8.3.

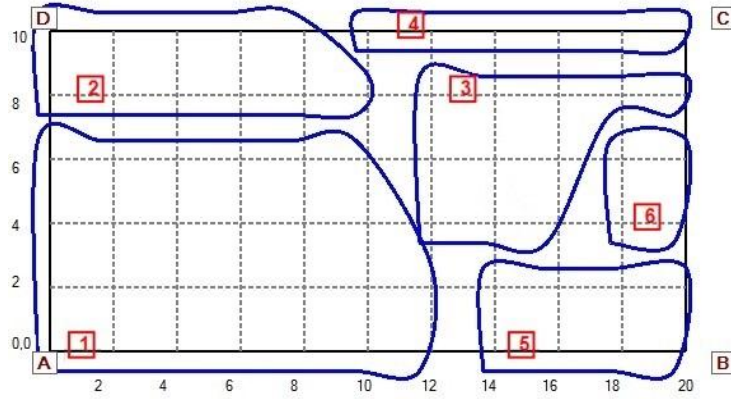


Figure 8.3: Example segments generated across the sensing area by using dynamic segmentation

Once S_m dynamic segments, where $m=1,2,3,\dots,M$, are determined across the sensing area, overall MEAN and STD of RSSI values received from each transmitter are calculated across each segment.

A *segment feature function* is generated by using these overall MEAN and STD values for each segment. Ranges of segment feature function can be shown as;

$$mean_{S_m T_j} - std_{S_m T_j} < RSSI_{T_j} < mean_{S_m T_j} + std_{S_m T_j} \quad (8.8)$$

Similarly *object location vector* is compared with *segment feature functions* and the object segment is determined by inclusion of *object location vector* elements in *segment feature function* ranges. Once object segment is determined, *object location vector* and the *fingerprint location vectors* in object segment are utilised to estimate the object location by using k-NN and weighted k-NN algorithms. An application program is developed to generate dynamic segmentation. Software algorithm for the object localisation by using dynamic segmentation is shown in Figure. 8.4

Begin

Step(1) : Select reference grid point in N grid points .

Step(2) : Determine Mean and STD of $RSSI_{T_j}$ values for total sensing area.

Step(3) : Generate feature function R_{T_j} for reference grid point .

Step(4) : Check fingerprint vector $F_J \in R_{T_j}$.

Step(5) : Determine first object segment S_1 .

Step(6) : Repeat procedure for next segments.

Step(7) : Determine object segment among the segments.

Step(8) : Estimated object point in object segment by using k-NN and weighted k-NN algorithm.

End

Figure 8.4: Algorithm to estimate the object location by using dynamic segmentation

8.4 Implementation

Applications of fingerprint localisations by using static and dynamic segmentation across the sensing area are described to determine the unknown object locations. Classical fingerprinting technique is also presented for comparison reasons. RSSI data transmission and collection are carried out by employing wireless transmitters and receivers. A server is used to collect the data and carry out the feature identification of segments. Object location detection is made across the object segment. A GUI is generated for all the operations.

8.4.1 Experimental test bed

Sensing area with 20mx10m dimensions and 2m grid space is employed during measurements. The area is free of any obstacles and experiments are conducted with line of sight measurements. Jennic JN5139 wireless sensor nodes are utilised as transmitters and receivers. 4 transmitters, T_j , are stationed at the corners of the sensing area and *fingerprint location vector* at each grid point contains 4 RSSI values. *Object location vectors* are collected at several object points. Measurements of RSSI values at each grid point are carried out and a fingerprint database is prepared with all the grid points.

8.4.2 Classical fingerprint approach

Initially, fingerprint mapping approach is utilised and unknown object locations are determined. *Object location vectors* at several object points are compared with *fingerprint location vectors* by using Euclidean distances. Classical k-NN and k-NN weighted algorithms are deployed and object locations are calculated. They are later compared with segmentation results. Selected object localisation results are presented in Table 8.3.

Object Coord. (x,y)	2-NN estimate	3-NN estimate	4-NN estimate	4-NN weighted estimate	Ave. estimated obj coord.	Error (m)
18 , 6	19 , 9	17 , 8	16 , 7	16.3 , 7.2	17.0 , 7.8	2.0
9 , 6	8 , 7	9 , 7	11 , 7	10.3 , 7.3	9.5 , 7.1	1.3
3 , 5	5 , 7	4 , 7	5 , 6	4.3 , 6.6	4.6 , 6.6	2.2
2 , 5	3 , 7	3 , 6	2.5 , 7	3.4 , 6.4	2.9 , 6.6	1.8
17 , 5	19 , 6	18 , 7	15 , 15	18.7 , 7.4	17.6 , 6.6	1.7
Average error						1.8

Table 8.3: Examples of estimated object coordinates by using k-NN algorithms across the total sensing area with dimensions 20mx10m with grid space of 2 m.

8.4.3 Static segmentation

3 Segments are organised across the sensing area and identified as C_1 , C_2 , and C_3 as shown in Figure 8.5. There are 66 *Fingerprint Location vectors* for 66 grid points.

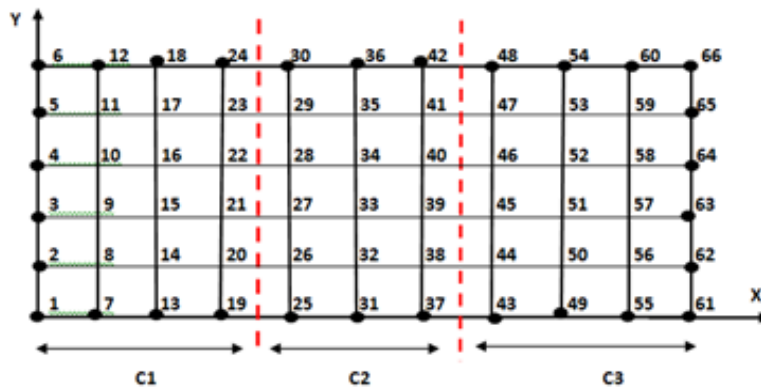


Figure 8.5: Sensing area, 20mx10m, with 3 segments C_1, C_2, C_3 . (grid space is 2 m)

Segments C_1 and C_3 have 24 grid points each and segment C_2 has 18 grid points. Overall Mean and STD of RSSI values received from each transmitter are calculated for each segment. A *segment feature function* for each segment is determined by using equation (8.2). Experimental *segment feature functions* for 3 segments are given in Table 8.4.

C ₁ feature function	C ₂ feature function	C ₃ feature function
$-84 \leq \text{RSSI}_A \leq -74$	$-83 \leq \text{RSSI}_A \leq -81$	$-73 \leq \text{RSSI}_A \leq -56$
$-75 \leq \text{RSSI}_B \leq -65$	$-79 \leq \text{RSSI}_B \leq -72$	$-74 \leq \text{RSSI}_B \leq -72$
$-74 \leq \text{RSSI}_C \leq -67$	$-81 \leq \text{RSSI}_C \leq -73$	$-76 \leq \text{RSSI}_C \leq -70$
$-78 \leq \text{RSSI}_D \leq -72$	$-72 \leq \text{RSSI}_D \leq -70$	$-73 \leq \text{RSSI}_D \leq -68$

Table 8.4: Feature functions for segment C₁ ,C₂ ,C₃ and 4 transmitters

Object segments are identified as explained in section 8.2 and estimated object coordinates with respect to actual object locations are calculated by using k-NN and weighted k-NN algorithms. A number of experiments are carried out. Selected object coordinates together with their estimated object locations are displayed in Table 8.5.

Segments	Object Coord. (x , y)	2-NN estimate	3-NN estimate	4-NN estimate	4-NN weighted estimate	Average Estimate Obj coord.	Error (m)
C3	18 , 6	18 , 8	18 , 6	15 , 6	17.9 , 6.7	17.2 , 6.6	1
C2	9 , 6	8.2 , 5.1	8.1 , 5.1	8.3 , 5.2	8.3 , 5	8.2 , 5.1	1.2
C1	3 , 5	2.1 , 4.3	2.2 , 4.2	2.2 , 4.4	2.3 , 4.2	2.2 , 4.2	1.1
C1	2 , 5	1.1 , 4	0.9 , 3.9	1.2 , 4.1	0.8 , 4.2	1 , 4	1.4
C3	17 , 5	16.1 , 4.1	16.3 , 4	16.2 , 4.2	15.8 , 3.9	16.1 , 4	1.3
Average error							1.2

Table 8.5: Estimated example object coordinates with static segmentation

Graphical display of object coordinates (18,6) , (9,6) , (3,5) and their estimated values by using static segmentation is given in Figure 8.6.

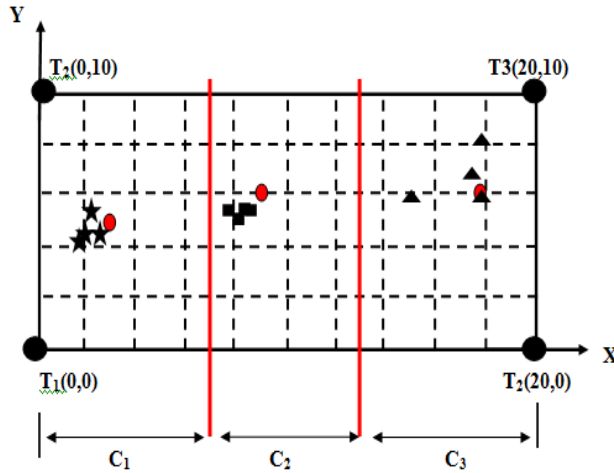


Figure 8.6: Graphical view of estimated object locations with static segmentation. Object is Red dot

An experimental result of static segmentation is presented in a test area of 20mx12m in Figure 8.7 as an example. Object coordinates are (8,8) and the average estimated object coordinates are calculated by AP as (7.4 , 9.1). The error distance is 1.2m.

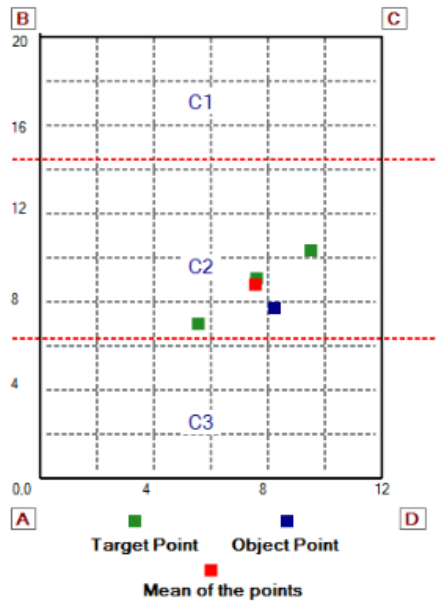


Figure 8.7: Experimental results of static segmentation in a 20mx12m test area. Object location is (8,8)

Flow chart of a software program, used in static segmentation, is presented in Figure 8.8.

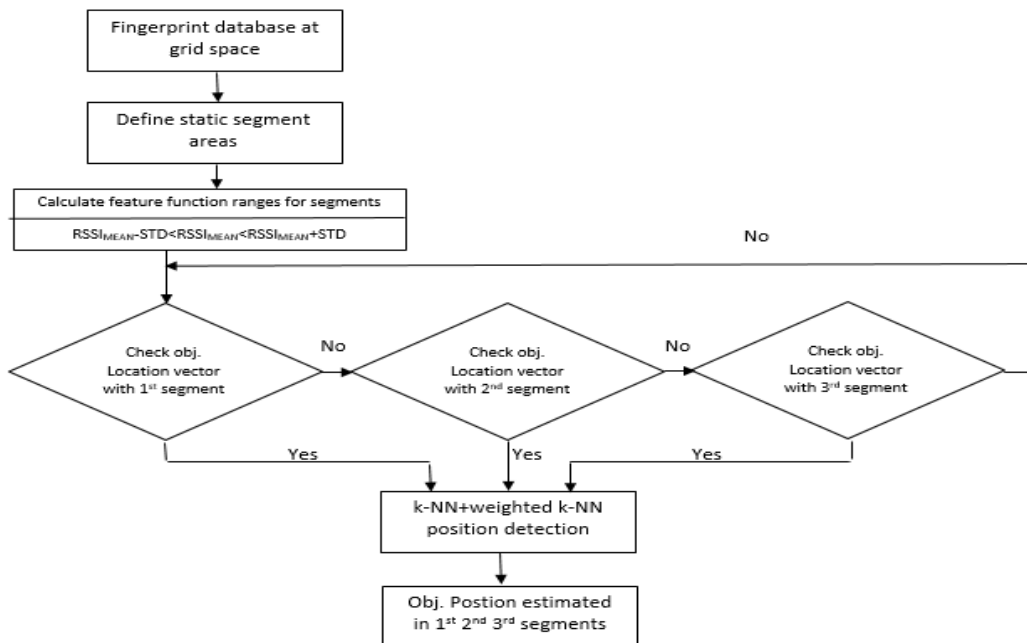


Figure 8.8: Flow chart of the software used for static segmentation

8.4.3.1 Static segmentation with different topology

Static segmentation approach is repeated for different indoor topologies. Test areas in different shapes and sizes are employed and similar methodology is applied. Some of the example localisation results for different object points are displayed here. An object location estimation is carried out in an L shaped test area with a grid space of 1mx1m. Initial

fingerprint mapping is carried out across the grid points. 5 segments are organised and their feature functions are determined. Object coordinates, (2,5), are estimated by using 2-NN, 3-NN and 4-NN algorithms. Average estimated object location is calculated as (2.0, 4.51) with an error distance of 0.5m. The results are shown in Figure 8.9.

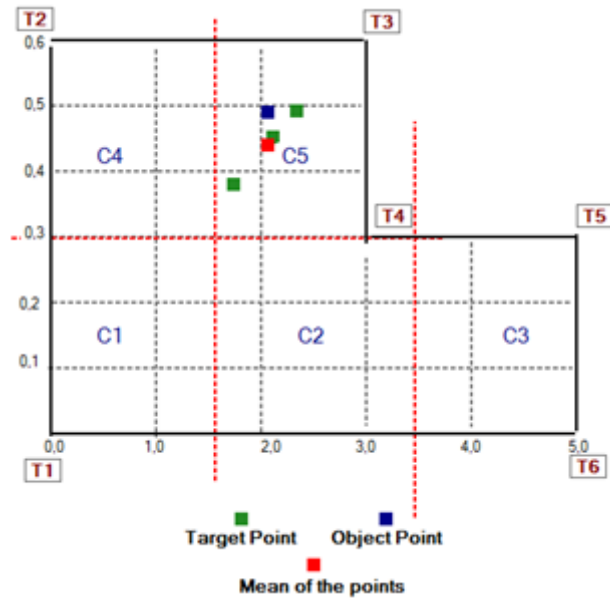


Figure 8.9: L shape test area with a grid space of 1mx1m. Object is at (2,5)

Feature functions of 5 segments which are employed during the experiments are given in Figure 8.10.

TAGS	C1	C2	C3	C4	C5
R1	221>R1>204	180>R1>163	152>R1>135	191>R1>174	141>R1>124
R2	154>R2>137	145>R2>128	130>R2>112	179>R2>163	192>R2>176
R3	129>R3>112	160>R3>143	154>R3>137	165>R3>148	213>R3>196
R4	151>R4>134	198>R4>181	200>R4>183	156>R4>139	207>R4>190
R5	142>R5>125	187>R5>170	218>R5>202	146>R5>129	196>R5>179
R6	143>R6>126	187>R6>170	218>R6>201	128>R6>111	148>R6>131

Figure 8.10 Feature functions of 5 segments with 6 transmitters.

Another test area with a T shape topology is utilised during the experiments. 6 transmitters are used and 4 segments are organised across the area. After generating the fingerprint mapping, segment feature functions are determined. Object segment C₂ for object location (5,3) is defined. Similar k-NN algorithms are applied and the example object location is estimated. Average estimated object location is calculated as (4.43, 3.61) with an error distance of 0.83m. See Figure 8.11.

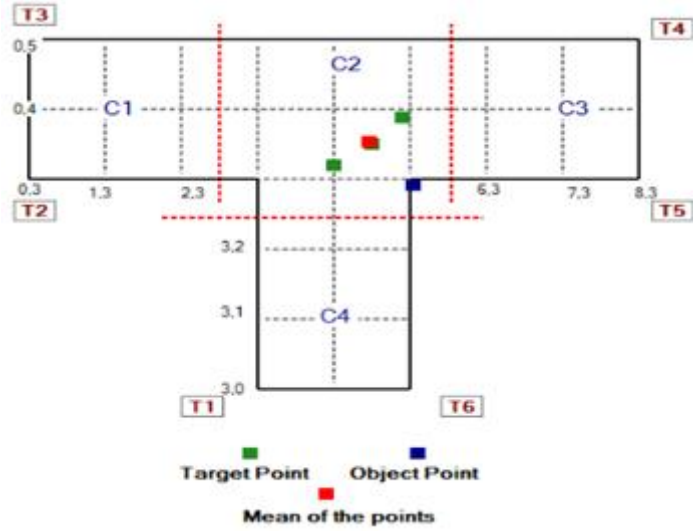


Figure 8.11: T shape test area with a grid space of 1mx1m. Object is at (5,3)

Feature functions for the T shape test area with 4 segments are presented in Figure 8.12 for 6 transmitters.

TAGS	C1	C2	C3	C4
R1	152>R1>135	167>R1>150	140>R1>123	204>R1>188
R2	210>R2>193	180>R2>163	148>R2>130	171>R2>154
R3	210>R3>193	181>R3>164	150>R3>133	153>R3>136
R4	150>R4>133	176>R4>159	209>R4>192	152>R4>135
R5	150>R5>133	176>R5>159	209>R5>192	166>R5>149
R6	147>R6>130	169>R6>152	157>R6>141	204>R6>186

Figure 8.12: Feature functions of 4 segments with 6 transmitters.

8.4.4 Dynamic segmentation

Dynamic segmentation is utilised by calculating the STD of RSSI values received from each transmitter across the sensing area. All RSSI values received at each grid point from one transmitter are used to calculate the STD value for that transmitter across the total sensing area. Hence there will be the same number of STD values as transmitters.

In an example case, grid point 1 in Figure 8.5 is selected as the reference grid point. STD value for each transmitter, T_j , across the sensing area is used together with $RSSI_{REF}$ value of each transmitter at reference point to generate *reference feature function* with feature ranges of $RSSI_{REF_{T_j}} \pm STD_{T_j}$. *Fingerprint location vectors* at other grid points are compared with *reference feature function*. Grid points, {1,2,3,7,8,9,13,14,15,19,20}, whose *Fingerprint location vectors* are included within the *reference feature function* are considered to be in segment 1 as shown in graphical example in Figure 8.2.

In this example, Grid point 4 at segment 1 boundary, is selected as the new reference grid point. Similar procedures are followed as in segment 1 and new grid points which are within the new *reference feature function* are determined.

Collection of these new grid points, {4,5,6,10,11,12,16,17,18,23}, is identified as segment 2. Feature functions for segments 1, 2 and 3 are determined and their corresponding RSSI ranges for each transmitter are presented as shown in Table 8.6.

Feature	Segments	Transmitter A	Transmitter B	Transmitter C	Transmitter D
F ₁	Segment 1	-50<RSSI _A <-46	-70<RSSI _B <-62	-67<RSSI _C <-62	-65<RSSI _D <-55
F ₂	Segment 2	-61<RSSI _A <-46	-67<RSSI _B <-63	-70<RSSI _C <-60	-60<RSSI _D <-45
F ₃	Segment 3	-66<RSSI _A <-53	-66<RSSI _B <-61	-76<RSSI _C <-63	-47<RSSI _D <-43

Table 8.6: Calculated feature functions for 3 dynamic segments F₁,F₂,F₃ across the sensing area

8.4.5 Environmental effects on dynamic segments

During calculations, the majority of the grid points are located in the correct segments. Due to the random nature of the recorded RSSI values, in rare cases, grid points from a remote part of the sensing area can be included in the current segment. This takes place due to the inclusion of remote grid points' fingerprint vectors in the feature function of the current segment. For example, under normal conditions, grid points 33 and 34 are not included in segment 1 in Figure 8.2. In order to eliminate these cases, once the grid points in the current segment are determined, these grid points are checked and the remote grid points among them are discarded. If the remote grid point coordinates are adjacent to other grid points, they are included in the current segment. Otherwise they are excluded from the current segment.

For example, grid points (1,7,13,19,2,8,14,20,3,9,15,33,34) in figure 8.5 are initially selected in segment 1. Proximity of each grid point is checked along x and y directions with each other. Firstly, those points that are adjacent to each other along the x direction are found to be (1,7,13,19) , (2,8,14,20) and (3,9,15). Secondly, the same procedures are carried out along the y direction and grid points (2,1,3), (8,7,9) , (14,13,15) and (20,19) are found to be adjacent. On the other hand, grid points (33,34), are found to be isolated from the rest of the grid points.

Hence two groups of grid points are generated. These groups are (1,2,3,7,8,9,13,14,15,19,20) and (33,34). Finally the two groups are compared in size and the largest group is taken as segment 1. Grid points in the smaller group are sent back for the segment reselection process. Once the grid points of a segment are decided, the boundaries of

the segment are drawn for the user's attention. A Flow chart of the software used for dynamic segmentation is displayed in Figure 8.13.

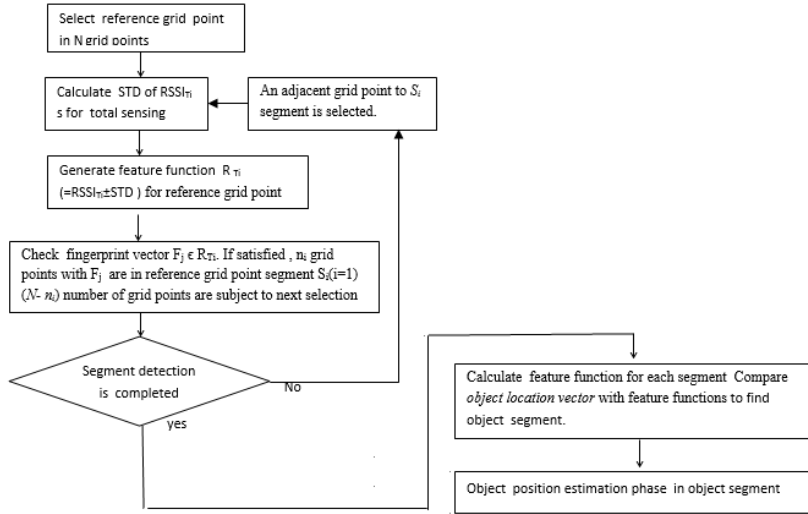


Figure 8.13: Flow chart of the software used for dynamic segmentation

8.4.6 Object localisation in dynamic segments

Once the segment areas and their grid points across the sensing area are realised as shown in Figure 8.3, localisation of the objects is carried out. The mean and STD of RSSI values for each transmitter are calculated across each segment. A *segment feature function* for each segment is realised, similarly, by using equation (8.8).

Object location vector is compared with *segment feature functions* of the segments. In case of an inclusion of *object location vector* by a *segment feature function*, the object is considered to be in that segment. Object coordinates are estimated by applying k-NN algorithms with *object location vector* and *fingerprint location vectors* at grid points in related object segment. Selected examples of estimated object coordinates by using dynamic segmentation are presented together with actual object coordinates in Table 8.7.

segments	Object Coord. (x , y)	2-NN estimate	3-NN estimate	4-NN estimate	4-NN weighted estimate	Average Estimated obj coord.	Error (m)
1	3 , 5	2.0 , 4.3	1.9 , 4.4	1.9 , 4.4	2.5 , 4.5	2 , 4.4	1.1
1	9 , 6	8.3 , 5.4	8.4 , 5.3	8.5 , 5.5	8.3 , 5.4	8.3 , 5.4	0.9
2	4 , 8	5.0 , 8.4	4.9 , 8.3	4.9 , 8.3	4.9 , 8.4	4.9 , 8.4	1.0
3	17 , 5	16.4 , 4.4	16.3 , 4.5	16.5 , 4.6	16.3 , 4.3	16.4 , 4.4	0.8
5	16 , 2	15.3 , 1.4	15.4 , 1.3	15.2 , 1.6	15.4 , 1.3	15.3 , 1.4	0.9
6	18 , 6	17.3 , 5.5	17.4 , 5.4	17.4 , 5.4	17.5 , 5.3	17.4 , 5.4	0.8
Average error							0.9

Table 8.7: Estimated object coordinates and error distances with dynamic segmentation and k-NN algorithms. (Test area is 20mx10m with grid space of 2m)

Graphical examples of object position detection by using dynamic segmentation are presented in Figure 8.14 and Figure 8.15.

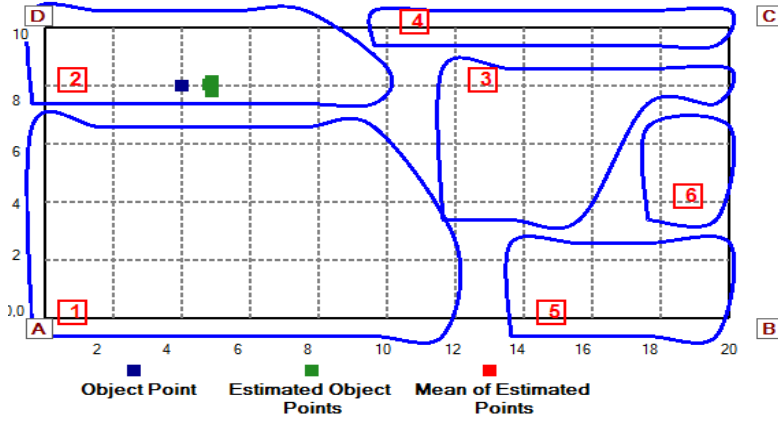


Figure 8.14: Object localisation by using dynamic segmentation. Object position is (4,8), estimated average object position is (4.9, 8.4).

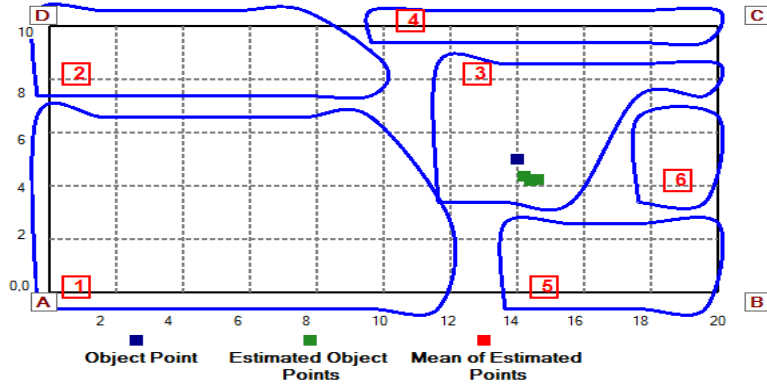


Figure 8.15: Object localisation by using dynamic segmentation. Object position is (14,5), estimated average object position is (14.8, 4.3).

Feature functions of 6 dynamic segments corresponding to 4 transmitter ranges for Figure 8.14 and 8.15 are given in Figure 8.16.

Segments	Transmitter - A	Transmitter - B	Transmitter - C	Transmitter - D
S1	-50>A>-58	-61>B>-71	-61>C>-71	-56>D>-64
S2	-51>A>-67	-63>B>-67	-62>C>-72	-46>D>-54
S3	-62>A>-72	-53>B>-63	-50>C>-56	-62>D>-70
S4	-59>A>-67	-55>B>-69	-38>C>-64	-62>D>-66
S5	-64>A>-70	-46>B>-50	-55>C>-63	-59>D>-79
S6	-64>A>-70	-44>B>-56	-47>C>-55	-60>D>-76

Figure 8.16: Feature functions of six dynamic segments in object localisation

In dynamic segmentation, a reference grid point is selected and a feature range of $RSSI_{REF_{T_i}} \pm STD_{T_i}$ for each transmitter is calculated. It is also possible to vary the width of these ranges by introducing a constant multiplier of “ α ” with STD_{T_i} where $1 \leq \alpha \leq 2$. This will in return change the number of dynamic segments. For example, segment number becomes 5

when $\alpha=1.2$ as shown in Figure 8.17. Feature functions of 5 segments are given in Figure 8.18.

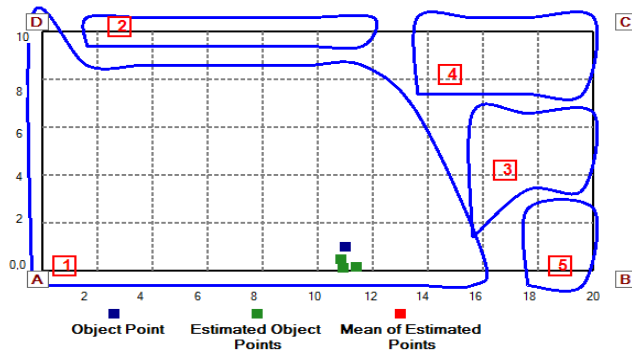


Figure 8.17: Object localisation by using dynamic segmentation, object position is (11,1), estimated object position is (11.3,0.2) .

Segments	Transmitter - A	Transmitter - B	Transmitter - C	Transmitter - D
S1	-52>A>-62	-60>B>-68	-60>C>-70	-56>D>-64
S2	-57>A>-65	-57>B>-73	-62>C>-70	-51>D>-55
S3	-62>A>-72	-45>B>-57	-49>C>-57	-57>D>-75
S4	-60>A>-70	-56>B>-62	-38>C>-56	-63>D>-69
S5	-64>A>-70	-40>B>-48	-52>C>-64	-56>D>-84

Figure 8.18: Segment feature functions for dynamic segmentation, object position is (11,1)

Similarly, segment number becomes 4 when $\alpha=1.8$ as shown in Figure 8.19. Feature functions of 4 segments are given in Figure 8.20.

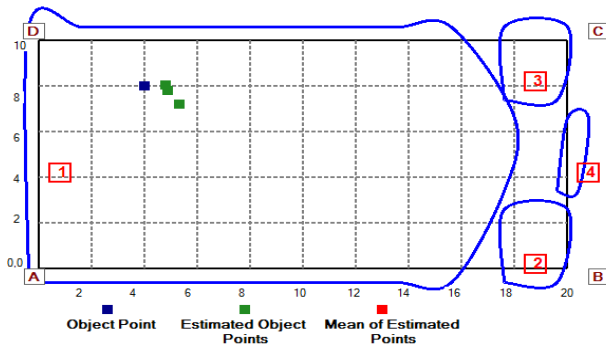


Figure 8.19: Object localisation by using dynamic segmentation, object position is (4,8), estimated object position is (4.9,7.6)

Segments	Transmitter - A	Transmitter - B	Transmitter - C	Transmitter - D
S1	-55>A>-63	-58>B>-68	-58>C>-68	-55>D>-65
S2	-64>A>-70	-40>B>-48	-52>C>-64	-56>D>-84
S3	-59>A>-75	-53>B>-63	-36>C>-50	-62>D>-72
S4	-66>A>-70	-50>B>-50	-50>C>-50	-67>D>-71

Figure 8.20: Segment feature functions for dynamic segmentation, object position is (4,8)

Example object localisation results by using dynamic segmentation in Figure 8.15, Figures 8.17, Figure 10.19 are tabulated in Table 8.8.

No of Segment	Object coordinates	2-NN	3-NN	4-NN	Weighted 4- NN	Ave Coord.	Error (m)
6	14 , 5	14.7 , 4.3	15 , 4.2	14.9 , 4.3	14.9 , 4.4	14.8 , 4.3	1
5	11 , 1	11.4 , 0.3	10.6 , 0.3	11.7 , 0.2	11.6 , 0.3	11.3 , 0.2	0.9
4	4 , 8	5 , 7.8	4.9 , 7.7	5.1 , 7.3	4.8 , 7.8	4.9 , 7.6	1.0
Average error =							0.95

Table 8.8: Dynamic segmntation results with different number of segments

8.5 System Evaluation

The idea of segmentation is introduced to search for the object location in a reduced computation time and to increase the accuracy of the position estimation. Initially, any indoor tracking area can be divided into segments according to its topology and the object search algorithm can be applied in one segment once the segment is selected. The selection process is carried out by considering the grid points across the test area and the RSSI values recorded at these grid points.

Fingerprint localisation systems in literature have localisation accuracies of around the grid size of their fingerprint maps. The static segmentation approach, introduced here, achieves an overall positioning accuracy of 1.2 metres. Dynamic segmentation gives better accuracy results of 0.9 metres while the classical fingerprint approach has a positioning accuracy of 1.8 metres.

In this chapter, a manual method, called static segmentation, is introduced where RSSI values at each grid point are averaged out to generate mean and STD values for each transmitter in each segment. A range of average mean \pm STD values is calculated for each transmitter. 4 ranges for 4 transmitters are identified as the feature function for each segment in the localisation process.

Object location vector is searched within the ranges of feature functions of all the segments. Once a match is obtained, k-NN algorithm is applied with the *object location vector* and *fingerprint location vectors* of object segment to determine the object location.

Automatic determination of segments is identified as dynamic segmentation. A grid point preferably at the corner of the test area is considered as a reference point to start the segmentation. Mean and STD of RSSI values for each transmitter are calculated across the total test area. Mean of recorded RSSI values for each transmitter at the reference point is also calculated and a range of mean \pm STD is determined for each transmitter .

A search is made with the RSSI values of all the transmitters at other grid points with these ranges. If RSSI values of transmitters at any grid point is within the ranges of the reference grid point then the corresponding grid point is considered in the same segment as the reference grid point.

Once the boundaries of segments are determined, local $\text{mean} \pm \text{STD}$ ranges are utilised for all the segments and *object location vector* is compared with them. Object segment is found when there is a match between the local segment $\text{mean} \pm \text{STD}$ range and the *object location vector* for each transmitter. k-NN algorithms are employed to localise the object position in the object segment.

Manual segment selection has the freedom of defining any section of the test area according to the structure of the indoor area. Accuracies obtained with the proposed system justify the manual selection as a valid segment selection. Dynamic segmentation, on the other hand, does not need any intervention and automatically decides on the segments. It gives good localisation accuracies.

8.6 Conclusion

Localisation techniques with static and dynamic segmentation are proposed in this chapter. Theoretical analysis of the segmentations are given in sections 8.2 and 8.3. The results show encouraging accuracy levels compared to other localisation accuracies. Localisation accuracies are evaluated based on two factors. Firstly, recordings of the RSSI values are carried out very carefully during the off-line phase of the experiments. They are recorded many times and averaged out to reduce the random behaviours among them. Outliers are also discarded from the mainstream recordings. Secondly, realisation of segments is carried out by using mean and STD of RSSI values corresponding to each transmitter.

Feature functions of the segments are developed with RSSI ranges for each transmitter. They are compared with *object location vectors* to pinpoint the object segment. Once the object segment is deployed, k-NN algorithms are employed to find the unknown object location in that segment.

The proposed segmentation approaches offer good localisation accuracies. Segmentation methods reduce the computation size and time to locate the objects. Differently shaped and sized segments can be introduced with respect to topology of indoor locations and the object locations can be estimated. The study in this chapter is published as a conference paper [50].

CHAPTER 9

CONCLUSIONS AND FUTURE WORK

9.1 Conclusions

The purpose of this study is to investigate various localisation techniques and to determine the techniques which generate the best positioning accuracies. Different techniques are utilised throughout the study and they are summarised as follows.

- Fingerprint based localisation,
- Centroid and weighted centroid,
- Adaptive centroid localisation,
- Triangular localisation,
- Neighbourhood referencing,
- Virtual fingerprint based localisation,
- Static and dynamic segmentation,

Additionally, LQI and RSSI characteristics are studied. Wireless sensor node radiation beam patterns are recorded and analysed. Relationships between radiation distances and LQI / RSSI values are investigated. Recorded LQI and RSSI values are calibrated with respect to distances.

Each localisation technique has its own advantages and disadvantages. Experimental results reveal that there are a few localisation techniques which give good positioning accuracies. Positioning accuracies achieved in this study are summarised in Table 9.1 in the presentation order of techniques utilised in this thesis.

As observed in Table 9.1, the best localisation accuracies are achieved with reference neighbourhood weighted localisation technique with error distances of 0.40 m. Error distances between the estimated object and the object positions are 0.77m with adaptive centroid using a grid space of 1m. Virtual fingerprint technique with exponential taper function gives 1.2m

accuracy for a grid space of 4m. Other localisation techniques introduce error distances between 0.8m and 2.4 m with respect to their grid spacing.

Localisation techniques		Accuracies (average error distance)
<i>Fingerprint 4-NN</i>	<i>(grid space is 1m)</i>	<i>0.82m</i>
<i>Fingerprint weighted 4-NN</i>	<i>(grid space is 1m)</i>	<i>0.81m</i>
<i>Weighted centroid</i>	<i>(grid space is 1m)</i>	<i>0.91m</i>
<i>First level adaptive centroid</i>	<i>(grid space is 1m)</i>	<i>0.90m</i>
<i>Second level adaptive centroid</i>	<i>(grid space is 1m)</i>	<i>0.77m</i>
<i>Triangular localisation</i>	<i>(grid space is 1m)</i>	<i>1.10m</i>
<i>Reference LandMarc (star)</i>	<i>(grid space is 2m)</i>	<i>1.25m</i>
<i>Reference Improved LandMarc</i>	<i>(grid space is 2m)</i>	<i>0.79m</i>
<i>Reference Neighbourhood weighted</i>	<i>(grid space is 2m)</i>	<i>0.40m</i>
<i>Virtual fingerprint (linear taper)</i>	<i>(grid space is 4m)</i>	<i>2.40m</i>
<i>Virtual fingerprint (exp-lin taper)</i>	<i>(grid space is 4m)</i>	<i>1.70m</i>
<i>Virtual fingerprint (exp-exp taper)</i>	<i>(grid space is 4m)</i>	<i>1.20m</i>
<i>Static segmentation</i>	<i>(grid space is 2m)</i>	<i>1.20m</i>
<i>Dynamic segmentation</i>	<i>(grid space is 2m)</i>	<i>0.90m</i>

Table 9.1: localisation techniques versus achieved accuracies

Grid spacing is an important factor during localisation procedures. Larger grid spaces represent sparse data recording at these grids and generate larger positioning errors. Localisation data must be recorded densely or denser data recording must be simulated across the test areas. Overall localisation accuracies and calculated error distances are approximately close to grid spacing. Experiments and position calculations, in this study, generally verify this hypothesis. This is in close agreement with similar localisation techniques in literature.

Another important factor which affects the accuracy of position detection is the environmental conditions along the RF propagation path. Any obstacles and walls indoors attenuate and reflect the radio signals and generate false readings or recordings. Hence data recording must be carried out under careful conditions and extra care must be taken during experiments.

Classical fingerprint based systems collect RSS values in LQI or RSSI forms in a server computer and organise them as databases with respect to signal positions or detection orders. Unknown object location fingerprints are compared with the location fingerprints in the database by using Euclidean distance models. Number of nearest fingerprints is selected by using k-nearest neighbourhood algorithm. The average values of their position coordinates are chosen as the estimated object location.

An improvisation to basic k-NN technique is introduced by using weight functions in the calculations. These functions are utilised with the coordinates of the nearest fingerprint points

with respect to signal distances. Shorter signal distances have more effects than the longer signal distances in the calculations. Weight functions increase the effects of longer distances next to shorter signal distances. Weight functions are inversely proportional to the distances between transmitters and receivers.

The basic fingerprint database contains the location fingerprint at every grid point across the tracking area. In general, the distribution of grids hence the measurements of RSS values are very coarse and this affects the localisation accuracy. The basic physical fingerprint database is organised as a virtual fingerprint database by introducing virtual grid points between physical grid points and virtual measurement values at these points. Every grid cell in the basic fingerprint is divided into a number of virtual sub cells. Consequently, the number of fingerprint readings is virtually increased across the test area. Linear and exponential interpolation algorithms are utilised across the distribution of signal strengths between adjacent physical grid points.

Similar k-NN and weighting k-NN techniques are applied to localise the unknown object positions. Localisation accuracies with an exponential interpolation algorithm is better than the standard fingerprint results.

In basic centroid localisation, the object location is determined as the average of the transmitter coordinates. This is a coarse position detection and it is improved by using weight functions between each transmitter and receiver pair. Hence weighted centroid localisation technique produces localisation accuracy better than centroid localisation.

An adaptive centroid localisation approach is utilised by using environmentally adapted RSSI values. Mean and standard deviation of RSSI values are used to develop a range of RSSI values to reduce the randomness among them. Another improvement is introduced by choosing a transmitter location where the minimum variations of RSSI values are received as the origin of the relative coordinate system. The distance values between the object receiver and transmitters are employed and the unknown object position is determined in a relative coordinate system. Calculations are transferred to a real coordinate system later and the object location is determined with a positioning accuracy of around 0.77m.

Segmentation is a localisation technique which divides the test area into areas of RSSI ranges. The test area is segmented into a number of sub areas and the range of RSSI values for transmitters in each sub area is defined. In the fingerprint localisation technique, a search mechanism is used to search an object fingerprint among the grid fingerprints. This search is done across the total grid space and in return takes a longer time.

In order to reduce this search time and effort, object RSSI recordings are checked with feature function of each sub area. A match between the object RSSI recordings and a segment feature function identifies the object segment. Finally, once the object segment is known, localisation procedures are only carried out in this sub area. Achieved positioning accuracy levels with static segmentation are around 1.2m and with dynamic segmentation are around 0.9m.

Neighbourhood weighted localisation technique is another technique which gives high accuracy levels. RSSI values and the physical distances are employed to determine the weights between the object and transmitters. 3 nearest nodes are selected with 3-NN algorithm and 3 closest nodes of each nearest node are deployed to calculate the object locations. Achieved accuracy levels are around 0.4m.

9.2 General discussion

A quick search of the literature reveals that there are many wireless localisation techniques developed for indoor areas. These techniques use different types of wireless sensor nodes with different properties and characteristics. Wireless sensor nodes with only basic transmitter and receiver properties generate positioning accuracies of around the utilised grid space. Similarly, basic Jennic JN5139 and JN5121 WSN devices are employed in this research and positioning accuracies of around 0.4m to 2.4m are obtained relative to grid spacing of 2m and 4m.

In literature, in order to improve these accuracy levels to below 0.1m, a second parallel system is often introduced with the wireless sensor nodes. For example a well known system, Cricket, uses an ultrasonic system next to an RF system. RF signals are used between transmitters and receivers for synchronisation of time measurements. Ultrasonic signals are transmitted and received to calculate the distances. Hence the distances can be accurately determined between the transmitters and receivers. The accuracy levels with these systems are around 0.1 m. If one requires further accuracy, optical and interferometric sub-systems are introduced with RF systems. Accuracy levels are around 2cm to 3cm with these systems.

An important factor in localisation techniques is the cost factor. Higher positioning accuracies require expensive systems and this increases the cost. Hence a correlation must be made and an optimum point must be found between the cost and operational requirements.

Some wireless sensor nodes are purpose built to contain two different signals, onboard memories, processor units and 2 way communication properties with different power levels.

These nodes are more effective at recording and processing the RF signals. They have many operational properties to allow signal and data trafficking between them.

Jennic JN5139 wireless sensor nodes are utilised in this study. These devices have simple communication and data transfer facilities between transmitters and receivers. They have no advanced signal control features. Improved models such as Jennic JN5168 have onboard advanced features such as time of flight engine etc. for data processing and localisation.

Fingerprint based localisation systems rely on how carefully the fingerprint database is prepared and how accurately the unknown location fingerprints are taken. In both cases, a number of RSS readings must be taken and their random behaviour must be reduced by using filtering and averaging techniques or algorithms such as an adaptive centroid algorithm.

An adaptive centroid localisation approach introduces a selection of RSSI values. RSSI values which are within the mean \pm STD interval are considered for positioning. A constant environmental attenuation factor is introduced related to environmental conditions on the selected RSSI values. New environmentally adapted RSSI values are generated by using this constant factor. This factor can be changed according to different environments.

Virtual localisation is an important approach to determine the RF signal amplitudes between the fingerprint nodes. Researchers usually measure the signal strengths at grid nodes but they have no information between these nodes. If the grid points are far apart, this affects destructively object localisation accuracies. One way to counter this is to introduce a large number of grid points and relevant RSSI measurements, but all these costs can be reduced by introducing virtual grid points and their RSS values with respect to special taper functions. Linear and exponential taper functions are employed and virtual RSSI distributions are developed across the test area.

The localisation process reveals a positioning error of 1.2m by using an exponential-exponential taper function with 416 virtual grid points while basic fingerprint gives an error of 3.1m with 24 physical grid points. A test area of 20mx12m with a grid space of 4m is used during the experiments. Hence the error levels of virtual fingerprint localisation are better than the basic fingerprint localisation results.

A neighbourhood weighted algorithm approach is another technique with low error margins. This algorithm is used with the well-known LandMarc localisation technique. Transmitter reference nodes are placed in star formation across the test area. Weighted 3-NN algorithm is utilised between the reference nodes. Weights are introduced between reference nodes by using both Euclidean distances and physical distances. Distances between the object

and the reference nodes are calculated with these weights. Triangulation techniques are employed to determine the object's coordinates.

Static and dynamic segmentation approaches are utilised to determine the object locations. An initial object search is carried out among the static or dynamic segments across the test area. Once the object segment is defined, object localisation is concentrated only in that segment. Localisation algorithms are applied with the fingerprint data across the object segment. Positioning accuracies are around 1.2m for static and 0.9m for dynamic segmentation with a grid space of 2m.

9.3 Outcomes

Many localisation approaches are developed in literature. Minimum accuracy levels achieved by using basic wireless sensor nodes are around 1 to 4 metres depending on the grid spacing and indoor topology. The main purpose of this study is to develop novel localisation systems with positioning accuracy levels around 1 metre or less by using basic Jennic wireless sensor nodes in rectangular indoor areas.

This study has introduced many new localisation approaches to enhance the localisation accuracies based on received signal strengths in LQI and RSSI form. Triangulations, trilateration, segmentation and virtual techniques are adapted to develop accurate object localisation. Many new developments are included such as determination of weight functions using Euclidean and physical distances, virtual fingerprinting using linear and exponential taper functions, neighbourhood weighting with reference nodes, environmental adaptivity and dynamic segmentation.

The objectives of this study are presented in the first chapter and they are successfully achieved throughout the work. Achievement of each objective is listed as follows.

9.3.1 Outcome 1: Research Literature

An extensive literature review is carried out in **Chapter 1**. More than 400 related publications are studied and the subject of object localisation is thoroughly investigated. Existing published research reveals that the localisation accuracies are around 1 to 4 metres depending on the grid spacing with simple wireless sensor nodes indoors. Very few publications dealt with Jennic devices and ZigBee standards. In this study, the main aim was to set up real life localisation systems with Jennic devices indoors and calculate the object positions as accurately as possible. Several localisation systems are introduced and tested. Their accuracy levels are compared with the accuracy levels in literature.

9.3.2 Outcome 2: Localisation systems

Design considerations of localisation systems are given in **Chapter 2**. Localisation techniques are investigated such as triangulation, trilateration, TOA, TDOA, AOA. Range free and range based localisation systems are studied. Fingerprint and LandMarc systems are summarised. RSS values are utilised in the majority of all localisation systems. They have Omni-directional properties and they can be detected conveniently from all directions.

RSS based localisation approaches are preferred in scientific community. Hence, RSS based localisation systems are implemented in this study. RSS values are received in LQI format from experimental Jennic devices and converted into RSSI format by software in the server. Different algorithms are developed to determine the object locations accurately across the indoor areas.

9.3.3 Outcome 3: LQI characteristics and Fingerprint localisation

Wireless sensor nodes transmit and receive radio signals in free space. Their antennas are omni-directional and RF signals propagate in all directions from transmitter antennas. Transmitter radiation beam patterns of experimental Jennic devices are plotted in **Chapter 3**. It is observed that they have generally spherical propagation patterns in all directions. Hence, uniform propagation of RF signals in all directions is assumed in the experiments for Jennic wireless sensor nodes.

A fingerprint based localisation approach is proposed. A fingerprint map is constructed across the test area. The system implemented gives a positioning accuracy of 0.82m by using k-NN algorithms. During the offline phase, extreme care is taken while recording the RSS data to avoid random amplitude variations. Experiments are always carried out in test areas where the majority of the obstacles are eliminated. Received LQI and RSSI values are filtered out before object position detection.

9.3.4 Outcome 4: Optimum weight functions

Localisation systems use weight functions to improve the localisation accuracies. Higher weights have more contribution to localisation accuracies. Different empirical weight functions are researched in indoor areas in **Chapter 3** and localisation experiments are carried out with these functions. Some of the weight functions are designed with Euclidean distances; other weight functions are designed with real distances between transmitters and receivers.

In this study, experiments show that weights which are designed with the cube of $(1/d_e)$ where d_e is the Euclidean distance between transmitters and receivers produce better positioning accuracies. Similarly, weight functions which use $(1/d)$ where d is the actual

distance between transmitters and receivers also generate better localisation accuracies with centroid localisation techniques.

9.3.5 Outcome 5: Weighted centroid localisation

A weighted centroid algorithm is utilised to determine the object locations in **Chapter 4**. Weights are calculated with respect to object distances from the transmitters. Object coordinates are determined by deploying these weights and the transmitter coordinates in the test area. Positioning accuracy levels of around 0.91m are achieved.

9.3.6 Outcome 6: Adaptive centroid localisation

A new approach is proposed by using centroid localisation adaptively in **Chapter 4**. RSSI values are affected by environmental conditions. These conditional effects are included adaptively with RSSI values. Mean and STD of RSSI values are used and ranges of RSSI values are determined. Localisation is carried out in 2 phases.

In first phase, a range of RSSI values in $\text{mean} \pm \text{STD}$ range is selected. An environmental threshold factor is identified and multiplied with the selected RSSI values. Object locations are estimated in phase 1 and average positioning accuracies of 0.9m are obtained.

A second phase is introduced after phase 1. A second similar selection process is introduced with RSSI values within the above range of $\text{mean} \pm \text{STD}$. A new environmental threshold constant is identified and estimations of object locations are carried out. Average localisation accuracies of 0.77m are obtained.

9.3.7 Outcome 7: Triangular localisation

A new localisation approach is proposed by using triangular segmentation across the test area in **Chapter 5**. Localisation has two stages. In the first stage, the test area is divided into an optimum number of triangles. LQI measurements are carried out at object locations. These measurements are converted into measurement distances by using a bi-sectioning algorithm with curve fitting procedures. Measurement distances are utilised with trigonometric methods and object locations are calculated. In the second stage, object location calculations are refined by introducing the weighted centroid localisation technique within the triangular sub-areas across the test area. Second level object localisation generates an average localisation accuracy of 1.1m.

9.3.8 Outcome 8: Reference node localisation

A novel localisation approach is proposed in **Chapter 6** by using transmitter reference nodes in star formation across the sensing area. This is similar to the LandMarc localisation system with different reference node topologies. The system uses less reference nodes.

Initially, LandMarc localisation system is utilised and an average object localisation accuracy of 1.2m is obtained. An improved LandMarc localisation system is introduced by selecting 3 nearest reference nodes to the object and 3 closest reference nodes to each nearest node. Localisation procedures between them reveal an average localisation accuracy of 0.79m. A hybrid weighted localisation approach employs a neighbourhood weighted 3-NN algorithm to determine the object locations. The proposed approach achieves an average positioning accuracy of 0.40m.

9.3.9 Outcome 9: Virtual localisation

A virtual localisation approach is proposed with fingerprint mapping in **Chapter 7**. Preparation of a large fingerprint database is time and effort consuming. On the other hand, large numbers of grid points are needed for better object accuracies. Hence, virtual grid points between physical grid points are organised. RSSI values are determined at these virtual grid points with respect to specific RSSI distribution functions. These distribution functions are linear and exponential functions. They are used to distribute RSSI values between grid points at virtual grid points. Application of fingerprint localisation techniques with virtual fingerprint databases gives better accuracies compared to basic fingerprint localisation. Minimum average positioning accuracy obtained is 1.2m in a rectangular indoor area of 4m grid space.

9.3.10 Outcome 10: Static segmentation

A new segmentation approach is proposed for indoor localisation in **Chapter 8**. Initially, the sensing area is divided manually into sub areas called segments. Each segment is identified by a feature function. Each feature function is composed of RSSI ranges of transmitters across the segment area. RSSI values recorded from transmitters with the object receiver are compared with these feature functions to see whether these values are included by any feature function or not. Once the object RSSI values are included in a feature function; this feature function and its segment is identified as the object segment. Localisation procedures are carried out only in that object segment. The average localisation accuracy achieved with static segmentation is 1.2m.

9.3.11 Outcome 11: Dynamic segmentation

A novel method of dynamic segmentation approach is proposed in **Chapter 8** where the segments are generated automatically across the test area. Once the fingerprint map is generated across the grid points, one grid point is selected as a reference grid point by its mean and STD values of RSSI values from transmitters.

A feature function is generated from these mean and STD values of the reference point. The search is carried out with RSSI values of other grid points whether they are included in the feature function of the reference point or not. In case of inclusions, those grid points and the reference point are considered as the first segment. Another grid point is selected as the next reference grid point adjacent to the first segment and the procedures are repeated.

Similarly, object RSSI values are compared with the feature functions of segments and the object segment is determined. Localisation procedures are carried out in the object segment to find the object location. The average localisation accuracy achieved with dynamic segmentation is 0.9m

9.4 Potential improvements of the research

In this study, several localisation approaches are implemented to determine the location of unknown objects with high accuracy indoors. Experimental areas contained a small number of obstacles. There are concrete walls at a distance surrounding the test area. RSS recordings in LQI format are carried out in large numbers at grid points and object locations. Experiments are repeated several times.

In view of the research work, various suggestions are brought forward and they are listed as follows:

- 1) During measurements, Jennic JN5139 WSN transmitters and receivers are utilised as source or destination according to the nature of experiments. One improvement would be to use wireless access points during data transfer to the base computer. Currently wired connections are used and this introduces physical difficulties and limitations. The number of transmitters and receivers are limited during experiments due to availability. Their numbers can be increased and denser node distributions can be utilised. This, in return, can assist to increase positioning accuracies. It also gives the opportunity to test larger areas indoors.
- 2) Jennic JN5139 devices are basic transmitters and receivers. They communicate with each other to transmit and receive LQI values. Hence there is a need to convert them to RSSI values for the application of some localisation algorithms. RSSI values define the RSS power in dBm and LQI values give an 8-bit representation of power. Hence, RSSI is preferred in accurate measurements. Other devices such as RF-Code communicate with each other and the server directly using RSSI values. These devices have power management and Wi-Fi capabilities. These advanced functions generate time savings and efficient

position calculations. Therefore, use of RF-Code devices can be a great advantage during experiments instead of Jennic devices.

- 3) Localisation procedures are carried out after LQI data is received and recorded in a database with present Jennic JN5139 devices. Next generation Jennic devices such as JN5168 have many improvements compared to JN5139. These devices have expansion boards, internet facility through a router, time of flight engine etc. Usage of these devices introduces better experimentation and intervention free data collection. As a result, localisation accuracies will be improved due to improved data collection.
- 4) Localisation accuracies can be improved by deploying wireless sensor nodes with dual transmission media. An example system is called Cricket which uses both RF and ultrasonic signals. Application of these signals between transmitters and receivers helps to determine the distances between them by using time of flight procedures. The distance between transmitter and receiver can be calculated electronically. Trigonometric methods are employed to find the coordinates of the unknown receiver by using these distances. An improvement would be the inclusion of Cricket devices in the experiments. Object localisation accuracies will be around a few centimetres.
- 5) Another improvement is to visualise the indoor objects in real time with PDAs and smartphones. Accurate positioning data can be interfaced to these devices through Wi-Fi and the indoor object position can be displayed with graphical visualisation techniques in real time.
- 6) Best accuracy improvements can be obtained by using optical and interferometric techniques. These techniques are rather costly. Positioning accuracies achieved with these systems are less than 2cm. Inclusion of these techniques and related devices in the experiments would increase the positioning accuracies.
- 7) Finally, object localisation is thoroughly investigated with Jennic JN5139 devices and a complete proposal can be suggested to locate objects in simple topology indoors.
 - LQI recordings, arriving from transmitters, are received by receivers. These recordings are stored in databases in a server computer.
 - Outliers are removed from recorded LQI values.

- LQI values are measured several times and recorded in a data base. Average of LQI values are taken to reduce the random variations among them. This generates a filtering and smoothing effects of LQI values.
- LQI values are calibrated with respect to distances and environmental conditions across the test area.
- LQI values are converted to RSSI values for adaptive localisation.
- RSSI values can be adaptively arranged so that only those within the adaptive range can be employed for localisation.
- LQI data recorded at object locations are also subjected to data correction and distances between object receiver and transmitters are determined as measurement distances.

Once LQI data is determined at grid points and at object locations, all localisation procedures in this study are recommended for position detection. They have good localisation accuracies with respect to grid spacing. They can be utilised according to required accuracies in indoor areas.

Several of these procedures attract attention due to high localisation accuracies achieved with respect to grid spacing during the study. These are:

- *Reference neighbourhood weighted, (0.4m)*
- *Adaptive centroid (0.77m)*
- *Dynamic segmentation (0.90m)*

The user can choose any one of these according to his/her indoor requirements. It can be possible to achieve a position detection accuracy of around 0.4m with simple Jennic JN5139 devices successfully. Localisation accuracy levels achieved with these devices and deployed techniques are quite encouraging considering similar advanced systems in literature.

Hakan Koyuncu 2014

REFERENCES

-
- [1] C. Randell, H. Muller; Low Cost Indoor Positioning System, report, Department of Computer Science, University of Bristol, UK.
 - [2] P. Bahl, V.N. Padmanabhan; RADAR: An in-building RF based user location and tracking system, in: Proceedings of IEEE INFOCOM 2000, Tel-Aviv, Israel (March 2000),
 - [3] Garmin Corporation, About GPS, <http://www.garmin.com/aboutGPS/>
 - [4] J. Hallberg, M. Nilsson and K. Synnes; Positioning with Bluetooth, 10th International Conference on Telecommunications, vol. 2, Feb 2003, pp. 954-958.
 - [5] A.Ward, A.Jones, A. Hopper: A new location technique for the active office, In IEEE personal Communication Magazine, Volume 4 no 5, pages 42-47, October 1997
 - [6] R.Want , A.Hopper,V.Falcao, J.Gibbons; The active Badge location system, ACM Transactions on Information systems Vol. 40, No. 1, pp. 91-102, January 1992
 - [7] L. M.Ni, Y. Liu, Y.C. Lau, A.P. Patil; LANDMARC: Indoor Location Sensing Using Active RFID; Wireless Networks 10, 701–710, 2004
 - [8] J. Hightower, R. Want, G. Borriello; SpotON: An indoor 3D location sensing technology based on RF signal strength, UW CSE00-02-02, February 2000, <http://www.cs.washington.edu/homes/jeffro/pubs/2000indoor/hightower2000indoor.pdf>
 - [9] <http://www.cl.cam.ac.uk/research/dtg/attarchive/projects.html>
 - [10] M.Hazas, A. Hopper ; A Novel Broadband Ultrasonic Location System for Improved Indoor Positioning, IEEE Transactions on mobile Computing, Vol. 5, No. 5, May 2006.
 - [11] N.B. Priyantha; The cricket indoor location system: PhD Thesis, Massachusetts Institute of Technology. 199 p, June 2005
 - [12] Y.Fukuju, M. Minami, H.Morikawa, T. Aoyama; Dolphin: An autonomous indoor positioning system in ubiquitous computing environment, in Proc of the IEEE Workshop on Software Technologies for Future Embedded Systems. 2003.
 - [13] R. J. Fontana, E. Richley, J. Barney; Commercialization of an ultra wideband precision asset location system, 2003 IEEE Conference on Ultra Wideband Systems and Technologies, November 2003, Reston, VA
 - [14] J. Hightower, G. Borriello; Location systems for ubiquitous computing. IEEE Trans. Computing., 34, pp 57–66, 2001.
 - [15] Y. Gwon, R. Jain, T. Kawahara; Robust indoor location estimation of stationary and mobile users, INFOCOM 2004, Hong Kong, March 2004.

-
- [16] J.Bohn; Prototypical implementation of location aware services based on a middleware architecture for Super-distributed RFID tag infrastructures. *Pers. Ubiquitous Computing*, 12, pp 155–166, 2008.
 - [17] T.Zhang, Y.X. Ouyang, C. Li, Z. Xiong; A scalable RFID-based system for location- aware services. *Proc. 3rd IEEE Int. Conf. Wireless Communications, Networking and Mobile Computing (WiCOM'07)*, Shanghai, China, September 21–23, Vol. 2, pp. 2116–2123 ,2007.
 - [18] N. S. Correal, S. Kyperountas, Q. Shi, M. Welbom; An UWB relative location system, *IEEE Ultra Wideband Systems and Technologies*, 2003, VA, USA
 - [19] R. J. Fontana; Ultra-wideband precision asset location system, 2002 IEEE Conference on Ultra Wideband Systems and Technologies, May 2002, Baltimore, MD.
 - [20] R. Merz, F. Chastellain, C. Botteron, A. Blatter, A.Farine; An Experimental Platform for an Indoor Location and Tracking System; <http://www.merz.li/documents/GNSS2008.pdf>
 - [21] G.Retscher, Q.Fu; Using Active RFID for Positioning in Navigation Systems, *Proceedings of the 4th International Symposium on Location Based Services and Telecartography*, Hong Kong, 2007
 - [22] S. Hinske; Determining the position and orientation of multi tagged objects using RFID technology, Institute for pervasive computing, dept of computer science, ETH Zurich.
 - [23] K.Zhang, M.Zhu, G.Retscher , F.Wu , W.Cartwright ; 3D Positioning Algorithm for Integrated RFID/INS Indoor Positioning System, *Proceedings of the 5th Location Based Service conference*, Salzburg, Austria,2008.
 - [24] V.W.Zheng, HIPS: A calibration-less Hybrid Indoor Positioning System Using Heterogeneous Sensors
 - [25] A. Benlarbi, J. C. Cousin; 3D Indoor micro Location Using a stereoscopic Microwave Phase sensitive device , *IEEE MTT-S Digest* ,2003 , pp 623-626
 - [26] H.Koyuncu, S.H.Yang; A survey of indoor positioning and object locating systems, *Int Journal of Computer Science and Network Security*,(IJCSNS), Vol 10,No 5, May 2010, pp 121-128
 - [27] P. Krishnan, A. Krishnakumar, W. H. Ju, C. Mallovs, S. Ganu; A System for LEASE: Location estimation Assisted by Stationary Emitters for Indoor RF Wireless Networks. In *IEEE Infocom*, volume 2, pages 1001–1011, March 2004
 - [28] D. Pandya, R. Jain, E. Lupu; Indoor location using multiple wireless technologies, *IEEE PIMRC*, Beijing, China, September 2003
 - [29] http://en.wikipedia.org/wiki/Wireless_sensor_network
 - [30] <http://blogs.dolcera.com/blog/2009/08/02/wireless-sensor-networks-a-report/>
 - [31] http://www.jennic.com/jennic_support/application_notes/jnan-1052_home_sensor_demonstration
 - [32] I.F.Akyıldız, W.Su, Y.Sankarasubramaniam, E.Cayirci: *Wireless sensor networks a survey*, *computer Networks* 38, 2002, pp 393
 - [33] R.Verdone, D. Dardari, G. Mazzini, A. Conti; *Wireless Sensor and Actuator Networks*, Academic Press/Elsevier, London, 2008.
 - [34] <http://www.lancs.ac.uk/pg/rutledge/pdf/ch2.pdf>
 - [35] <http://www.cse.yorku.ca/~dusan/Zigbee-Standard-Talk.pdf>
 - [36] <http://en.wikipedia.org/wiki/MiWi>

-
- [37] G.J. Pottie, W.J. Kaiser; Wireless integrated network sensors, *Communications of the ACM* 43 (5), pp 551–558, 2000.
 - [38] E. Callaway, P. Gorday, L.Hester; Home Networking with IEEE 802.15.4: A Developing Standard for Low-Rate Wireless Personal Area Networks, *IEEE Communications Magazine*, August 2002 pp 70-77
 - [39] http://en.wikipedia.org/wiki/IEEE_802.15.4
 - [40] S. Safaric, K. Malaric; ZigBee wireless Standard, 48th International Symposium ELMAR-2006, Zadar, Croatia pp 259-262, 07-09 June 2006,
 - [41] S.C. Ergen; Zigbee/IEEE 802.15.4 Summary, <http://pages.cs.wisc.edu/~suman/courses/838/papers/zigbee.pdf>. 2004
 - [42] C. Drane, M. Macnaughtan, C. Scott; Positioning GSM telephones, *IEEE Commun. Mag.*, vol. 36, no. 4, pp. 46–54, 59, Apr. 1998.
 - [43] H.Koyuncu, S.H.Yang; A 2D positioning system using WSNs in indoor environment, *Int.Journal of Engineering and Computer Science*, Vol 11, No 3, pp 70-77 ,June 2011.
 - [44] H.Koyuncu, S.H.Yang; A study of indoor positioning by using trigonometric and weight centroid localization techniques , *Int. Journal of Computer Engineering Research*, Vol 2, No 4, pp 60-67, October 2011
 - [45] H.Koyuncu, S.H.Yang; An Improved adaptive localization approach for indoor positioning by using environmental thresholds with wireless sensor nodes, *IET Wireless Sensor Systems*, pp 1-9 ,2014 ,doi: 10.1049/iet-wss.2013.0100
 - [46] H.Koyuncu, S.H.Yang; Comparisons of Indoor localization techniques by using reference nodes and weighted k-NN algorithms, *Third European conference of computer science*. 3, pp 46-51, ISBN 978-1- 61804-140-1, December 2012.
 - [47] H.Koyuncu, S.H.Yang; Indoor Positioning with Virtual Fingerprint mapping by using linear and exponential taper functions, *IEEE International conference on Systems, Man and Cybernetics (CSMC)* ,IEEE Proceedings, pp 1052-1057,ISSN 978-1-4799-0652-9 ,October 2013.
 - [48] H.Koyuncu, S.H.Yang; Virtual 2D positioning system by using Wireless sensors in indoor environment, *International Journal of Wireless and mobile networks (IJWMN)*, Vol 5, No 6 , December 2013, pp 21- 36.
 - [49] H.Koyuncu, S.H.Yang; Improved Fingerprint localization by using static and dynamic segmentation, *International Conference on Computational Science and Computational Intelligence (CSCI'14)*, IEEE CPS proceedings, Las Vegas USA, pp 149-156, March 2014,
 - [50] P. Ali-Rantala, L. Ukkonen, L. Sydanheimo, M. Keskilammi, and M. Kivikoski, “Different kinds of walls and their effect on the attenuation of radiowaves indoors,” in *Proceedings of the IEEE Antennas and Propagation Society International Symposium*, vol. 3, pp. 1020–1023, Columbus, Ohio, USA, June 2003.
 - [51] C. Alippi, G. Vanini; A RF map-based localization algorithm for indoor environments. In *ISCAS '05: Proceedings Of the IEEE International Symposium of Circuits and Systems*. IEEE Computer Society, May 2005.
 - [52] N. B. Priyantha, A. Chakraborty, H. Balakrishnan; The cricket location-support system. In *Proceedings of the 6th annual international conference on Mobile computing and networking*, pages 32–43. ACM Press, 2000.

-
- [53] N.Bulusu, J.Heidemann, D.Estrin.D ; GPS-less low cost outdoor localization for small devices, IEEE personal communication, vol 7 ,pp 28-34 ,2000
 - [54] K. Almuzaini, A. Gulliver, "Range-Based Localization in Wireless Networks Using Density-Based Outlier Detection," *Wireless Sensor Network*, Vol. 2 No. 11, pp. 807-814, 2010
 - [55] F.Reichenbach, J.Blumenthal, D.Timmermann ; improved precision of coarse grained localization in wireless sensor networks 9th DSD conference, Dubrovnik, Croatia pp 630-637,2006
 - [56] D.Li, K.Wong, Y.Hu , A.Sayeed ; detection classification and tracking of targets in distributed sensor network, IEEE signal processing magazine ,Vol 19,No 2, pp 17-29 ,2002
 - [57] J. Small, A. Smailagic, D. P. Siewiorek ;Determining User Location For Context Aware Computing Through the Use of a Wireless LAN Infrastructure, Dec 2000, [Online] Available: <http://www-2.cs.cmu.edu/~aura/docdir/small00.pdf>.
 - [58] A. Nasipuri, K. Li; A directionality based location discovery scheme for wireless sensor networks. In Proceedings of ACM International Workshop on Wireless Sensor Networks and Application, pages 105–111, Sept. 2002.
 - [59] N. Patwari, A. O. Hero, M. Perkins, N. S. Correal, R. J. O’Dea; Relative location estimation in wireless Sensor networks. IEEE Transaction on Signal Processing, 51:2137–2148, Aug. 2003.
 - [60] R.I. Hartley, P. Sturm; Triangulation, <http://users.cecs.anu.edu.au/~hartley/Papers/triangulation/triangulation.pdf>
 - [61] B. Cook, G. Buckberry, I. Scowcorft, J. Mitchell, T. Allen; Indoor location using trilateration characteristics. In: London Communications Symposium, LCS 2005, London, UK, 8-9 September 2006
 - [62] P. Enge, P. Misra; Special issue on GPS: The Global Positioning System. *Proceedings of the IEEE*, 87(1):3–172, January 1999.
 - [63] J. Werb, C. Lanzl; Designing a Positioning System for Finding Things and People Indoors. *IEEE Spectrum*, 35(9):71–78, Sept.1998.
 - [64] C. Medina,J.C.Segura, A.D.Torre; Ultrasound indoor positioning system based on low-power wireless sensor network providing sub-centimeter accuracy, *Sensors*,vol.13,pp 3501-3526, 2013
 - [65] R.Peng, M.L.Sichitiu; Angle of arrival localization for wireless sensor Networks, Dept of Electrical and Comp engineering, North Carolina State University, research publications pp 2-7, 2006
 - [66] K.Kaemarungsi, P.Krishnamurthy; Modeling of indoor positioning systems based on location Fingerprinting IEEE infocom, ISBN: 0-7803-8356-7, 2004
 - [67] E.Kaplan, C.J.Hegarty; Understanding GPS: principles and applications. Boston, MA: Artech House; 2005.
 - [68] K.Pahlavan, A.H.Levesque; Wireless information networks, 2nd Ed. New York: John Wiley & Sons; 2005.
 - [69] M.Youssef, A.Agrawala; Horus location determination system. In: Association of computing machinery (ACM), MOBISYS, pp 205–219, 2005
 - [70] S.J.Ingram, D.Harmer, M.Quinlan; Ultra Wide Band indoor positioning systems and their use in emergencies. In: IEEE conference on position location and navigation symposium, pp 706–715, 2004.

-
- [71] T. Sansanayuth, P. Suksompong, C. Chareonlarnnopparut, A. Taparugssanagorn; RFID 2D-localization improvement using modified LANDMARC with linear MMSE estimation, Communications and Information Technologies (ISCIT), pp 133-137, 4-6 Sept. 2013
 - [72] A.Bekkali, H.Sanson, M.Matsumoto; RFID indoor positioning based on probabilistic RFID map and kalman filtering. In: 3rd IEEE international conference on wireless and mobile computing, networking and communications, IEEE WiMob, 2007.
 - [73] K.Yamano, K.Tanaka, M.Hirayama, E.Kondo; Self-localization of mobile robots with RFID system by using support vector machine. In: Proceedings of 2004 IEEWRSI international conference on intelligent robots and systems, Sendai, Japan, 2004.
 - [74] T.King, S.Kopf, T.Haenselmann, C.Lubberger, W.Effelsberg; COMPASS: a probabilistic indoor positioning system based on 802.11 and digital compasses. In: WinTeck, p. 24–40, 2006.
 - [75] K.Hinckley, M. Sinclair; Touch-sensing input devices. In: Proceedings of the SIGCHI conference on human factors in computing systems, pp 223–230, 1999.
 - [76] S.Schuhmann k.Herman, K.Rothwemel, J.Blumenthal, D.Timmermann; Improved weight centroid localization in smart ubiquitous environment, UIC 2008 proceedings of 5th int conference on ubiquitous intelligence and computing, pp 20-34, 2008
 - [77] S. P. Fekete, A. Kroller, C. Buschmann, S. Fischer, D. Pfisterer: Koordinatenfreies Lokation sbewusstsein. In it - Information Technology, 47, 2, pp. 70–78, 2005.
 - [78] S. Pandey, F. Anjum, B. Kim, P. Agrawal; A low-cost robust localization scheme for WLAN. In Proceedings of the 2nd Int'l Workshop on Wireless Internet, 2006.
 - [79] D. Niculescu and B. Nath; DV Based Positioning in Ad hoc Networks in Journal of Telecommunication Systems, 2003.
 - [80] T. He, C.Huang, B.Blum, J.Stankovic, T.Abdelzاهر; Range-free localization and its impact on large scale sensor networks. In Transactions on Embedded Computing Systems, vol 4, 4, pp. 877-906, 2005.
 - [81] E. Elnahrawy, X. Li, R. P. Martin: Using Area-Based Presentations and Metrics for Localization Systems in Wireless LANs. In Proceedings of the 29th IEEE International Conference on Local Computer Networks (LCN'04), Washington, USA, 2004.
 - [82] B. W. Parkinson, J. J. Spilker; Global Positioning System: Theory and Applications, Vol. 1. In Progress in Astronautics and Aeronautics, American Institute of Aeronautics and Astronautics, vol. 163, pp. 29–56, 1996.
 - [83] M. Youssef, A. Agrawala, U. Shankar; WLAN Location Determination via Clustering and Probability Distributions. In Proceedings of IEEE per Com 2003, March 2003.
 - [84] R.Want; An introduction to RFID technology. IEEE Pervasive Computing, vol 5(1), pp25–33, 2006.
 - [85] M.Baudin; RFID applications in manufacturing. Draft, 2005.
 - [86] A.Stelzer, K.Pourvoyeur, A.Fischer; Concept and application of LPM—a novel 3-D local position measurement system. IEEE Trans. Microwave Theory Techniques; vol 52(12), pp 2664–2692, 2004.
 - [87] H.J.Lee, M.C. Lee; Localization of mobile robot based on radio frequency identification devices. In: SICE-ICASE, international joint conference, pp 5934–5939, October 2006.
 - [88] S.S.Han, H.S.Lim, J.M.Lee; An efficient localization scheme for a differential-driving mobile robot based on RFID system. IEEE Trans. Ind. Electron., vol 54, pp 3362–3369, 2007.

- [89] B.Xu, W.Gang; Random sampling algorithm in RFID indoor location system. In: IEEE international workshop on electronic design, test and applications (DELTA'06), 2006.
- [90] W.T.Hill; Electromagnetic Radiation Wiley, ISBN 978-3-527-40773-6, 2009.
- [91] K.Pahlawan and P.Krishnamurthy ; Principles of wireless networks ,A unified approach ,Prentise Hall PTR,New Jersey ,2002.
- [92] R. Bansal; Fundamentals of Engineering Electromagnetics, CRC Press, May 2006
- [93] J.Small, A.Smailagic, D.P.Siewiorek; determining user location for context aware computing through the use of a wireless LAN Infrastructure, Project aura Report, Carnegie Mellon University, 2000.
- [94] B.Sklar; Rayleigh fading channels in mobile digital communication systems, IEEE Communication Magazine ,vol 35, pp 90-100, 1997.
- [95] J.Yin, Q.Yang, L.Li; Adaptive Temporal Radio maps for indoor Location Estimation, 3rd IEEE international conference on pervasive computing and communications ,Hawai , pp 85-94,2005.
- [96] T.S.Rappoport; Wireless Communications: principles and practise, Prentice-Hall Inc., New Jersey, 1996
- [97] S.C.Ergen; ZigBee/IEEE 802.15.4 Summary, [http:// pages.cs.wisc.edu/~suman/courses /838/papers/ zigbee.pdf](http://pages.cs.wisc.edu/~suman/courses/838/papers/zigbee.pdf)
- [98] R. Grossmann; Localization in Zigbee-based wireless sensor networks, Technical Report, University of Rostock, Institute MD, April 2007.
- [99] <http://www.jennic.com/support/forums>
- [100] http://www.jennic.com/support/datasheets/jn5139_module_datasheet
- [101] M. Sugano, T. Kawazoe ,M. Murata ; Indoor localization system using RSSI Measurement of wireless sensor network based on ZigBee Standard, IASTED international multi conference on wireless and optical communications , 2006
- [102] http://en.wikipedia.org/wiki/Bisection_method
- [103] <https://ece.uwaterloo.ca/~dwharder/NumericalAnalysis/10RootFinding/bisection/>
- [104] <http://www.cee.vt.edu/ewr/environmental/teach/smprimer/outlier/outlier.html>
- [105] S.Walfish; A review of statistical outlier methods, Pharmaceutical technology, pp 1-5, 2008.
- [106] F.Augusto, A.Garcia; Tests to Identify Outliers in Data Series, Introduction section, Mathworks.com, 2010
- [107] http://en.wikipedia.org/wiki/Dixon's_Q_test#Example
- [108] ITU-R criteria for propagation data and prediction methods for the planning of indoor radio communication and local area networks ITU-R RecP 1238,1999
- [109] W.Ren, L. Xu, D.Zoo, Z.Deng; Positioning algorithm using a wireless sensor Networks, Journal of data acquisition and processing, Vol 24, No 6, pp757-761, 2009
- [110] B.Li.,J.Salter,A.Dempster,C.Rizos; Indoor positioning techniques based on wireless LAN, Proceedings of Auswireless, Sydney, Australia, 2006

- [111] J.Blumenthal, R.Grossmann, D.Timmermann; Weighted centroid localization in Zigbee based sensor networks, IEEE symposium on intelligent signal processing WISP, Madrid, Spain 2007
- [112] http://en.wikipedia.org/wiki/Weight_function
- [113] http://www.jennic.com/files/support_files/JN-DS-JN5139MO-1v6.pdf
- [114] http://www.jennic.com/files/support_documentation/JN-AN-1052- ZigBee-Home-documentation/Sensor-Demo-1v3.pdf
- [115] K.Benkic, M.Malajner, P.Planinsic; Using RSSI value for distance estimation in wireless sensor networks based on Zigbee, Systems ,signals and image processing , IWSSIP, pp 303-306, 2008
- [116] M.Bal, H.Xue, W.Shen, H. Ghenniwa; A 3D indoor location tracking and visualization system based on WSNs, IEEE 978-1-4244-6587 pp 1534-1590, 2010
- [117] J.Ma, Q.Chen, D.Zhang, L.M.Ni; An empirical Study of radio signal strength in sensor Networks, technical report, dept of comp sci and eng Hong Kong univ of sci and tech, March 25,2006
- [118] D. Zhan, J.Ma, Q.Chen and L.M.Ni; An RF based system for tracking transceiver free objects, in proceedings of percom, 2007.
- [119] R.Behnke, D.Timmermann ; AWCL as an efficient improvement of coarse grained localization , Proceedings of WPNC 2008, 5th workshop on positioning ,navigation and communication, IEEE ,pp 243-250 ,2008
- [120] W.J.Feng, X.W.Bi; A novel Adaptive cooperative location Algorithm for wireless sensor Networks, International journal of Automation and computing, pp 1-6, 2009
- [121] H.Koyuncu and Shuang Hua Yang, “An improved adaptive localisation approach for indoor positioning by using environmental thresholds with wireless sensor nodes”, IET Wireless sensor systems. 2014, pp. 1–9, doi: 10.1049/iet-wss.2013.0100
- [122] M.Zhu ; Novel Positioning Algorithms for RFID-Assisted 2D MEMS INS Systems, Proceedings of the Institute of Navigation , GNS 2008 conference, Savannah, Georgia, US ,2008
- [123] S.T. Sheu, Y.M. Hsu, H.Y. Chen; Indoor Estimation Using Smart Antenna System with Virtual Fingerprint Construction Scheme, The Eighth International Conference on Mobile Ubiquitous Computing, Systems, Services and Technologies, pp.281-286, 2014
- [124] P. Lamon, I. Nourbakhsh, B. Jensen, R. Siegwart; Deriving and Matching Image Fingerprint Sequences for Mobile Robot Localization, IEEE International Conference on Robotics and Automation, Korea, 2001
- [125] Y. Zhao, Y. Liu , L.M. Ni; VIRE: Active RFID-based Localization Using Virtual Reference Elimination, International Conference on Parallel Processing, pp. 56, 2007
- [126] [http://en.wikipedia.org/wiki/Segmentation_\(image_processing\)](http://en.wikipedia.org/wiki/Segmentation_(image_processing))
- [127] K. Chen, V. Rajlich; Case study of feature location using dependence graph. In A. von Mayrhauser and H. Gall, editors, *proceedings of the 8th International Workshop on Program Comprehension*, pages 241–252. IEEE Computer Society Press, June 2000.
- [128] D. Edwards, S. Simmons, N. Wilde; An approach to feature location in distributed systems. Technical report, Software Engineering Research Center, 2004